115
5-2-91 QS (2)

DOE/NE/34046-1
HBEP-61(3P27)
UC-523

High Burnup Effects Program

High Burnup Effects Program-Final Report

April 1990

Prepared for
U.S. Department of Energy
Assistant Secretary for Nuclear Energy
Office of Light Water Reactor Safety and Technology
under Contract DE-FG06-80ET 34046

DOE/NE/34046-1

Battelle
Pacific Northwest Laboratories

DISCLAIMER

PACIFIC NORTHWEST LABORATORY
operated by
BATTELLE MEMORIAL INSTITUTE
for the
UNITED STATES DEPARTMENT OF ENERGY
under Contract DE-AC06-76RLO 1830

Printed in the United States of America

Available to DOE and DOE contractors from the
Office of Scientific and Technical Information, P.O. Box 62, Oak Ridge, TN 37831;
prices available from (615) 576-8401. FTS 626-8401.

Available to the public from the National Technical Information Service,
U.S. Department of Commerce, 5285 Port Royal Rd., Springfield, VA 22161.

DISCLAIMER

DOE/NE/34046-1
HBEP-61(3P27)
Distribution Category UC-523

DOE/NE--34046-1

DE91 011127

High Burnup Effects Program

High Burnup Effects Program-Final Report

J. O. Barner
M. E. Cunningham
M. D. Freshley
D. D. Lanning

APRIL 1990

A synopsis of the High Burnup Effects Program is presented in this report. The initial objectives of the program, accomplishments relative to those objectives, the organization of the program, and a summary of the major technical findings are included.

Prepared for
U.S. Department of Energy
Assistant Secretary for Nuclear Energy
Office of Light Water Reactor Safety and Technology
under Contract DE-FG06-80 ET 34046

BATTELLE
PACIFIC NORTHWEST LABORATORIES
RICHLAND, WASHINGTON 99352

ACKNOWLEDGEMENTS

The authors would like to take this opportunity to acknowledge and express our appreciation for the support and interest of the High Burnup Effects Program sponsoring organizations, especially those individuals who represented the sponsoring organizations, for their encouragement, continual support, active involvement, and feedback. Battelle, Pacific Northwest Laboratories (BNW) feels that the High Burnup Effects Program was unique in many respects; among them being the longevity of the program and the extent to which the participants interacted and cooperated during the ten year duration of the program. Without the dedicated support of the participants, the HBEP would not have succeeded and the knowledge gained by this program would not have been developed.

We would also like to acknowledge the support and help of individuals and other organizations within BNW whose contributions were critical to the success of the HBEP. Our thanks and recognition go to:

- Lee Daniel who organized and directed the preirradiation characterization of the Task 2 and the original Task 3 archive fuel materials.
- Harold Kjarmo who organized and directed the characterization of the supplementary Task 3 archive fuel materials.
- Evan Jenson and Jim Coleman who, respectively, performed the EPMA and SEM analyses of the Task 2C GE fuel examined at BNW.
- Wendy Bennett who helped develop the data base used by BNW and, since 1984, was responsible for maintaining the data base. Wendy was also a key player in preparing many of the graphics used in the reports and for the Review Meetings.
- Carl Beyer, Rick Williford, and Kitty Hsieh Rising whose efforts during Task 1 helped to define and develop the scope for Tasks 2 and 3.
- The Contracts staff who established and monitored the numerous and complex participant contracts and subcontracts for performance of work.
- The Duplicating personnel who reproduced over 70 reports and handouts published during the life of the program while dealing with often tight schedules and unusual requests.

ACRONYMS AND ABBREVIATIONS

BN - Belgonucleaire
BNFL - British Nuclear Fuels Limited
BNW - Battelle, Pacific Northwest Laboratories
BWR - boiling-water reactor
ECN - Netherlands Energy Research Foundation
EOL - end-of-life
EPMA - electron probe microanalysis
FBFC - Franco-Belge de Fabrication de Combustibles
FGA/CEA - Fragema/CEA
FGR - fission gas release
GBBPR - grain boundary bubble precipitation radius
GE - General Electric Company
HBEP - High Burnup Effects Program
HFR - High Flux Reactor
JRC - Joint Research Center - Petten
KWU/CE - Kraftwerk Union/Combustion Engineering
LHGR - linear heat generation rate
LWR - light-water reactor
PIE - postirradiation examination
PWR - pressurized-water reactor
SEM - scanning electron microscope
TVO - Teollisuuden Voima Oy
WEC - Westinghouse Electric Corporation
XDR - xenon depletion radius
WNL - UKAEA Windscale Nuclear Laboratory
XRF - x-ray fluorescence

CONTENTS

FIGURES

TABLES

1.0 SUMMARY AND CONCLUSIONS

This is the final report of the High Burnup Effects Program (HBEP). It has been prepared to present a summary, with conclusions, of the HBEP. The HBEP was an international, group-sponsored research program managed by Battelle, Pacific Northwest Laboratories (BNW). The principal objective of the HBEP was to obtain well-characterized data related to fission gas release (FGR) for light water reactor (LWR) fuel irradiated to high burnup levels (Freshley 1981).

The HBEP was organized into three tasks as follows:

- Task 1 - High Burnup Effects Evaluations. The objective of the work carried out under this task was to compile and assess the publicly available information on fission gas release from high burnup UO_2 fuel. Work carried out under this task resulted in a report titled High Burnup Effects: A State-of-the-Technology Assessment (HBEP-01).(a) Provided in this report was a review and evaluation of the open literature related to high burnup effects in LWR fuel, plus an assessment of critical data needs.

- Task 2 - Fission Gas Sampling. The objective of the work carried out under this task was to obtain fission gas release data from existing commercial fuel rods with peak-pellet burnup levels to 55 MWd/kgM. Activities carried out within this task included acquiring existing irradiated fuel rods, continuing the irradiation of some rods to high burnup levels, performing power-bumping on selected rods, and then performing extensive postirradiation examinations (PIE). Data were acquired from 45 rods with rod-average burnup levels ranging from 22 to 47 MWd/kgM. Qualification of the Task 2 data was presented in Qualification of Fission Gas Release Data from Task 2 Rods (HBEP-25).

- Task 3 - Parameter Effects Study. The objective of the work carried out under this task was to obtain well-characterized data, with an emphasis on fission gas release, from fuel rods specifically built, charac-

---

(a) HBEP reports specifically referenced in this report are listed in Section 5.0, REFERENCES. All HBEP reports are listed in Appendix B.

terized, and irradiated for the HBEP to peak-pellet burnup levels in excess of 80 MWd/kgM. Work carried out within this task began with the fabrication of fuel rods for irradiation to rod-average burnup levels exceeding 60 MWd/kgM. Anomalies in the as-built condition of the rods were discovered during the PIE of rods irradiated for one-cycle. As a result, rods from other sources were acquired to complement the original Task 3 rods. Extensive PIE was performed on 37 rods with rod-average burnup values ranging from 25 to 69 MWd/kgM. Qualification of the Task 3 data was presented in Qualification of Fission Gas Release Data from Task 3 Rods (HBEP-60).

The original objective of the HBEP was to obtain a large quantity of high-quality, high-burnup level data. At the completion of the program, the following conclusions may be made:

- It was confirmed that the dependency of FGR upon design and irradiation history parameters, known to be applicable at lower burnup levels, was also applicable at higher burnup levels; specifically
  - For rods of similar design, rods operated at low LHGR levels had less FGR than rods operated at high LHGR levels, a result principally related to fuel temperatures.
  - Rods with high internal helium gas pressure had less FGR than rods with low helium pressures, a result principally related to the effect of diluting the released fission gas.
- The net EOL transient (power-bumping) FGR was found to be dependent on a) the terminal LHGR level, b) the burnup level, c) the length of the hold period, and d) the pre-transient state of the grain boundary bubble network.
- A burnup and time dependence of grain boundary bubble precipitation was confirmed; depletion of matrix xenon and precipation of bubbles at grain interfaces are thermally-driven FGR mechanisms.
- At pellet-edge burnup levels greater than approximately 60 MWd/kgM, burnup-dependent microstructural changes occur at the periphery of the pellet; these changes are characterized by a loss of definable grain structure and the formation of a high volume of porosity. Observed

along with the microstructural changes is a transfer of fission gas from the UO_2 matrix to the porosity. This is the result of an athermal mechanism and results in the potential of enhanced release of fission gas from the pellet rim that can increase total FGR during normal operation. During the period of the HBEP, this "rim effect" emerged as the one "new" high-burnup effect.

During the course of the HBEP, a program that extended over 10 years, 82 fuel rods from a variety of sources were characterized, irradiated, and then examined in detail after irradiation. The study of fission gas release at high burnup levels was the principal objective of the program and it may be concluded that no significant enhancement of fission gas release at high burnup levels was observed for the examined rods. The rim effect, an as yet unquantified contributor to athermal fission gas release, was concluded to be the one truly high-burnup effect. Though burnup enhancement of fission gas release was observed to be low, a full understanding of the rim region and rim effect has not yet emerged and this may be a potential area of further research.

2.0 INTRODUCTION

The HBEP was an international, group-sponsored program managed by BNW. The sponsors included fuel manufacturers, utility representatives, and government entities from Europe, Japan, and the United States; a list of the participants is provided as Table 2.1. The principal objective of the HBEP was to obtain well-characterized data on FGR for typical LWR fuel irradiated to high burnup levels (Freshley 1981).

To meet the objective of obtaining useful and well-characterized data on rods irradiated to high burnup levels, the HBEP was organized into three tasks. The first task, High Burnup Effects Evaluation, began in September 1978 with the first organization meeting of the HBEP and concluded in May 1979. A major portion of the work conducted under this task was a compilation and assessment of the publicly available information on high burnup fuel fission gas release. This work was reported in HBEP-01 and formed the basis for the experimental work carried out under Tasks 2 and 3 of the HBEP. The principal conclusion of Task 1 was that the then current data base was not adequate to define the effects of burnup on fission gas release.

Tasks 2 and 3 comprised the experimental work carried out by the HBEP. Under Task 2, Fission Gas Sampling, 45 existing fuel rods, either at moderate burnup levels or undergoing irradiation to higher burnup levels, were identified, acquired, and subjected to PIE. Some rods were also subjected to power-bumping irradiations. This task began in November 1979 and concluded in 1987. Under Task 3, Parameter Effects Study, the HBEP had built a series of fuel rods for irradiation to high burnup levels. Four design variations and three variations in operational history were used to study the effect of design and operation parameters on high burnup FGR. The original Task 3 rods were subsequently supplemented by acquisition of other rods after fabrication anomalies were discovered in the original Task 3 rods. A total of 37 rods were eventually subjected to PIE under Task 3. This task began in November 1979 and concluded in 1990.

The objective of this report is to provide a synopsis of the HBEP, including a review of the program organization, activities, accomplishments, and conclusions. Presented in this report is the following material.

- A program overview and chronology (Section 3).
- An overview of major technical findings and conclusions (Section 4).
- A summary of fuel rod design and operation data (Appendix A).
- A bibliography of material prepared by the HBEP, and tables cross-referencing data with reports (Appendix B).
- A brief summary of the examination techniques employed during post-irradiation examination (Appendix C).

TABLE 2.1. Listing of HBEP Sponsors

Organization	Country
Advanced Nuclear Fuels Corporation[a] (ANF)	USA
Babcock-Brown Boveri Reaktor (BBR)	FRG
Babcock and Wilcox (B&W)	USA
Belgonucleaire (BN)	Belgium
British Nuclear Fuels Limited (BNFL)	UK
Central Research Institute of Electric Power Industry (CRIEPI)	Japan
Centre d'Etude de l'Energie Nucleaire (CEN)	Belgium
Combustion Engineering, Incorporated (CE)	USA
dell'Energia Nucleare e delle Energie Alternative (ENEA)[b]	Italy
Department of Energy, U.S. Government (DOE)	USA
Electric Power Research Institute (EPRI)	USA
Fragema (FGA)[c]	France
General Electric Company (GE)	USA
Hitachi, Limited	Japan
Japan Atomic Energy Research Institute (JAERI)	Japan
Mitsubishi Heavy Industry, Limited (MHI)	Japan
Netherlands Energy Research Foundation (ECN)	The Netherlands
Nuclear Fuels Industry, Limited (NFI)	Japan
Risø National Laboratory (Risø)	Denmark
The Paul Scherrer Institute[d] (PSI)	Switzerland
Siemens AG[e]	FRG
Studsvik Energiteknik AB (Studsvik)	Sweden
Toshiba Corporation	Japan
Technical Research Center of Finland (VTT)	Finland
Westinghouse Electric Corporation (WEC)	USA

(a) Formerly Exxon Nuclear Company, Incorporated.
(b) Formerly Comitato Nazionale per l'Energie Nucleaire (CNEN).
(c) Formerly Framatome.
(d) Formerly the Swiss Federal Institute for Reactor Research (EIR).
(e) Formerly Kraftwerk Union Aktiengesellschaft (KWU).

3.0 PROGRAM OVERVIEW

This section provides an overview of the HBEP and the activities carried out by the HBEP. Included is a discussion on a) the goals/objectives of the HBEP, b) the organization and chronology of the HBEP, and c) the fuel types and operational histories investigated by the HBEP.

3.1 HBEP GOALS/OBJECTIVES

The primary objective of the HBEP, as stated in Freshley (1981), was to "provide information on the high burnup (60-65 MWd/kgM peak) behavior of Zircaloy-clad UO_2 LWR fuel with emphasis on obtaining well-characterized data related to the effect of fuel temperature on fission gas release during irradiation of PWR and BWR fuels to high burnup levels." It was intended that the HBEP would provide modeling-quality data. The scope of the program was modified throughout its duration as dictated by results that were obtained and to reflect the responses, interests, and needs of the participants.

3.2. HBEP ORGANIZATION AND CHRONOLOGY

The HBEP was organized into three tasks, with the first task being a review of existing high-burnup fission gas release data and the second and third tasks being experimental to obtain the data recommended, by the first task, as being needed.

The HBEP participants provided funding (or work in-kind) for the program and directed the general scope of the program. BNW developed and proposed the program, provided the management, directed the specific work activities, and qualified and disseminated the data. The majority of activities were carried out by subcontractors; the HBEP subcontractors and the activities they performed are listed in Table 3.1.

The program scope outlined in the following sections reflects the as-performed program. As the program progressed, the scope was expanded (in terms of number of rods and postirradiation examinations) relative to the original scope. The expanded scope was made possible because of the

availability of additional funding from a) investment of participant prepayments and b) favorable currency exchange rates on subcontracts.

3.2.1 Task 1 - High Burnup Effects Evaluation

Organizational efforts by BNW to develop the HBEP began in 1978 and culminated in September 1978 with the first organizational meeting. Ten participants at this meeting committed to sponsoring Task 1 of the HBEP. Activities conducted under Task 1 included:

- evaluation of the state-of-the-technology relative to high-burnup FGR;
- assessment of the publicly available data relative to the development of a correlation for predicting high-burnup FGR;
- identification of data needs for the development of a high-burnup FGR correlation;
- evaluation and identification of existing data and irradiated fuel rods for possible use by the HBEP; and
- development of a program plan for Tasks 2 and 3.

Task 1 was completed in May 1979 and the results were presented to the sponsors at the first review meeting held on May 4, 1979.

The activities and results of Task 1 were documented in HBEP-01 and a supplementary paper on analysis of the data and FGR models was prepared (HBEP-10 and Beyer 1982). Conclusions presented in these documents included:

- there was a need for well-qualified FGR data from fuel operated with centerline temperatures ranging from 1000 to 2000°C for burnup levels in excess of 30 MWd/kgM (this was the expected operating temperature range for LWR fuels);
- the majority of the data available up to the initiation of the HBEP was obtained under non-typical LWR conditions;
- data obtained under typical LWR conditions was often lacking in details needed for complete evaluation; and
- data available in the open literature was <u>not</u> useful for establishing the effects of burnup on FGR from LWR fuels.

Following the conclusion of Task 1, a program plan for Tasks 2 and 3 was developed and the second program review meeting was held in November 1979. Twenty four potential HBEP participants attended this meeting and the work scope for Tasks 2 and 3 was agreed upon.

3.2.2 Task 2 - Fission Gas Sampling

Task 2 was initiated in November 1979 when the HBEP sponsors agreed to the work scope. The objectives of Task 2 were to:

- provide FGR data on fuel rods irradiated in commercial reactors over the burnup range 20 to 55 MWd/kgM;
- provide FGR data on fuel rods irradiated in commercial reactors to high burnup levels at low LHGR/temperature levels that were subsequently power-bumped(a) to high LHGR/temperature levels; and
- provide an interim correlation for high-burnup FGR.

The first two objectives were clearly met, with the acquisition of FGR data from fuel rods having peak-pellet burnup levels to 55 MWd/kgM (rod-average burnup levels to 47 MWd/kgM). While factors relevant to developing a correlation for FGR to moderately high burnup levels were identified, the data obtained did not lend itself to incorporation into a single FGR correlation. Therefore, given the varying levels of participant interest in model development, activities by BNW to develop a correlation were limited to "qualification of the data" for use in performance modeling correlations. "Qualification" refers to a broad scope of activities that include a consistent summarization of the data, determining levels of significance for the as-reported data, correlating observations such as microstructure and EPMA data, providing best-estimate evaluations of parameters such as rod-average burnup and fuel temperature, and identifying behavior as either anomalous or self-consistent.

(a) Power-bumping refers to short-period irradiations wherein rods undergo a relatively rapid increase to LHGR levels greater than normal steady-state LHGR levels. The peak LHGR level is then held for a sufficient period to allow near-equilibrium fission gas release; see Section 7.1.3 of Freshley 1981.

A total of 45 rods were acquired and examined. The major activities carried out under Task 2 consisted of acquisition of suitable existing irradiated fuel rods; characterization of archive non-irradiated fuel pellets; continued- or re-irradiation (including power-bumping) of some rods; PIE of the rods; data handling and qualification; and disposal of the irradiated material. A total of 38 reports[a] were prepared by either BNW or the subcontractors to document the Task 2 activities (Appendix B). Summaries of the Task 2 data, including evaluations relative to high-burnup FGR, were provided in HBEP-25 and HBEP-50. A summary of the rods included in Task 2 is provided as Table 3.2.

Task 2 was divided into three subtasks; those subtasks were:

Task 2A - Fission Gas Sampling of Existing Rods. Existing rods at moderate burnup levels were acquired and PIE was performed on those rods; 20 rods were included in this subtask.

Task 2B - Fission Gas Sampling of Reirradiated Rods. Existing rods were acquired and their irradiation was continued to high burnup levels. PIE was performed on these rods following completion of the irradiation; nine rods were included in this subtask.

Task 2C - Fission Gas Sampling of Bumped Rods. Sibling rods to some of the rods used in Subtasks 2A and 2B were acquired, and then subjected to power-bumping irradiations in a test reactor. PIE was performed on these rods following the bumping irradiations; 16 rods were included in this subtask.

3.2.3. Task 3 - Parameter Effects Study

Task 3 was initiated in November 1979 along with Task 2. The objective of Task 3 was to provide well-characterized data on the effects of fuel temperature, burnup, power history, and different fuel characteristics with an emphasis on FGR. Data obtained from Task 3 were expected to be of modeling quality because of detailed preirradiation characterization of the fuel and rods and operation under typical and well-known conditions. Because of the anomalies present in the fuel rods built for Task 3, the original objective of the task was modified.

(a) Some HBEP reports include both Task 2 and Task 3 data.

Initially, 44 rods were manufactured for the HBEP with 40 rods planned for irradiation in the BR-3 reactor. However, PIE of rods irradiated for 1-cycle revealed two serious anomalies from the fabrication of the rods: the presence of a significant (~20%) fraction of argon in the initial fill gas(a) and the presence of high-enrichment UO_2 particles distributed throughout the fuel matrix. These two anomalies were considered to be serious impediments to obtaining the original objectives of the task.

Following the conclusion in 1985 that the Task 3 rods had not been fabricated to specification, a decision was made to reduce the number of original Task 3 rods to be included in Task 3 and supplement the matrix with rods from other sources. There were two principal criteria for selecting the rods to be used to supplement the original Task 3 rods; those criteria were rods with the maximum possible burnup level and rods with archive non-irradiated fuel pellets available for characterization. After adding rods from other sources to the sixteen original Task 3 rods that were retained, a total of 37 rods were included in Task 3; a summary of the characteristics of those rods is provided as Table 3.3.

Activities carried out under Task 3 included fabrication of fuel and rods; acquisition of additional rods; characterization of archive non-irradiated fuel pellets; irradiation of the fuel rods; PIE of the rods; data handling and qualification; and disposal of the irradiated material. A total of 21 reports were prepared by either BNW or the subcontractors to document the Task 3 activities (Appendix B). A summary of the Task 3 data, including evaluations relative to high-burnup FGR, was provided in HBEP-60.

3.2.4. Chronology

The overall chronology of the HBEP is summarized in Figure 3.1. As previously mentioned, Task 1 was conducted from September 1978 through May 1979 and culminated with HBEP-01, the first draft of the program plan, and the first program review meeting. Tasks 2 and 3 were initiated in November 1979 with the agreement of the initial participants on the scope of those

---

(a) This had the effect of raising fuel temperatures 50 to 150°C relative to pure helium as a fill gas.

tasks. Task 2 was completed[a] in November 1987 with the issuance of the final version of HBEP-25. Task 3 was completed in January 1990 with the issuance of the final version of HBEP-60. Details on the actual chronology of the HBEP are contained in the BNW-prepared handouts for the review meetings (see listing in Appendix B).

3.3 FUEL TYPES AND OPERATIONAL HISTORIES

Fuel rods for the HBEP were both acquired from existing sources and fabricated for the program. There were three sources of rods for Task 2 and five sources of rods for Task 3. Rods were selected or fabricated to represent both PWR and BWR designs, variations of designs (e.g., annular versus solid pellets, rod fill gas pressure variations, grain size variations) and variations in operational histories.

3.3.1 Task 2 Rods and Rodlets

Fuel rods for Task 2 were acquired from three sources and had been irradiated in four different reactors. PWR rods were acquired from both British Nuclear Fuels Limited (BNFL) that had been irradiated in the BR-3 reactor and from Kraftwerk Union/Combustion Engineering (KWU/CE) that had been irradiated in the Obrigheim PWR. BWR rods were acquired from both KWU/CE that had been irradiated in the Würgassen BWR and from General Electric Co. (GE) that had been irradiated in the Monticello reactor. The characteristics of the Task 2 rods are summarized in Table 3.2.

3.3.1.1 BNFL PWR Rods

Twelve fuel rods manufactured by BNFL and irradiated in the BR-3 reactor located in Mol, Belgium were acquired and evaluated under Task 2A. A wide variety of fuel and rod designs were covered by the twelve 1-meter long rods. All rods contained solid pellets, though there were three primary variations of fuel density and ^{235}U enrichment. In addition, seven of the rods were pressurized (1.5 MPa helium) while five of the rods were non-pressurized (0.1 MPa helium) and two of the rods had annealed cladding rather than the

---

(a) Except for disposal of some rods and waste materials.

standard cold-worked cladding; a summary of the fuel and rod design features is provided in Table A.1.

These rods were irradiated in Assembly 373 during BR-3 cycles 3A, 3B, 4A, and 4B. Peak-in-life LHGR values occurred during the first irradiation cycle, with maximum local LHGR values exceeding 40 kW/m. Rod-average burnups ranged from 40 to 47 MWd/kgM with rod-average FGR values ranging from 3.2 to 10.7%. Plots of the irradiation histories are provided in Figure A.1.

Data obtained from sibling Assembly 366, irradiated in BR-3 during Cycles 3A and 3B, were also supplied to the HBEP; this data was reported in HBEP-25 (Section 8.1) and by Grimoldby and Crossley (1982).

3.3.1.2. KWU/CE PWR Rodlets

Twenty-one rod segments (rodlets) manufactured by KWU/CE and irradiated in the Obrigheim PWR were acquired and evaluated under Tasks 2A, 2B, and 2C. The rodlets had been irradiated in Obrigheim as part of seven-rodlet strings that were linked together to form a full-length rod; only rodlets from the central five positions of the rodlet strings were acquired for the HBEP. All rodlets contained solid pellets and there were two variations in fuel pellet diameter and pellet-cladding gap. Fifteen of the rodlets were nearly identical in design while the remaining six rodlets included three variations: Gd_2O_3 addition, large grain size, or low gas pressure. A summary of the fuel and rodlet design features is provided in Table A.2.

The fifteen "standard" rodlets were from three rodlet-strings, each of which was irradiated for either two, three, or four consecutive cycles, beginning with Obrigheim Cycle 8. This resulted in three rodlet groups with nominal rodlet-average burnups of 25, 35, and 45 MWd/kgM, respectively. Maximum local LHGR values occurred near the beginning of the irradiations and were in the range of 24 to 28 kW/m. Plots of the irradiation histories are provided in Figure A.2.

The six "variant" rodlets were from three additional rodlet-strings, all irradiated for three commercial cycles beginning with Obrigheim Cycle 8; rodlet-average burnups ranged from 30 to 36 MWd/kgM and rodlet-average FGR values ranged from 0.7 to 7.3%. Less variation in the LHGR history occurred for these rodlets, compared to the "standard" rodlets, except for the Gd_2O_3

rodlets; rodlet-peak LHGR values ranged from 24 to 30 kW/m. Plots of the irradiation histories are provided in Figure A.3.

Twelve of the "standard" rodlets were power-bumped in the High Flux Reactor (HFR) in The Netherlands. Rodlet-average terminal LHGR values ranged from 28 to 45 kW/m with hold periods of 48 or 191 hours at the peak LHGR level. Rodlet-average FGR values after bumping ranged from 12.2 to 55.8%; the three non-bumped sibling rodlets had rodlet-average FGR values of 1.3 to 26.0%.(a) A summary of the power-bumping irradiation conditions is listed in Table A.3.

3.3.1.3 KWU/CE BWR Rodlets

Four rod segments (rodlets) manufactured by KWU/CE and irradiated in the Würgassen BWR were acquired and evaluated under Tasks 2A and 2B. As with the PWR rodlets, the BWR rodlets were irradiated in seven-rodlet strings; all four HBEP rodlets were irradiated in the second position from the bottom of a rodlet-string. All rodlets were nominally identical; a summary of the fuel and rodlet design features is provided in Table A.4.

The four rodlets were irradiated in four different rodlet-strings for either three or four consecutive cycles, beginning with Würgassen Cycle 2. This resulted in rodlet-average burnups ranging from 28 to 34 MWd/kgM, respectively; rodlet-average FGR values ranged from 0.1 to 0.4%. Maximum local LHGR values occurred near the beginning of the irradiations and were in the range of 30 kW/m. Plots of the irradiation histories are provided in Figure A.4.

3.3.1.4 GE BWR Rodlets

Eight rod segments (rodlets) manufactured by GE and irradiated in the Monticello BWR were acquired and evaluated under Tasks 2A, 2B, and 2C. Four rodlets had been linked together to form a full-length rodlet-string for irradiation in the reactor; rodlets from the central two positions were acquired for the HBEP. All rodlets contained solid pellets and there were

---

(a) The nonbumped siblings from the 25 and 45 MWd/kgM groups had FGR in the expected range of 1 to 5%; the nonbumped sibling from the 35 MWd/kgM group had 26% FGR, thus implying high pre-bump FGR for the power-bumped rodlets from that group.

two variations in fuel pellet diameter and cladding inner diameter. A summary of the fuel and rodlet design features is provided in Table A.5.

The eight rodlets were from four rodlet-strings, all of which were irradiated for five consecutive cycles, beginning with Monticello Cycle 3. This resulted in rodlet-average burnups ranging from 24 to 34 MWd/kgM. Maximum local LHGR values occurred during the first half of the irradiations and were in the range of 18 to 20 kW/m. Plots of the irradiation histories are provided in Figure A.5.

Four of the rodlets were power-bumped in the R-2 reactor at Studsvik, Sweden. Rodlet-peak terminal LHGR values ranged from 36 to 45 kW/m with hold periods of 48 hours at the peak LHGR level. The power-bumped rodlets had rodlet-average FGR values of 2.6 to 5.2% while the non-bumped rodlets had rodlet-average FGR values of 0.2%. A summary of the bumping irradiation conditions is listed in Table A.6.

3.3.2 Task 3 Rods

Task 3 rods were acquired from five sources and were irradiated in two different reactors. All PWR-type rods were irradiated in the BR-3 reactor and were acquired from Fragema/CEA (FGA/CEA), BN, Westinghouse Electric Co. (WEC), or were fabricated for the HBEP. The commercial BWR rods were acquired from Teollisuuden Voima Oy (TVO) and were irradiated in the TVO-1 reactor. The Task 3 rods are summarized in Table 3.3.

3.3.2.1 FGA/CEA PWR Rods

Three fuel rods manufactured by CEA for FGA/CEA and irradiated in the BR-3 reactor were acquired and evaluated under Task 3. All three of the 1-meter-long rods contained annular pellets; the principal difference between rods was the initial fill gas pressure. A summary of the fuel and rod design features is provided in Table A.7.

The FGA/CEA rods were irradiated during BR-3 Cycles 4B through 4D2. Peak-in-life LHGR values occurred during the first and third operating cycles, with maximum rod-average LHGR values being approximately 23 kW/m. Rod-average burnup values ranged from 51 to 69 MWd/kgM with rod-average FGR values ranging from 1.4 to 3.8 %. Plots of the irradiation histories are provided in Figure A.6.

3.3.2.2 BN PWR Rods

Six fuel rods manufactured by FBFC for BN and irradiated in the BR-3 reactor were acquired and evaluated under Task 3. All six of the 1-meter-long rods contained solid pellets and were essentially identical in design. A summary of the fuel and rod design features is provided in Table A.8.

The BN rods were irradiated during BR-3 Cycles 4B, 4C, and 4D2. Peak-in-life LHGR values occurred during the first operating cycle, with maximum rod-average LHGR values being approximately 27 kW/m. Rod-average burnup values ranged from 41 to 56 MWd/kgM with rod-average FGR values ranging from 1.7 to 4.0%. Plots of the irradiation histories are provided in Figure A.7.

3.3.2.3 WEC PWR Rods

Three fuel rods manufactured by FBFC for WEC and irradiated in the BR-3 reactor were acquired and evaluated under Task 3. One of the 1-meter-long rods contained solid pellets, the other two rods contained annular pellets. A summary of the fuel and rod design features is provided in Table A.9.

The WEC rods were irradiated during BR-3 Cycles 4A through 4C. Peak-in-life LHGR values occurred during the first operating cycle, with maximum rod-average LHGR values ranging from 18 to 20 kW/m. Rod-average burnup values ranged from 42 to 46 MWd/kgM with rod-average FGR values ranging from 0.3 to 0.5%. Plots of the irradiation histories are provided in Figure A.8.

3.3.2.4 Original Task 3 PWR Rods

Sixteen fuel rods manufactured for the HBEP and irradiated in the BR-3 reactor were retained under Task 3 following the discovery of the two fabrication anomalies. Four principal design differences were represented by the sixteen rods. Five rods had standard solid pellets with high fill gas pressure, five rods had standard solid pellets with low fill gas pressure (to simulate a BWR pressure), three rods had standard annular pellets with a moderately high fill gas pressure, and three rods had large-grain solid pellets(a) with high fill gas pressure. The matrix was designed to study the effects upon fission gas release of solid versus annular pellets, high versus

(a) The large grains were formed by the addition of 0.46 wt% Nb_2O_5.

low fill gas pressure, and standard versus large-grain fuel. A summary of the fuel and rod design features is provided in Table A.10.

The original Task 3 rods were irradiated during BR-3 Cycles 4C through 4D2. Peak-in-life LHGR values occurred during the first operating cycle, with maximum rod-average LHGR values being approximately 30 kW/m. Rod-average burnup values ranged from 25 to 62 MWd/kgM with rod-average FGR values ranging from 2.5 to 11.3%. Plots of the irradiation histories are provided in Figure A.9.

3.3.2.5 TVO-1 Commercial BWR Rods

Nine commercial BWR fuel rods manufactured by ABB ATOM[a] and irradiated in the TVO-1 reactor were acquired and evaluated under Task 3. All nine of the full-length (3.7 m) rods were typical ABB ATOM commercial BWR rods (solid pellet, 0.4 MPa fill gas pressure). A summary of the fuel and rod design features is provided in Table A.11.

The TVO-1 rods were irradiated for a total of five or six cycles during TVO-1 Cycles 2 through 7. Peak-in-life LHGR values occurred during the first and third operating cycles, with maximum rod-average LHGR values being approximately 18 to 27 kW/m. Rod-average burnups ranged from 44 to 50 MWd/kgM with rod-average FGR values ranging from 0.3 to 16.7%. Plots of the irradiation histories are provided in Figure A.10.

(a) Formerly ASEA-ATOM.

TABLE 3.1. HBEP Subcontractors(a)

Subcontractor	Activity
ABB ATOM	preirradiation characterization and irradiation history data for Task 3 TVO-1 rods
BN/CEN	1) BR-3 irradiations 2) supplied Task 3 fuel rods 3) shipments of Task 3 rods between Mol an WNL
ECN	1) axial gamma scanning of Task 2 power bumped KWU/CE PWR rodlets 2) postirradiation examinations of Task 2 HFR-bumped rodlets
FBFC/BNFL	manufacture of original Task 3 fuel and rods
FGA/CEA	supplied Task 3 fuel rods
GE	1) supplied and shipped Task 2 rodlets 2) postirradiation examinations of Task 2 rodlets
JRC	nondestructive examination and power bumping of Task 2 KWU/CE PWR rodlets
KWU	nondestructive examination of Task 2 KWU/CE rodlets
KWU/CE	supplied Task 2 rodlets
Risø	XRF on Task 3 fuel cross-sections
Studsvik	power bumping of Task 2 GE rodlets
Transnubel	shipment of XRF fuel cross-sections from WNL to Risø
TVO	supplied Task 3 fuel rods
WEC	supplied Task 3 fuel rods
WNL	postirradiation examinations of Tasks 2 and 3 fuel rods
Transnuclear	shipping of TVO-1 rods

(a) Characterization examinations on nonirradiated archive fuel pellets, and SEM/EPMA examinations on fuel sections from power-bumped Task 2 Rodlet 5D17-4, were performed at BNW.

TABLE 3.2. Summary Characteristics of Task 2 Rods

Rod/ Rodlet	Source	Task[a]	Rod-Average Burnup, MWd/kgM	Peak-Pellet Burnup, MWd/kgM	FGR, %	Type
DF	BNFL	2A	47.4	58.0	3.9	high pressure
BK	BNFL	2A	47.2	57.8	4.0	high pressure
AK	BNFL	2A	41.5	51.2	3.9	high pressure
AU	BNFL	2A	43.5	53.0	3.4	high pressure
AP	BNFL	2A	40.0	49.0	4.7	high pressure
BN	BNFL	2A	44.1	52.9	3.2	annealed cladding
BW	BNFL	2A	44.3	53.1	7.3	annealed cladding
DE	BNFL	2A	41.5	51.4	10.7	low pressure
AL	BNFL	2A	46.5	57.0	6.3	low pressure
BH	BNFL	2A	40.8	50.3	7.3	low pressure
CQ	BNFL	2A	42.8	52.1	6.1	low pressure
BP	BNFL	2A	42.0	47.6	6.3	low pressure
D198	KWU/CE	2C	22.6	(b)	45.9	standard
D199	KWU/CE	2C	24.9	(b)	47.9	standard
D200	KWU/CE	2C	25.2	(b)	38.2	standard
D201	KWU/CE	2C	25.2	(b)	25.5	standard
D202	KWU/CE	2A	24.4	(b)	4.1	standard
D205	KWU/CE	2C	32.5	(b)	48.3	standard
D206	KWU/CE	2C	35.1	(b)	55.8	standard
D207	KWU/CE	2C	35.4	(b)	53.8	standard
D208	KWU/CE	2C	35.3	(b)	31.8	standard
D209	KWU/CE	2A	34.7	(b)	26.0	standard
D219	KWU/CE	2C	41.7	(b)	33.2	standard
D226	KWU/CE	2C	45.1	(b)	44.1	standard
D227	KWU/CE	2C	45.6	(b)	24.4	standard
D220	KWU/CE	2C	45.6	(b)	12.2	standard
D228	KWU/CE	2B	43.7	(b)	1.3	standard
D244	KWU/CE	2A	30.7	(b)	2.1	Gd_2O_3 added
D245	KWU/CE	2A	29.7	(b)	(c)	Gd_2O_3 added
D267	KWU/CE	2B	33.1	(b)	0.8	large grain
D268	KWU/CE	2B	31.6	(b)	0.7	large grain
D346	KWU/CE	2B	36.3	(b)	7.3	low pressure
D347	KWU/CE	2B	34.9	(b)	7.1	low pressure
S26H	KWU/CE	2A	28.3	(b)	0.3	standard
S34H	KWU/CE	2A	27.9	(b)	0.1	standard
S17W	KWU/CE	2B	34.1	(b)	0.4	standard
S24W	KWU/CE	2B	33.8	(b)	0.3	standard
8D10-2	GE	2A	28.9	30.6	0.1	standard
8D10-1	GE	2C	31.4	33.2	5.2	standard
0A07-3	GE	2A	24.0	25.2	0.1	standard
0A07-1	GE	2C	26.8	28.2	(d)	standard
5D17-4	GE	2C	32.2	34.2	5.2	standard
5D04-3	GE	2B	33.5	34.6	0.2	standard
8D14-3	GE	2C	30.3	32.6	2.6	standard
8D14-2	GE	2B	32.1	33.8	<0.2	standard

(a) Task 2A and 2B rodlets were commercially irradiated; Task 2C rodlets were power bumped following their commercial irradiation.
(b) For the KWU/CE PWR and BWR rodlets, rod-average and peak-pellet burnup differed by ≤5% because of the flat axial profile; therefore, no differentiation was made between rod-average and peak-pellet burnup values.
(c) No fission gas recovered; measuring chamber leakage suspected.
(d) Rodlet failed during bumping irradiation.

TABLE 3.3. Summary Characteristics of Task 3 Rods

Rod/ Rodlet	Source	Rod-Average Burnup, MWd/kgM	Peak-Pellet Burnup, MWd/kgM	FGR, %	Type
BR-3 Rods					
BK370	FGA/CEA	50.9	62.0	1.4	annular, high pressure
BK363	FGA/CEA	66.7	79.2	3.8	annular, moderate pressure
BK365	FGA/CEA	69.4	83.1	2.4	annular, high pressure
3-74	BN	41.5	53.5	3.2	standard
3-89	BN	41.7	51.2	4.0	standard
3-86	BN	54.7	67.2	1.7	standard
3-128	BN	56.1	68.2	2.6	standard
3-138	BN	55.8	69.2	2.6	standard
3-337	BN	54.6	68.0	1.9	standard
01-7-A	WEC	46.1	55.0	0.5	solid-pellet
03-8-C	WEC	43.3	51.9	0.3	annular-pellet
08-8	WEC	42.4	51.1	0.3	annular-pellet
BSH-01	HBEP	25.0	30.9	8.6	standard
BSH-06	HBEP	59.8	72.2	8.4	standard
BSH-08	HBEP	54.2	64.5	6.5	standard
BSH-11	HBEP	52.2	62.6	4.3	standard
BSH-12	HBEP	50.2	60.2	4.1	standard
BSM-21	HBEP	25.3	31.1	9.6	low pressure
BSM-25	HBEP	55.8	66.0	8.5	low pressure
BSM-27	HBEP	56.9	67.3	7.1	low pressure
BSM-29	HBEP	49.1	60.2	3.3	low pressure
BSM-30	HBEP	53.7	65.3	5.2	low pressure
BAH-41	HBEP	28.6	34.3	3.3	annular-pellet
BAH-50	HBEP	61.0	72.2	2.5	annular-pellet
BAH-51	HBEP	62.4	74.1	(a)	annular-pellet
BLH-61	HBEP	27.3	33.2	11.3	large grain
BLH-64	HBEP	52.2	62.5	6.2	large grain
BLH-65	HBEP	50.3	56.5	5.6	large grain
TVO-1 Rods					
H8/36-6	TVO	44.6	51.4	11.2	standard
F1/3-6	TVO	45.9	51.8	12.7	standard
A1/8-6	TVO	44.9	50.9	3.4	standard
E8/27-6	TVO	43.7	49.5	1.0	standard
H8/36-4	TVO	46.6	54.9	17.3	standard
A3/6-4	TVO	47.8	54.9	1.0	standard
A1/8-4	TVO	48.5	55.5	0.3	standard
H5/27-4	TVO	45.5	52.4	6.6	standard
E8/27-4	TVO	45.5	52.4	6.2	standard

(a) Cladding apparently breached during postirradiation handling.

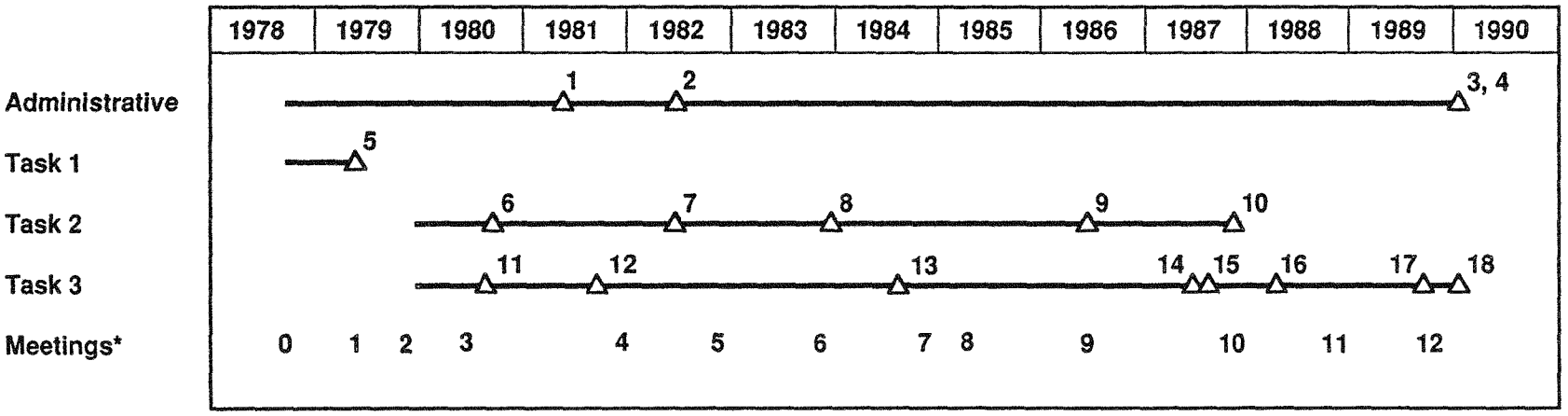

Administrative

1-Final Version (Revision 3) of Program Plan Completed
2-All Participant Agreements Signed
3-Final Version of HBEP-61 Issued
4-HBEP Completed

Task 1

5-Task 1 Completed

Task 2

6-Irradiation of Task 2 BNFL Rods Completed
7-Irradiation of Task 2 KWU/CE Rods Completed
8-Irradiation of task 2 GE Rods Completed
9-Task 2 PIE Completed
10-Final Version of HBEP-25 Issued

*See Table B.3.

Task 3

11-Design and Fabrication of Task 3 HBEP Rods Completed
12-Irradiation of Task 3 Rods Begun
13-Standard PIE of Task 3 1-Cycle Rods Completed
14-BR-3 Irradiations Completed
15-TVO-1 Rods Shipped to WNL
16-Shipment of All Task 3 Rods to WNL Completed
17-Task 3 PIE Completed
18-Final Version of HBEP-60 Issued

38909107.2

FIGURE 3.1. Chronology of the HBEP

4.0 MAJOR TECHNICAL FINDINGS

The principal emphasis of the HBEP was on fission gas release occurring at high burnup levels. The focus was on the ability to adequately account for enhancement in fission gas release caused by mechanisms associated strictly with burnup level, if indeed it occurred.(a) Presented in this section is a summary of the technical findings on rod-average FGR for both normal operation and bumping irradiations, results of the special examinations and identification of the rim effect, and finally a comparison of the HBEP data set to other available data.

Two general objectives were identified at the beginning of the HBEP. In general, the first objective was to obtain modeling-quality data related to the release of fission gas at high-burnup levels. This objective was met by a) characterizing non-irradiated archive fuel specimens, b) obtaining detailed LHGR histories and deriving best-estimate temperature histories using the GT2R2 code (Cunningham and Beyer 1984); see HBEP-25 and HBEP-60, c) obtaining FGR data from rods ranging in rod-average burnup level from 23 to 70 MWd/kgM (peak-pellet burnup levels ranging from 23 to 83 MWd/kgM) that were subjected to a variety of operating histories, and d) obtaining extensive PIE data ranging from basic nondestructive examinations to detailed radial profiles of fission product retention. The second objective was to develop a model that would account for the observed fission gas release at high-burnup levels. This objective was subsequently modified to focus on a) identifying burnup-related effects in the fuel, b) identifying correlations between fuel microstructure, xenon retention, and fuel temperature, and c) quantifying the release of fission gas from the rim region. An empirical correlation relating athermal release of matrix-retained xenon from the rim region to pellet-edge burnup was developed.

(a) The assumption being that changes in the fuel at high burnup levels could affect the FGR relative to FGR levels predicted based upon data obtained at low burnup levels.

4.1 FISSION GAS RELEASE DURING NORMAL OPERATION

Rod-average fission gas release[a] for the non-bumped rods[b] examined as part of the HBEP is presented as a function of rod-average burnup in Figure 4.1.[c] However, while the format of Figure 4.1 is convenient for presenting the data, it is not fully useful for evaluating the data because it does not reflect nor account for the variety of fuel designs and thermal histories that are represented. Therefore, the effect of design and operational variables upon FGR will be the focus the following discussion. The high burnup "rim effect" is discussed separately in Sections 4.3.1, 4.4, and 4.5.4.

4.1.1 Linear Heat Generation Rate

Thermally-induced fission gas release is principally dependent on the level of fuel temperature, which is in turn dependent on LHGR and fuel/rod design. In general, FGR can be expected to increase with increasing fuel temperature (in the thermally-driven regime above a temperature threshold). To evaluate this expectation, rod-average FGR as a function of lifetime-average rod-average LHGR is presented in Figure 4.2 for the rods irradiated in BR-3. Maximum LHGR values typically occurred during the first irradiation cycle.

FGR values from the lower LHGR level Task 3 rod groups (FGA/CEA and WEC rod groups, symbols F and W in Figure 4.2a) show no strong correlation with LHGR while the higher LHGR level Task 3 BN rods generally exhibit increasing FGR with increasing LHGR (symbol B in Figure 4.2a). There is no clear trend for the Task 2 BNFL rods (symbol N in Figure 4.2a). The lack of an apparent trend relating FGR with LHGR for the Task 2 BNFL rods is likely due to three causes: first, there is a variety of fuel/rod designs within the Task 2 BNFL rod group which affect fuel temperature and, thus, FGR; second, compared to

---

(a) The total fission gas release for the rod as measured during postirradiation examination.

(b) Because the FGR for the power-bumped rods was principally a function of the bumping irradiations (see Section 4.2), those data are not included in Figure 4.1.

(c) Because of the fabrication anomalies of the original Task 3 fuel rods, throughout this section the presentation of data obtained from those rods has been separated from data obtained from the other rods.

the Task 3 rods, LHGR values for the BNFL rods were greater during the first irradiation cycle and significantly lower during the subsequent cycles, thus the lifetime-average rod-average LHGR value is not as representative of the entire irradiation history for the Task 2 BNFL rods as for the Task 3 rods; and third, fuel-cladding contact during the peak LHGR period was likely, thus minimizing fuel temperature and FGR differences among the BNFL rods.

Fission gas release values for the Task 3 BWR rods (TVO-1) correlated with position within the fuel assembly; i.e., FGR tended to decrease with increasing distance of the rods from the control blade. Because movement of the control blade can produce local LHGR variations along the length of the rods, the larger FGR from rods closest to the control blade was attributed to the effects of the local LHGR variations.

Original Task 3 Rods - A trend of increasing FGR with increasing irradiation-average LHGR for the original Task 3 rods (Figure 4.2b) is apparent. The BAH rods, with lower fuel temperatures at equivalent LHGR levels, had less dependence of FGR upon LHGR level.

4.1.2 Quantity of Fill Gas

The release of fission gas from the fuel to the rod fill gas affects fuel temperature and thermally-dependent FGR by changing the fill gas composition and thermal conductivity. For any specific quantity of released fission gas, the thermal effect of the released fission gas will be reduced as the initial volume of helium fill gas is increased. The volume of helium fill gas may be increased by increasing either, or both, the initial helium pressurization level and the rod void volume.

For the HBEP rods, the Task 2 BNFL rods had two different initial pressurization levels, and thus differing initial volumes of helium, while other design parameters remained the same. Differences in FGR due to the different initial pressurization levels are illustrated in Figure 4.3, where it may be seen that the Task 2 BNFL rods with a higher initial helium pressurization level (symbol o) had the lower FGR for a given irradiation-maximum LHGR value.

Original Task 3 Rods - The effect of initial helium pressurization was to be studied by comparing the BSH and BSM rod types from the original Task 3 rods;

the BSH rods having the higher initial pressurization and, thus, the greater quantity of helium. However, sufficiently high fission gas release generally occurred in both rod types so that EOL gas thermal conductivities were approximately equal for both. Therefore, operating fuel temperatures were similar for both rod types and, as a result, FGR levels were similar for both rod types. No measured data are available to indicate whether the onset of significant degradation of fill gas thermal conductivity for the BSH rods was delayed relative to the BSM rods.

4.1.3 Fuel Pellet Design

For a given LHGR value, annular-pellet fuel rods are expected to operate at lower fuel temperatures and have lower FGR than solid-pellet fuel rods; this is particularly expected to occur where the fuel is operating above the athermal release temperature range. Annular-pellet versus solid-pellet behavior can be directly compared for one Task 3 rod group, i.e., the WEC rods. The difference in FGR between the solid-pellet and annular-pellet WEC rods was minimal; 0.5% versus 0.3%, respectively. These rods operated at low LHGR levels and temperatures (see Section 3.1.3 of HBEP-60); therefore, the FGR was primarily athermal, i.e., recoil release, and the FGR difference is probably not significant.

Original Task 3 Rods - The BSH and BAH rod types of the original Task 3 rods, while having different pellet designs, had equal volumes of initial fill gas; therefore, the principal difference was the presence (or absence) of an annulus. As illustrated in Figure 4.4, the solid-pellet rods had the higher FGR. For equivalent LHGR values, the FGR values for the BAH rods (symbol A) are approximately 1/3 those of the BSH rods (symbol H). The lower FGR values for annular-pellet rods are likely due to one principal factor: the annular-pellet rods, at equivalent LHGR levels, operate at lower fuel temperatures because of the shorter heat transfer distance.

4.1.4 Fuel Grain Size

Increasing the fuel grain size is postulated to reduce fission gas release by increasing the average diffusion distance to the fuel grain

boundary. The large-grain (true grain size[a] of 48 μm) Task 2 rodlets (D267 and D268) had significantly lower FGR than similarly designed standard-grain (true grain size of 10 μm) Rodlet D202; i.e., 0.8% versus 4.1% FGR, respectively. The large-grain and standard-grain rodlets were operated at approximately the same LHGR values (compare Figures A.2 and A.3) with the standard-grain rodlet having operated at slightly higher maximum LHGR levels than the large-grain rodlets, while the large-grain rodlets were irradiated to a higher burnup level than the standard-grain rodlet. The differences in operation are not a likely cause for the significant difference in FGR, thus indicating the possibility that the grain size differences were a factor in the FGR differences.

Original Task 3 Rods - The BSH (standard-grain) and BLH (large-grain) rod types of the original Task 3 rods were intended to investigate the effect of fuel grain size; true grain sizes were 16 and 78 μm, respectively. Fission gas release data as a function of irradiation-average rod-average LHGR for the two rod types are presented in Figure 4.5. No clear difference in FGR between the standard-grain (symbol H), and the large-grain (symbol L), rod types is evident. This conclusion should be moderated by noting that a) thermal feedback occurred in the 3-cycle rods resulting in increased fuel temperatures and FGR; and b) the Nb_2O_5 addition used to enhance large grain formation may also have resulted in an increase in the diffusion rate of the fission gas in the large-grain size fuel relative to the standard-grain size fuel (Franklin, Djurle, and Howl 1985; Une, Tanabe, and Oguma 1988).

4.1.5 Effect of Fuel Fabrication Anomalies Upon FGR for Original Task 3 Rods

The original Task 3 rods were fabricated with two inadvertent anomalies: argon contamination of the initial fill gas and fuel enrichment microheterogeneities.[b] The rods acquired from BN to supplement Task 3 were nearly identical in design to the original Task 3 rods, but did not have the

---

(a) True grain size is defined as the as-measured linear intercept value multiplied by 1.57.

(b) The fuel pellets in the original Task 3 rods were produced from mechanically blended fractions of 89.4% and 3.0% ^{235}U enriched UO_2 powders. As a result, small 89.4% ^{235}U enriched particles or islands, up to 100 μm in diameter, existed in the as-sintered pellets.

anomalies and, thus, may be used to help determine the possible effects of the anomalies on the FGR for the original Task 3 rods. Fission gas release data for the standard fuel rods from the two rod groups are compared in Figure 4.6. At equivalent irradiation-average LHGR levels, the BN rods (symbol B) clearly had lower FGR than the original Task 3 BSH rods (symbol H). Although the BSH rods had somewhat higher early-in-life LHGR values than the BN rods, the difference in FGR is likely due to the as-fabricated differences between the two rod types. In particular, the presence of argon in the fill gas of the original Task 3 rods would increase fuel temperatures relative to the BN rods and, thus, would be expected to increase FGR relative to the BN rods. It is also conjectured that increased localized fuel temperatures associated with the enrichment microhetero-geneities may have contributed to the higher levels of FGR for the BSH rods relative to the BN rods; however, it is difficult to quantify the effect of the enrichment microheterogeneities.

4.1.6 Predicted and Measured FGR

Fission gas release for the HBEP rods was predicted using the ANS-5.4 (NRC 1982) fission gas release model with modified diffusion coefficients (Beyer and Meyer 1976) and the best-estimate temperature histories.(a) Predicted and measured FGR values for the non-bumped Task 2 and Task 3 HBEP rods and rodlets are compared in Figures 4.7 and 4.8, respectively.

For the moderate burnup level Task 2 rods (Figure 4.7), the predicted FGR values generally lie within an acceptable factor of 2 (as indicated by the dashed lines) for rods having less than 10% FGR. However, the predicted values tend to be less than the measured values. The generally good agreement between the measured and predicted FGR values for the Task 2 rods indicates that the modified ANS-5.4 FGR model adequately predicts the FGR for these rods to rod-average burnup values of 47 MWd/kgM.

(a) See HBEP-25 and HBEP-60 for details of how best estimate temperature histories and FGR predictions were obtained. For most rods, modifications to the assumed LHGR history, and some fuel behavior models (for example, rate of fuel swelling) were made; significant modifications were required for some Task 3 rods to obtain temperature histories that appeared to be appropriate for the observed end-of-life conditions of the rods.

For the higher burnup level Task 3 rods, the rod-average FGR was generally underpredicted for the lower temperature rods; i.e., the annular-pellet FGA/CEA rods and the 2-cycle BN rods. A likely cause of underprediction for the FGA/CEA rods is the effect of the particular microstructure and porosity in these rods that is not accounted for by the ANS-5.4 model. Particularly for the Task 3 rods, it may be concluded that the non-modified GT2R2/ANS-5.4 combination was not adequate to model the measured fission gas release at high burnup levels.

Original Task 3 Rods - Measured and predicted rod-average FGR values for the original Task 3 rods are compared in Figure 4.9. Fission gas release was underpredicted for a significant number of rods, particularly for those rods that might have been expected to have operated at lower temperatures (BSH, BAH, and BLH rod types). The likely cause of the underprediction is the inability of the ANS-5.4 model to account for the athermal FGR from the rim region, the possible effects of the enrichment microheterogeneities, and the effect of the Nb_2O_5 addition on gas diffusion rates in the large grain fuel pellets.

4.1.7 Cladding Waterside Corrosion and Fuel-Cladding Bonding

Cladding waterside corrosion is also related to high burnup operation of LWR fuel rods. The cladding waterside corrosion was evaluated by both visual examination and measurement of oxide thickness.(a) For the PWR-type rods irradiated in the BR-3 reactor, the oxide layer was generally uniform and had a thickness ranging from 4 to 10 μm. It should be noted that the rods irradiated in BR-3 were exposed for a shorter period of time and to lower coolant temperatures than what would be typical for commercial PWR rods of equivalent burnup levels. Cladding waterside corrosion on the standard BWR rods irradiated in TVO-1 consisted of a base oxide layer plus nodules. The base oxide layer was up to 30 μm thick; the nodules had a mean thickness up to 55 μm, with a maximum observed nodule thickness of 120 μm.

Fuel-cladding bonding and cladding interior surface oxidation was also observed and recorded. For the PWR-type rods irradiated in BR-3, fuel-

---

(a) Thickness was measured on 500X magnification photos of fuel cross sections taken during optical microscopy.

cladding bonding was not observed for the majority of the rods; the exception being the original Task 3 rods. Similarly, areas of enhanced cladding interior surface oxidation were observed only for the original Task 3 rods; these areas were generally associated with the presence of a high-enriched fuel particle. Some patchy areas of cladding interior surface oxidation were observed for some of the other rods irradiated in BR-3. The BWR rods irradiated in TVO-1 had open fuel-cladding gaps and no indications of fuel-cladding bonding were found. Cladding interior surface oxidation was generally less than 10 μm thick.

4.2 FISSION GAS RELEASE DURING POWER-BUMPING

As part of Task 2, twelve PWR rodlets and four BWR rodlets were power-bump tested at the end of their steady-state irradiations. Fission gas release was directly measured after the bumping irradiations, and for the PWR rodlets, analysis of ^{85}Kr activity in the plenum region was used to non-destructively evaluate FGR before and after the bumping irradiations.

4.2.1 Net FGR During Bumping Irradiations

Net FGR during the bumping irradiations is presented as a function of peak LHGR level in Figure 4.10. For the PWR (KWU/CE) rodlets, the net FGR was evaluated from pre- and post-bump analyses of the ^{85}Kr activity in the fuel rodlet plenums. For the BWR (GE) rodlets, the net FGR was assumed to be equal to the post-bump measured FGR; this was because of the low FGR measured for the sibling non-bumped rodlets. Several observations are possible based on the data presented in Figure 4.10 (trend lines are provided in the figure):

- The 45-MWd/kgM PWR rodlet group released more fission gas during the bumping irradiation, as a function of LHGR, than the 25 MWd/kgM PWR rodlet group.
- The 35-MWd/kgM PWR rodlet group released less fission gas during the bumping irradiation than the other two PWR rodlet groups.
- Within each rodlet group, rodlets with long hold periods (approximately 190 h) at the peak LHGR level generally released more fission gas than rodlets with shorter hold periods (48 h).

- Net-bumping FGR[a] increases approximately linearly with peak LHGR during the bumping irradiation, with an apparent LHGR threshold (LHGR intercept for zero net bumping FGR) for FGR during power-bumping between 25 kW/m and 30 kW/m.

The difference in net-bumping FGR between the 35 MWd/kgM PWR rodlet group and the 25 and 45 MWd/kgM PWR rodlet groups has been attributed to the differences in FGR that existed for the rodlets at the end of the steady-state irradiation (see HBEP-25). In essence, the 35 MWd/kgM rodlet group had much greater FGR during the steady-state irradiation and thus, had already released much of the gas that would have been released during the bumping irradiation.

The BWR rodlets had much less FGR during the bumping irradiations than the PWR rodlets. This was attributed to three principal factors (see HBEP-25):

- Differences in the axial power profiles during the bumping irradiations. Because of differences in rod lengths, the GE rodlets had a greater peak-to-average LHGR ratio than the KWU/CE rodlets, i.e., 1.40 versus 1.09, respectively. Thus, for equal peak LHGR during the bumping irradiation, the GE rodlets had lower rod-average LHGR levels.
- Differences in the fuel radial temperature profile due to differences in the cladding surface temperature and heat flux. Cladding surface temperatures for the GE and KWU/CE rodlets were 264°C and 338°C, respectively. Because of their larger diameter, the GE rodlets had a lower heat flux across the fuel-cladding gap. As a result, at equal LHGR levels, the GE rodlets had a fuel pellet surface temperature approximately 100°C lower than the KWU/CE rodlets and, thus, lower temperatures throughout the fuel pellet.
- Differences in the prebump inventories of retained fission gas within the fuel because of differences in the prebump LHGR and fuel temperature histories. The fission gas in the BWR fuel was still largely retained

---

(a) Net-bumping FGR is considered to be the FGR that occurs only during the bumping irradiation.

within the fuel matrix and, therefore, not as "easily" released to the rodlet free volumes compared to the PWR rodlets which likely had substantial amounts of fission gas stored on the grain boundaries at the time of the bumping irradiation.

It is also postulated that differences in the application and release of hydrostatic stresses could account for the observed differences between the PWR and BWR fuels.(a)

During the planning for the power-bump testing of selected rodlets it was assumed that a 48-h hold period would be sufficient to achieve near-equilibrium FGR (see Freshley 1981). Additional power-bump irradiations using a 190-h hold period were included as a check on this premise. As shown from the data presented in Figure 4.10, extending the hold period from 48 h to 190 h resulted in the release of additional fission gas indicating that the 48-h hold period was not sufficient to achieve equilibrium FGR at these heat ratings.(b)

Thus, the HBEP power-bumping irradiations a) confirmed a dependency of FGR on LHGR level, b) showed an increase in FGR (at equal LHGR levels) as burnup level increased, and c) showed an increase in FGR as the hold times increased from 48 to 190 h at the LHGR levels tested.

4.2.2 ^{85}Kr Analysis of Fission Gas Release

Nondestructive analysis of FGR, based on measuring the activity of ^{85}Kr in rod and rodlet plenums, was performed on the bumped PWR rodlets in Task 2 and the commercial BWR rods in Task 3.(c) A comparison of ^{85}Kr-predicted and puncture-measured FGR values is presented in Figure 4.11. In general, the non-destructive ^{85}Kr method provided good estimates of the rod-average FGR.

(a) Paper presented by S. Gehl, EPRI, during the workshops conducted in conjunction with the HBEP Program Meeting held June 9-10, 1986 in Wengen, Switzerland. Also, see Knudsen et al. (1988).

(b) A recent paper by Knudsen et al. (1988) reached the conclusion that hold periods in excess of 86 h can be necessary to achieve equilibrium FGR at a peak bumping LHGR of 40 kW/m.

(c) These measurements were made on separate equipment but using similar analyses.

4.3 FUEL MICROSTRUCTURE AND FISSION PRODUCT RETENTION

To help illuminate the relationship between fuel microstructure and local retention of fission products, three special postirradiation examinations were performed in addition to the standard postirradiation examinations (visual, rod puncture and gas analysis, ceramography). The special examinations included electron probe microanalysis (EPMA) and x-ray fluorescence (XRF) for radial profiles of retained fission products and scanning electron microscopy (SEM) to supplement the optical microscopy examinations of the fuel microstructure. See Appendix C for a brief explanation of each of these analytical techniques and their limitations. Several observations/conclusions were reached relative to fuel microstructure and fission product retention/release; they are discussed in the following.

4.3.1 Development of Fuel Rim Region

The fuel pellet periphery is a region of very high local burnup.(a) This region, for high burnup rods, is often characterized by high concentrations of porosity, loss of definable grain structure, and depletion of xenon from the UO_2 matrix (as measured by EPMA). Actual loss of xenon from the rim region is more questionable, as illustrated by XRF data which indicate little or no loss of total xenon from the rim region (see HBEP-60). This region is termed the "rim region" and the change in microstructure, transfer of matrix xenon to the porosity, and potential release of xenon from this region are characteristic of the "rim effect." An example of the microstructure in the rim region is provided as Figure 4.12.

The development of the fuel rim region can be evaluated, as a function of pellet-edge burnup, by measuring the rim region thickness, and the rim region matrix retention of xenon. Assuming a simple linear dependence and extrapolating the data to the burnup level of no observable effect, a threshold burnup level may be defined for the onset of observable rim region effects.

(a) Pellet-edge burnup (depending on fuel enrichment, pellet diameter, neutron spectrum, and general burnup level) is commonly a third, or more, greater than the pellet-average burnup. Pellet-edge burnup was evaluated from the EPMA-determined radial profiles of neodymium concentration.

The thickness of the fuel rim region was estimated from both optical microscopy (500X magnification) and SEM (200X to 4400X magnification), and from the radial profiles of matrix-retained xenon. The increase in rim region thickness with increasing pellet-edge burnup is illustrated in Figure 4.13. It is noted that the thickness of the rim region is generally greater when defined by the EPMA data than by the optical data. This difference is conjectured to be due to changes in the fuel matrix that were not observed optically but which resulted in the loss of matrix xenon. However, both sets of data extrapolate to a similar threshold burnup level.

The EPMA data was also used to estimate the depletion of matrix-retained xenon from the rim region; increasing depletion (decreasing retention) of matrix xenon with increasing pellet-edge burnup is illustrated in Figure 4.14. Extrapolating the data in either Figures 4.13 or 4.14 to zero rim thickness shows that the threshold burnup level for the onset of the rim effect is estimated to be in the 50 to 60 MWd/kgM range at the pellet-edge, i.e., outside surface.

4.3.2 Correlation Between GBBPR and XRD

Correlations exist between microstructural features and xenon retention. One such correlation is the radial extent of the grain boundary bubble network (also referred to as the grain boundary bubble precipitation radius - GBBPR) and the radial extent of matrix depletion of xenon (also referred to as the xenon depletion radius - XDR). The GBBPR is determined visually at 500X magnification; the XDR is determined from a radial EPMA examination. These features are schematically defined in Figure 4.15. Grain boundary bubble precipitation radius as a function of XDR for the Task 3 rods is presented in Figure 4.16. The data in Figure 4.16 are scattered because of the difficulty in precisely defining the GBBPR and XDR. However, for all cases the GBBPR does not extend beyond the XDR.(a) A correlation between GBBPR and XDR was also observed for the Task 2 bumped KWU/CE PWR rodlets, as illustrated in Figure 4.17.

(a) Data for the FGA/CEA rods are not included in Figure 4.16. That is because for the FGA/CEA rods, no central or transition zone for xenon retention could be defined though an intergranular bubble network was observed for some cross-sections.

4.3.3 Effect of Fuel Grain Growth

It has been assumed that grain size must be doubled in order to obtain significant local FGR through grain boundary sweeping (HBEP-25). No correlation between a doubling of grain size and local FGR (as measured by EPMA and XRF) was discerned for the HBEP fuels. This is illustrated in Figure 4.18 in which the observed grain growth and EPMA-measured xenon retention for the bumped Task 2 PWR rodlets are overlayed. The nonbumped rods from Task 2 and the rods from Task 3 also showed no correlation between grain growth and the EPMA-measured xenon profiles.(a)

4.3.4 Correlation of Fuel Temperatures and Fuel Microstructure/Xenon Retention Features

Correlations between fuel temperatures and fuel microstructure/xenon retention features can be useful in developing models to predict high-burnup FGR. One principal correlation that was determined was for the GBBPR as a function of temperature. For the Task 2 bumped rodlets (both PWR and BWR), best-estimate temperature histories assigned a peak-in-life fuel temperature of approximately 1100°C to the GBBPR observed during PIE (see Tables 4.12 and 6.11 of HBEP-25). This temperature also applied to the XDR because the GBBPR and XDR were both observed to occur at approximately the same fuel radius. Therefore, it appears that significant fission gas release and microstructural changes, for rods that are power-bumped, occurs in fuel regions operated at temperatures in excess of 1100°C according to BNW's evaluation.

The correlation between fuel temperature and GBBPR was also observable for the Task 3 fuel rods. Estimated peak-in-life temperatures for the GBBPR varied from 1100 to 1300°C(b) (see Table 4.3 of HBEP-60). The range in temperature associated with the GBBPR is likely due to the difficulty in precisely defining the GBBPR combined with the rapid rate of change in fuel temperature with radius occurring in this region of the fuel. As with the

---

(a) For the TVO-1 rods, the onset of grain growth apparently correlates with the extent of the central region of xenon depletion. However, the maximum grain growth was only approximately 30% which is not expected to have a significant effect on local FGR.

(b) The annular-pellet FGA/CEA rods had GBBPR at estimated fuel temperatures of less than 1000°C.

Task 2 power-bumped rodlets, the XDR for the Task 3 fuel generally correlated with the GBBPR. Best-estimate temperatures for the XDR range from 900 to 1150°C (the annular-pellet FGA/CEA rods had no discernible XDR). Therefore, it appears that significant FGR and microstructural changes, for rods operated at steady-state as well as power-bumped, occurs in fuel regions operated at temperatures in excess of 1100°C according to BNW's evaluation.

4.3.5 Dark-Etch Rings

Etching of fuel cross-sections for optical microscopy often revealed zones that visually appeared much darker than other portions of the fuel cross-section; an example is provided in Figure 4.19. These "dark-etch" zones were usually in the form of circumferential rings of varying thickness and radius and correlated with high levels of intragranular porosity.

4.4 PREDICTION OF RIM REGION ATHERMAL FISSION GAS RELEASE

As has been discussed in the previous section, microstructural changes to the periphery of the pellet occur at high burnup levels and can be correlated with increasing burnup levels. These changes are manifested by an increase in porosity, loss of definable grain structure, and a transfer of xenon from the UO_2 matrix to the porosity. Correlations for the change in rim region width and the loss of matrix-retained xenon, both as a function of burnup, were developed to form the basis of an empirical correlation for the loss of matrix-retained xenon from the rim region (see HBEP-60).

The optically-determined rim region width, as a function of pellet edge burnup, may be defined as follows:

$$W = 2.19 \cdot (BU - 48.8); \; BU > 48.8$$

where W is the rim region width in μm and BU is the burnup at the pellet edge or outer surface in MWd/kgM. This correlation is a linear least squares fit to the data listed in Table 5.1 of HBEP-60.

Using the EPMA-determined radial profiles of matrix-retained xenon, the fractional loss of matrix xenon from the rim region may be defined as:

$$F_r = 0.00625 \cdot (BU - 62.2);\ BU > 62.2$$

where F_r is the fraction of xenon produced in the rim region that has been lost from the UO_2 matrix. This correlation is a linear least squares fit to the data listed in Table 5.1 of HBEP-60.

The above two terms may be combined to provide an empirical model to predict the fraction of total xenon produced in the pellet that is lost from the UO_2 matrix in the rim region. The model may be stated as:

$$R_r = V_r \cdot F_r \cdot P_r$$

where R_r is the loss of xenon from the UO_2 matrix in the rim region, expressed as a fraction of the total xenon production for the cross-section; V_r is the volume fraction of the pellet that is in the rim region (dependent on the rim width W); and P_r is the ratio of average xenon production in the rim region to average xenon production in the remainder of the fuel cross-section. Each of these terms is more fully discussed in HBEP-60. The term R_r overpredicts the actual amount of xenon lost from the rim region because not all xenon lost from the UO_2 matrix is released to the void volume in the rod. It is more likely that most of the gas is still contained in the rim region porosity.

4.5 COMPARISON OF HBEP DATA TO OTHER DATA SOURCES

The FGR data set from the HBEP compares well with other sources of well-qualified FGR data. Four areas of comparison are presented, i.e., steady-state FGR, transient FGR, fuel microstructure/xenon retention correlations, and onset of the rim effect.

4.5.1 Steady-State Fission Gas Release Comparisons

The TVO-1 rods, irradiated in a commercial BWR reactor, were observed to have a wide range of FGR values over a narrow range of rod-average burnup. However, the range of FGR data was not unusual when compared to FGR data from other ABB ATOM rods (Andersson et al. 1986), as illustrated in Figure 4.20. The HBEP FGR values fall within the range of the ABB ATOM data, even though the HBEP rods are at greater burnup levels. Two observations from

Figure 4.20 are worthy of note. First, the lower bound of the FGR data is apparently increasing with burnup level. This is interpreted as an indication of athermal FGR increasing with burnup level. Second, the upper bound of the FGR data is approximately constant with burnup level. This is interpreted to indicate no apparent burnup effect upon thermally activated or high temperature FGR.

For the nonbumped PWR-type rods, only three of the 49 rods had FGR values in excess of 10% (see Tables 3.2 and 3.3). In comparison, observed FGR values for commercially-irradiated full-length PWR rods are often less than 2% at rod-averaged burnup levels to 40 MWd/kgM (Pati and Garde 1985). A more recent compilation (Pati, Garde, and Clink 1988) showed FGR values less than 4% at rod-average burnup levels to 56 MWd/kgM. Because the HBEP PWR-type rods generally had higher rod-average LHGR values than commercial PWR rods, the generally higher FGR values for the HBEP PWR-type rods are not considered unreasonable.

Fission gas release data at the end of two cycles of irradiation from sibling BNFL fuel Assemblies 373 (Task 2) and 366 (data supplied to the HBEP) are compared as a function of lifetime-maximum LHGR level in Figure 4.21. A separation in FGR results between the pressurized and non-pressurized rods may also be inferred, though not statistically supported. It may be concluded that the behavior of the Assembly 373 and 366 rods was consistent when the difference in LHGR levels is accounted for. Additional discussion on the comparison of these two assemblies may be found in Section 8.1 of HBEP-25.

4.5.2 Fission Gas Release During Power-Bumping

Fission gas release data for the power-bumped KWU/CE PWR rodlets may be compared to other KWU/CE PWR rodlets power-bumped in the HFR (LaVake and Gaertner 1984). Six of 68 rodlets tested by KWU/CE were comparable to the HBEP rodlets because of similar holding times at peak bumping LHGR, similar prebump burnup levels, and similar fuel types. The net bumping FGR data for the HBEP and KWU/CE rodlets are compared in Figure 4.22. The FGR data from the KWU/CE rodlets generally lie within the data band of the HBEP rodlets, the exception being one rodlet from each of the KWU/CE burnup groups. This comparison indicates that the HBEP bumping results were generally comparable

to results obtained from bump testing similar KWU/CE rodlets under similar conditions.

The HBEP power-bumping FGR data indicated an increase in net FGR during the bumping irradiations, at equivalent bumping LHGR levels, as burnup level increased from 25 to 45 MWd/kgM. The increase in FGR with burnup level is attributed to more fission gas in the UO_2 matrix both available for release and readily releasable. This apparent burnup level dependency on FGR during transients has also been observed by a) Pati and Garde (1985) as burnup increased from 25 to 35 MWd/kgM, b) Manzel, Sontheimer, and Stehle (1985), and c) Knudsen et al. (1988). Therefore, the HBEP results are in general agreement with other data.

4.5.3 Fuel Microstructure/Xenon Retention Correlation

Other investigators have published comments on correlations between fuel microstructure and matrix retention of xenon. First, for BWR-type rods irradiated in the Halden Boiling Water Reactor, the GBBPR was found to occur at approximately the same radius as the XDR (Lanning 1986a). Best-estimate lifetime-peak fuel temperatures assigned to these radii ranged from 1100 to 1250°C (Lanning 1986b), which are in good agreement with the temperature estimates from the HBEP fuel cross-sections. Second, for commercial PWR rods, a similar correlation between GBBPR and XDR has also been reported by Manzel, Sontheimer, and Stehle (1985); they assigned a temperature of 1200°C to the two radii. Thus, the HBEP data and analyses are in general agreement with other data and analyses.

4.5.4 Onset of Rim Effect

From the optical microscopy, SEM, and EPMA evaluations, it is concluded that the threshold pellet-edge burnup level for the initial manifestation of a rim effect is approximately 50 to 60 MWd/kgM. Other estimates of the burnup threshold level for the rim effect have been generated; they include: a) pellet-edge burnup value of greater than 68 MWd/kgM for PWR fuel (Pati, Garde, and Clink 1988); and b) pellet-edge burnup value of greater than 60 MWd/kgM for PWR fuel (Baron, Forat, and Maffeis 1988). Thus, the HBEP results and conclusions are in general agreement with other published data.

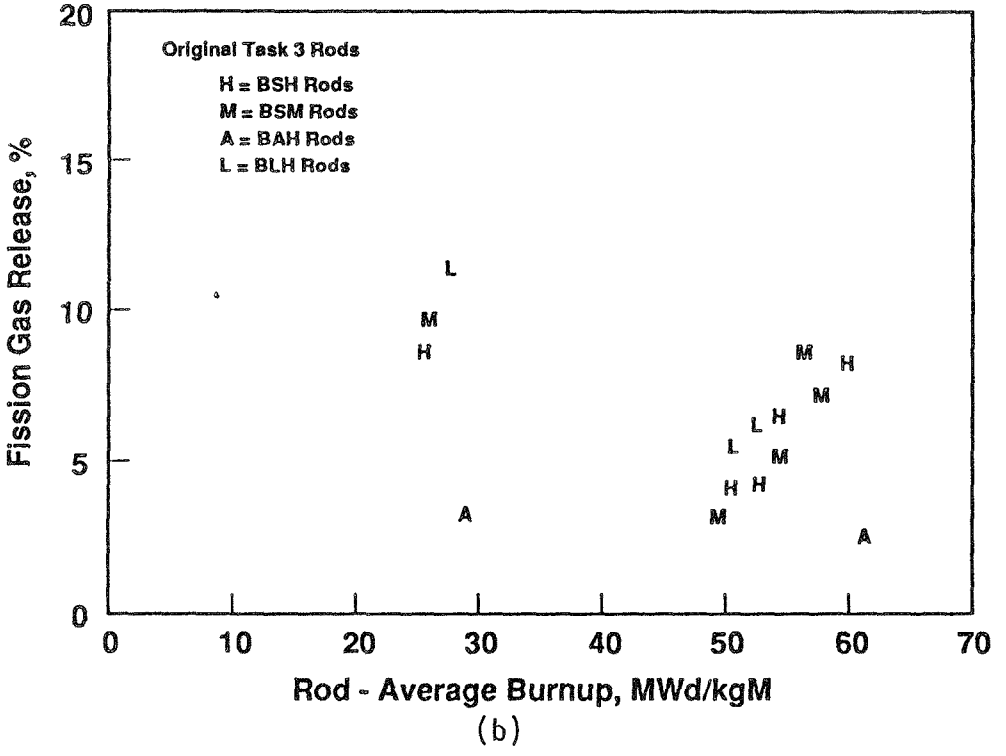

(b)

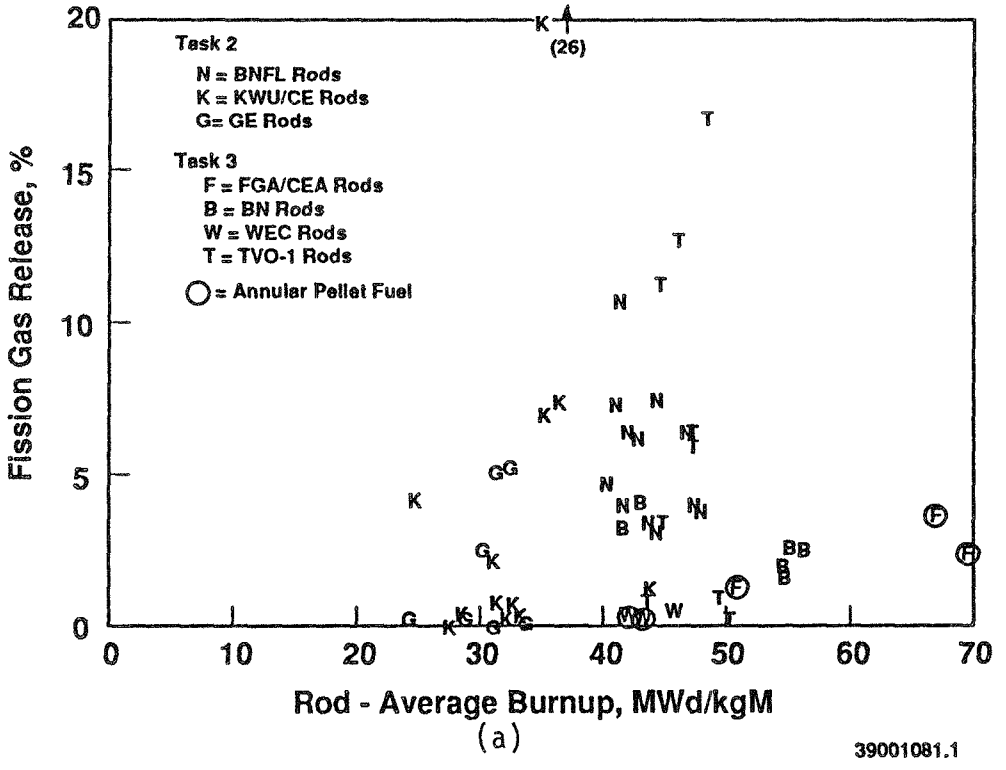

(a)

FIGURE 4.1. Fission Gas Release Data for HBEP Non-Bumped Rods and Rodlets. a) Participant-Origin Rods; b) Original Task 3 Rods

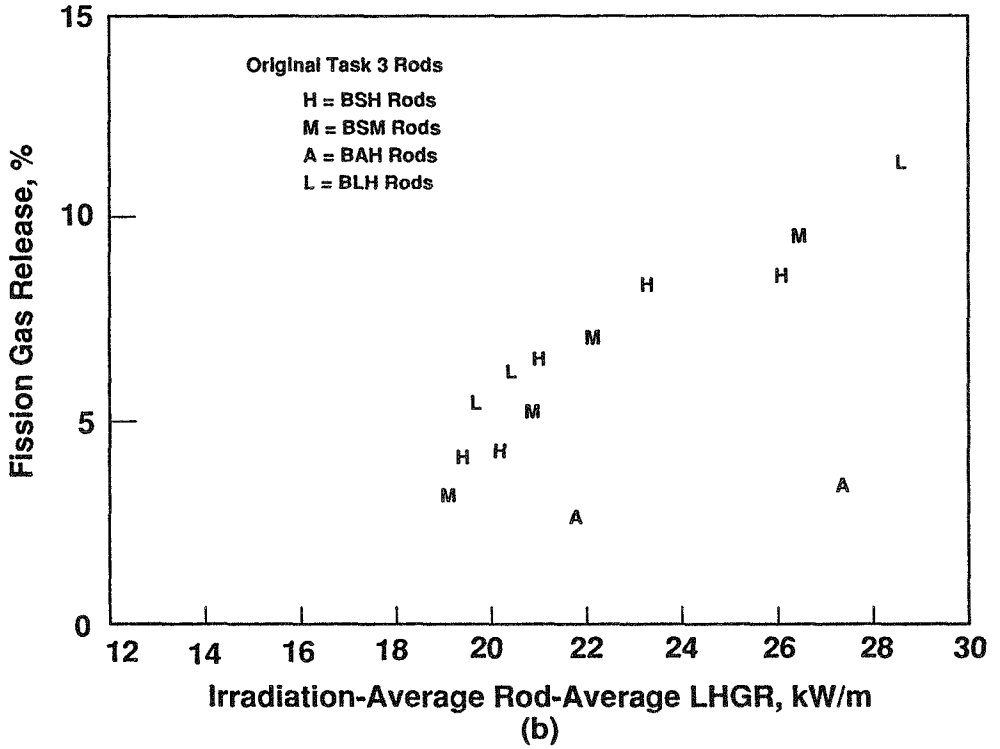

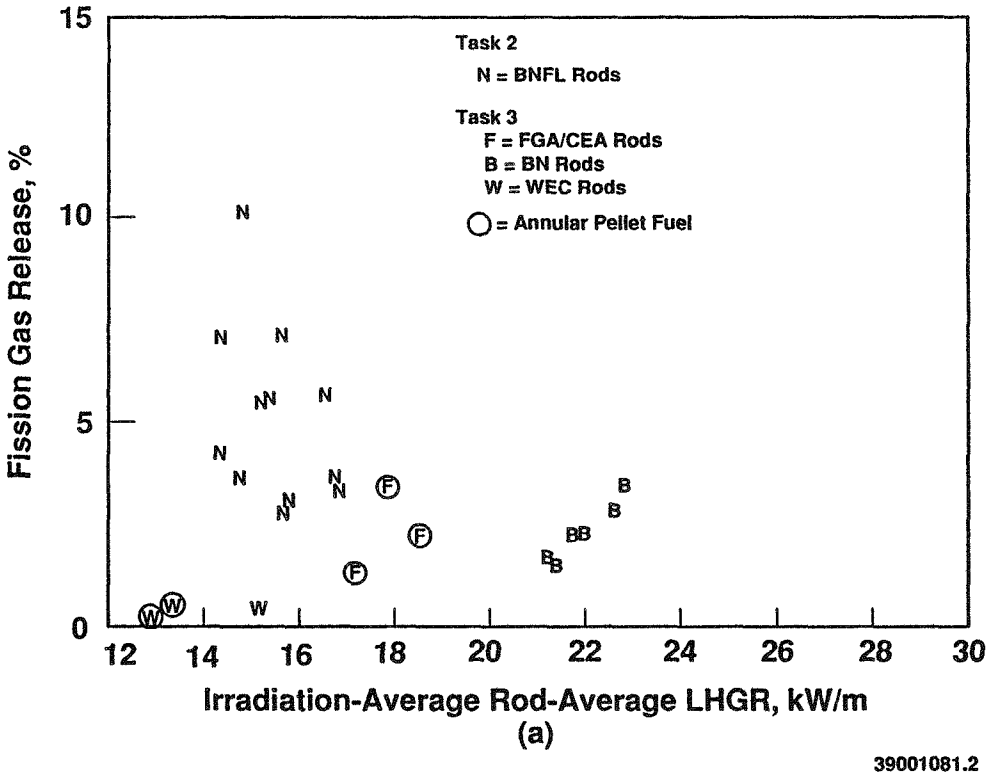

FIGURE 4.2. Fission Gas Release Data as a Function of Lifetime-Average Rod-Average LHGR for HBEP Rods Irradiated in BR-3. a) Participant-Origin Rods; b) Original Task 3 Rods.

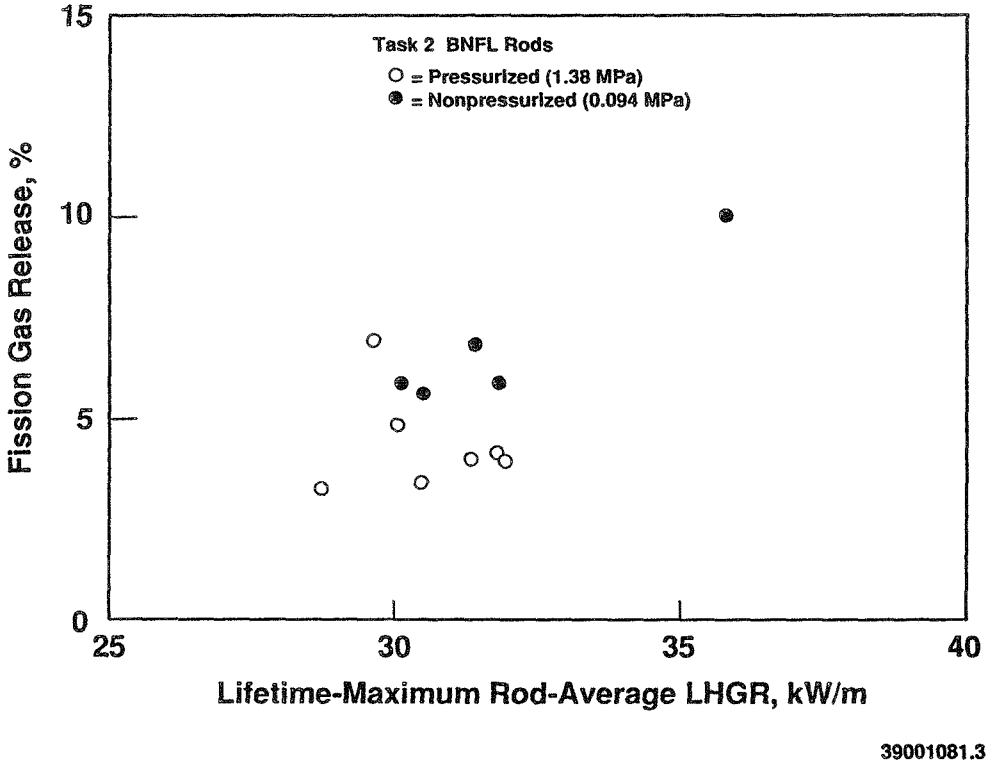

FIGURE 4.3. Fission Gas Release Data as a Function of Lifetime-Maximum Rod-Average LHGR for HBEP Task 2 BNFL Rods

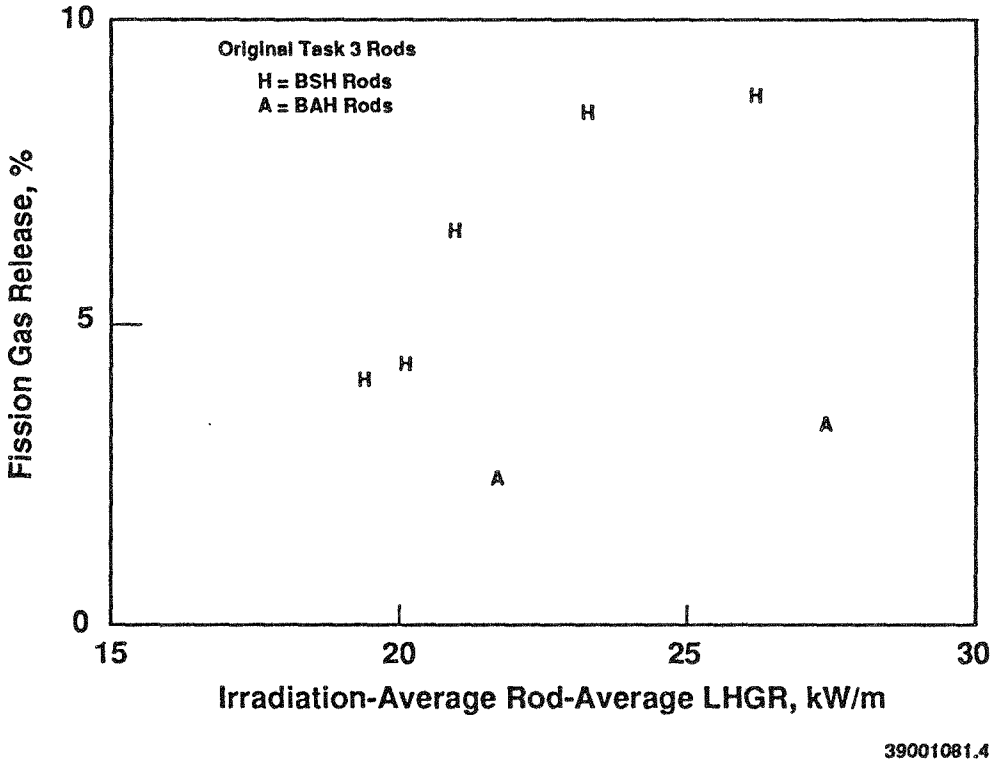

FIGURE 4.4. Comparison of Fission Gas Release Data from Solid-Pellet and Annular-Pellet Original Task 3 Rods

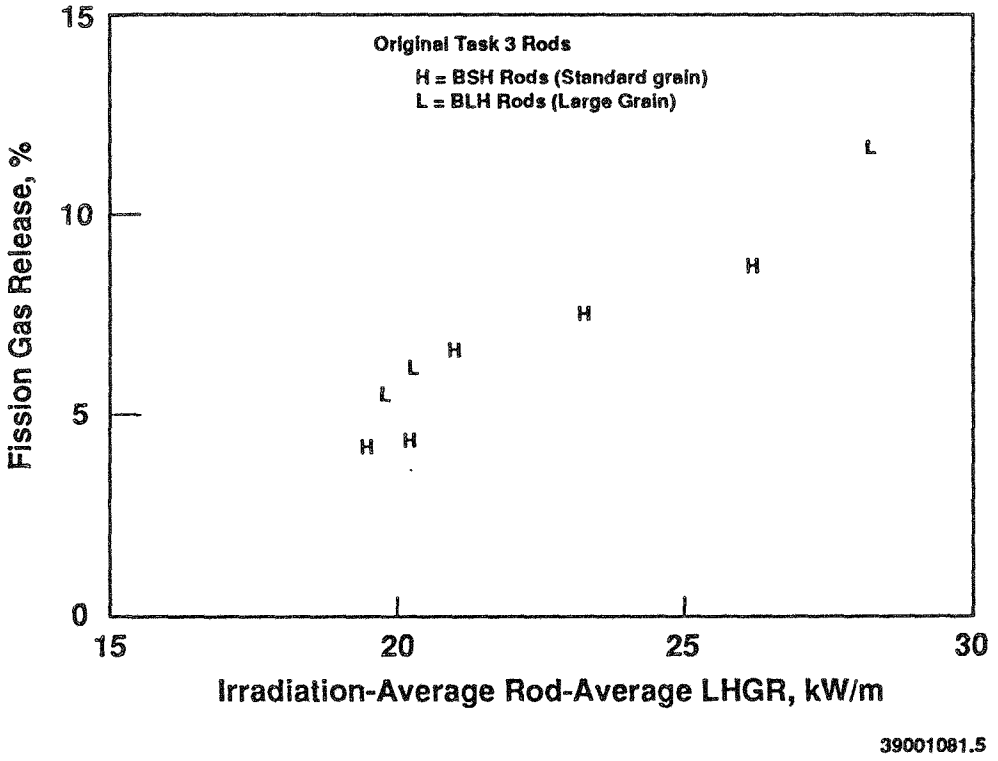

FIGURE 4.5. Comparison of Fission Gas Release Data from Standard-Grain and Large-Grain Original Task 3 Rods

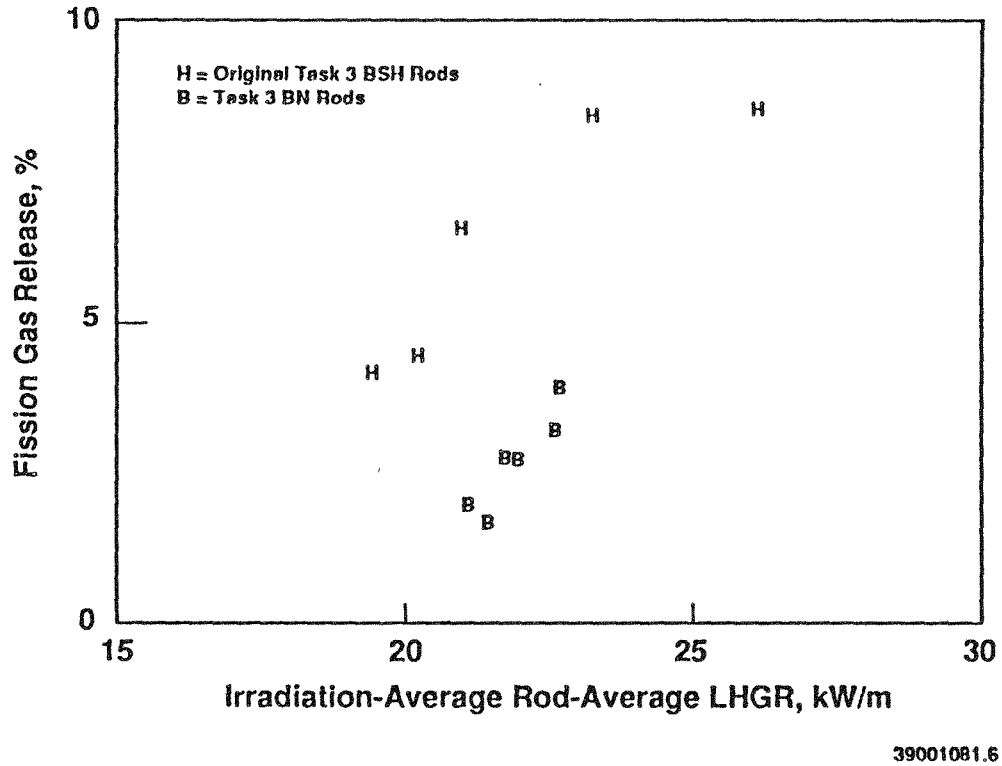

FIGURE 4.6. Comparison of Fission Gas Release Data from Task 3 BN Rods and Original Task 3 BSH Rods

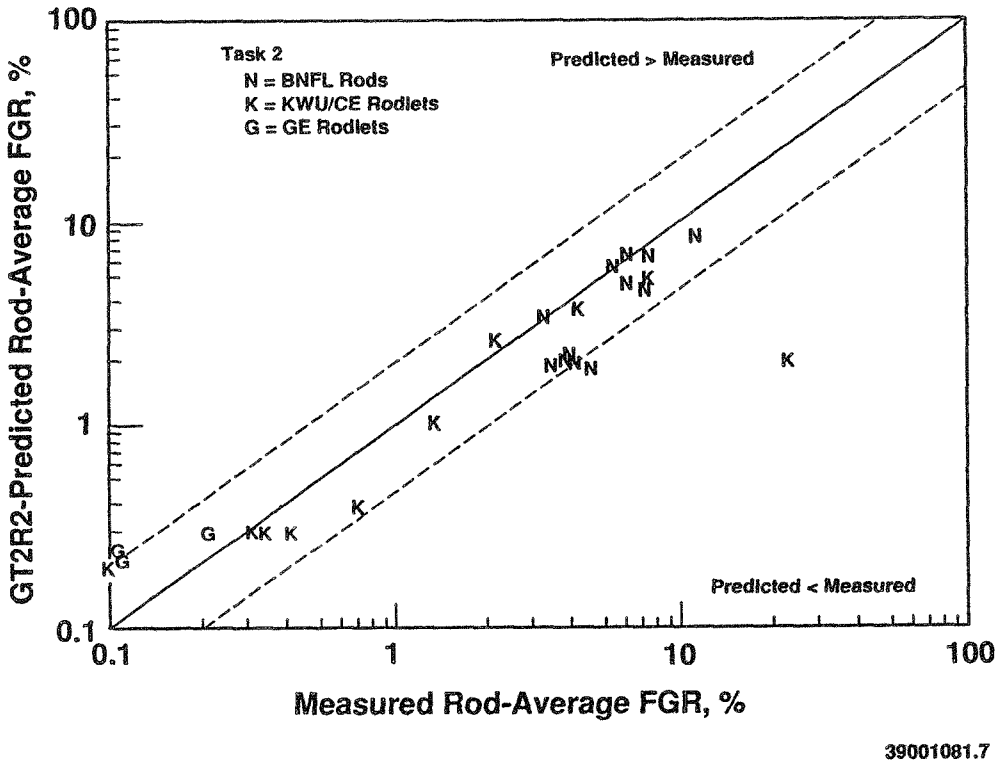

FIGURE 4.7. Comparison of GT2R2-Predicted and Measured Fission Gas Release Values for Non-Bumped Task 2 Rods and Rodlets

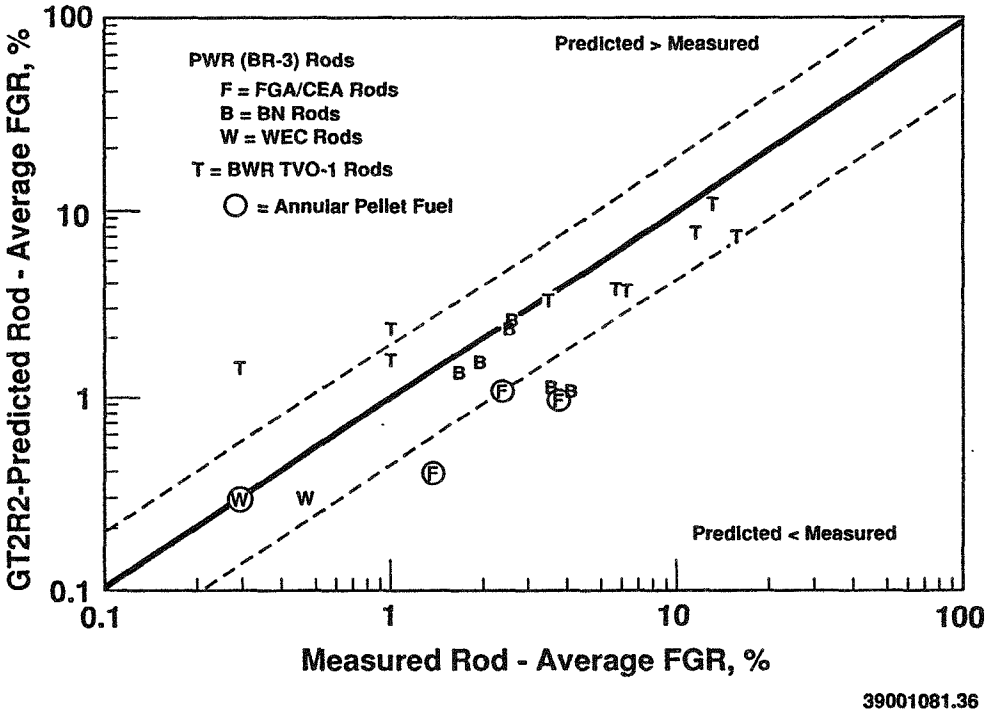

FIGURE 4.8. Comparison of GT2R2-Predicted and Measured Fission Gas Release Values for Supplemental Task 3 Rods

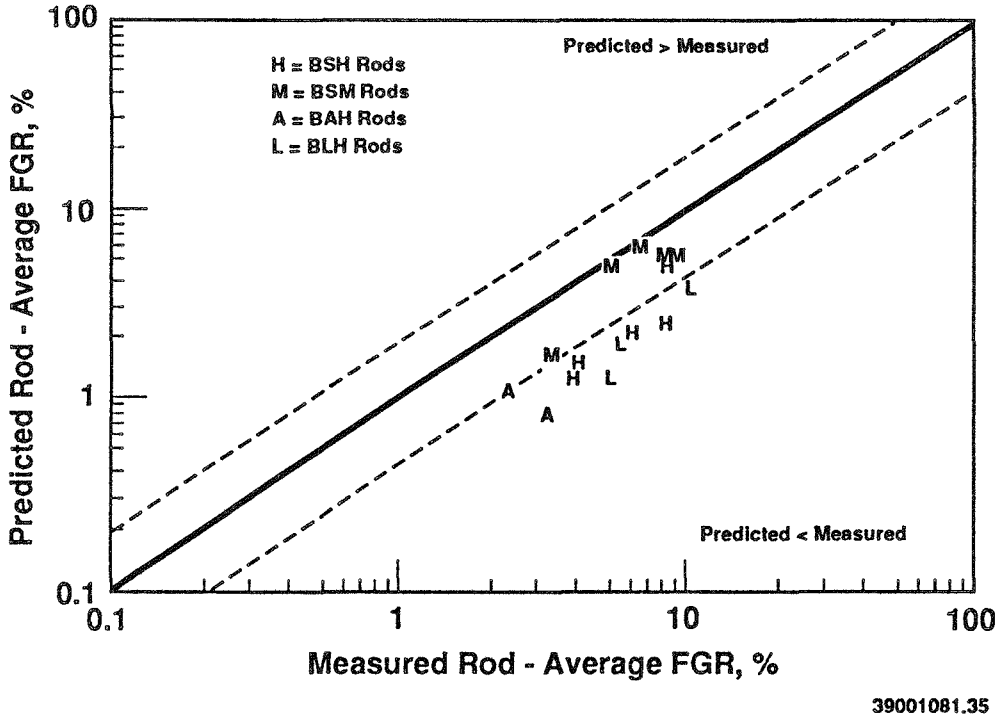

FIGURE 4.9. Comparison of GT2R2-Predicted and Measured Fission Gas Release Values for Original Task 3 Rods

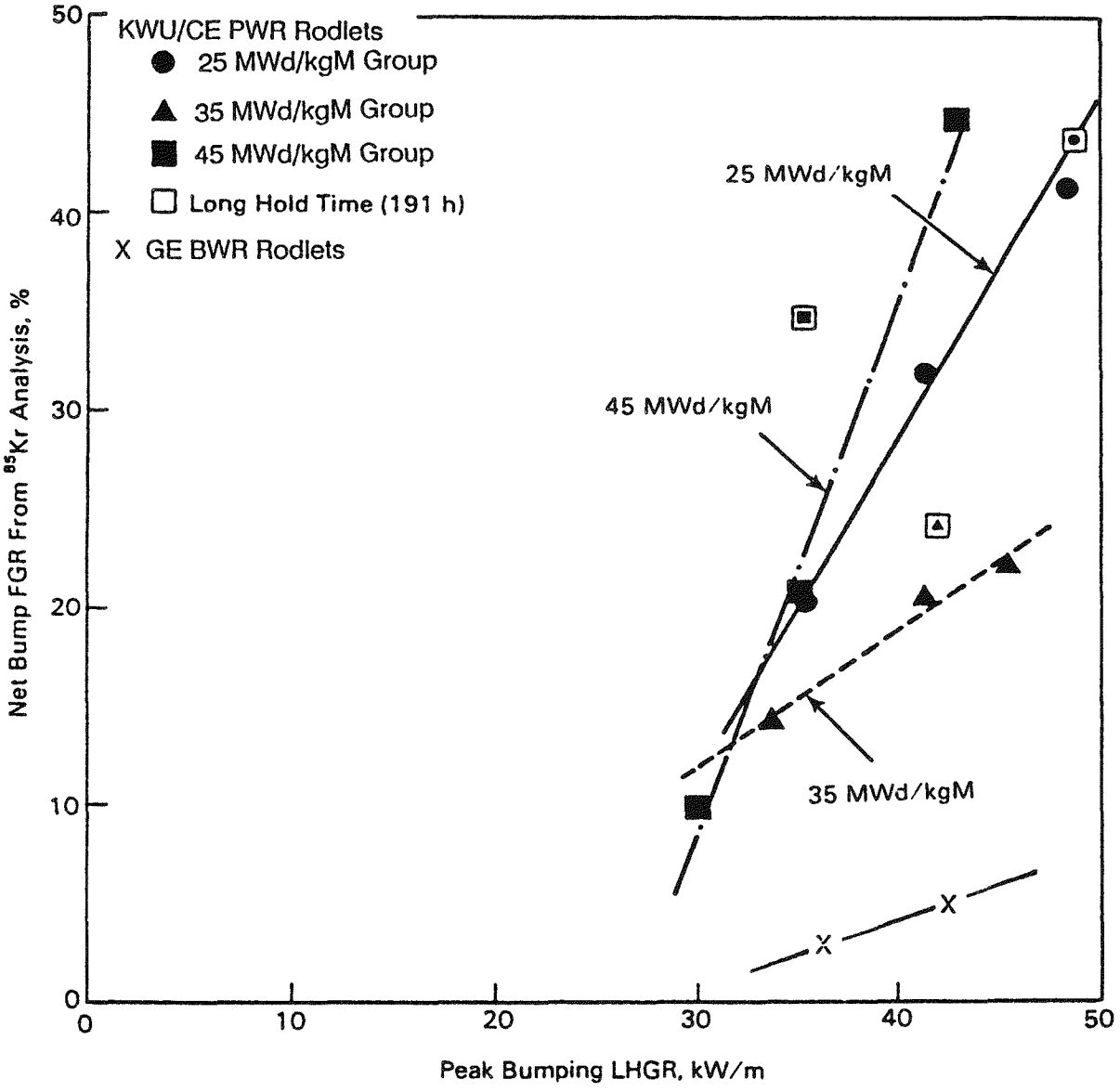

FIGURE 4.10. Net Fission Gas Release During Power-Bumping Irradiations as a Function of Peak Bump LHGR Level

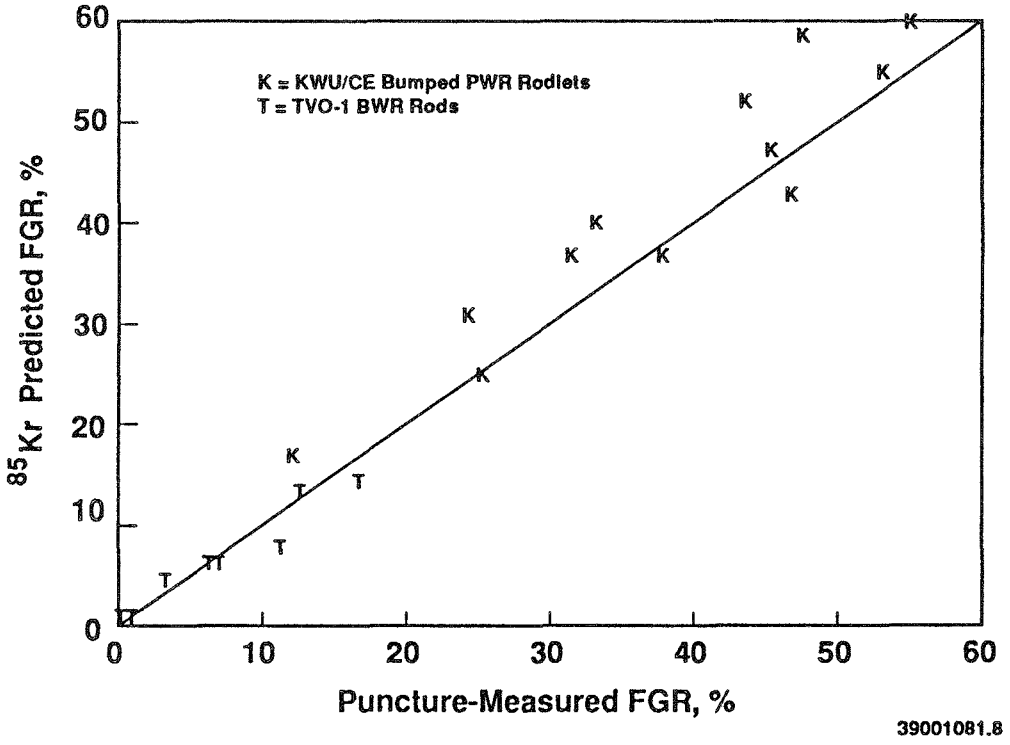

FIGURE 4.11. Comparison of ^{85}Kr-Predicted and Puncture-Measured Fission Gas Release Values

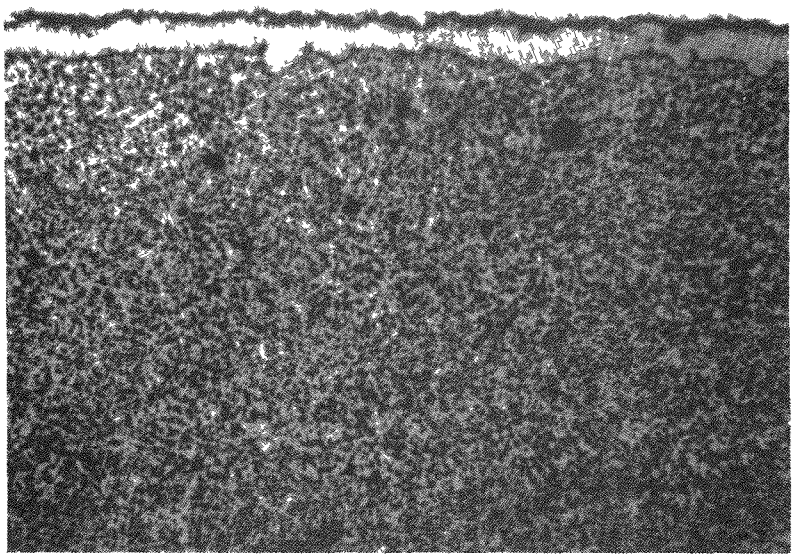

Rod BK365 (PWR-Type) at 83 MWd/kgM (Pellet-Average)

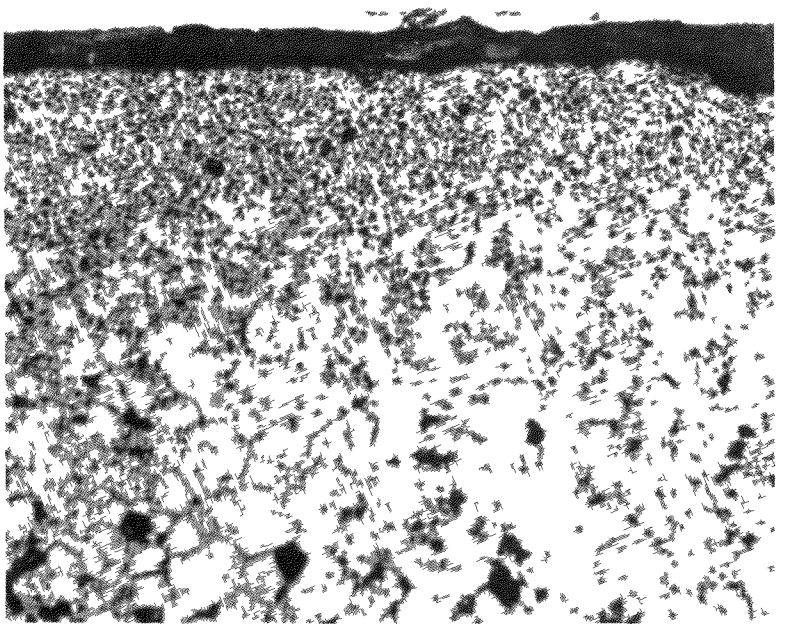

Rod H8/36-6 (BWR) at 49.5 MWd/kgM (Pellet-Average)

FIGURE 4.12. Example of Fuel Microstructure in Pellet Rim Region (both photos at 500X, etched)

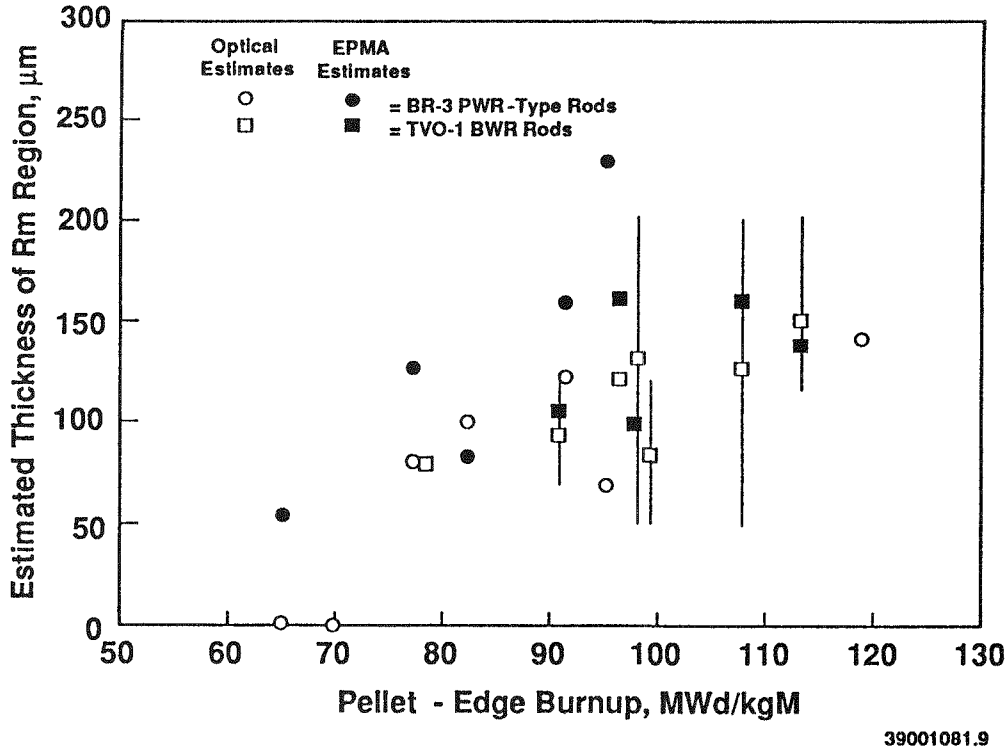

FIGURE 4.13. Estimated Rim Region Thickness as a Function of Pellet-Edge Burnup Level

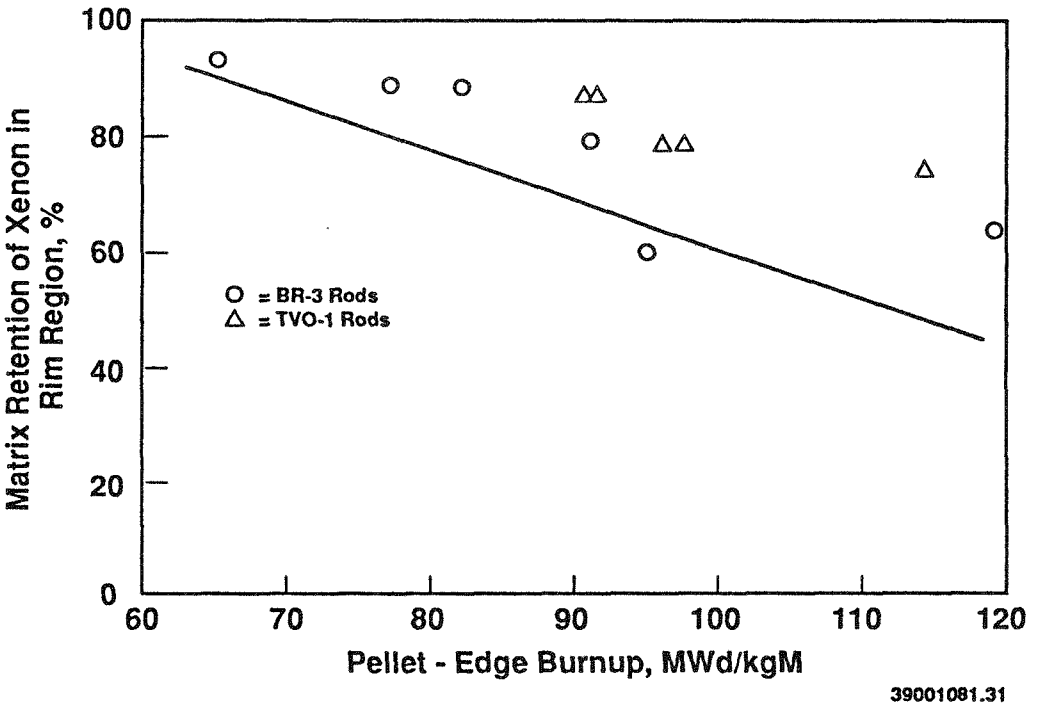

FIGURE 4.14. Estimate of Matrix Retention of Xenon in the Rim Region (from EPMA measurements)

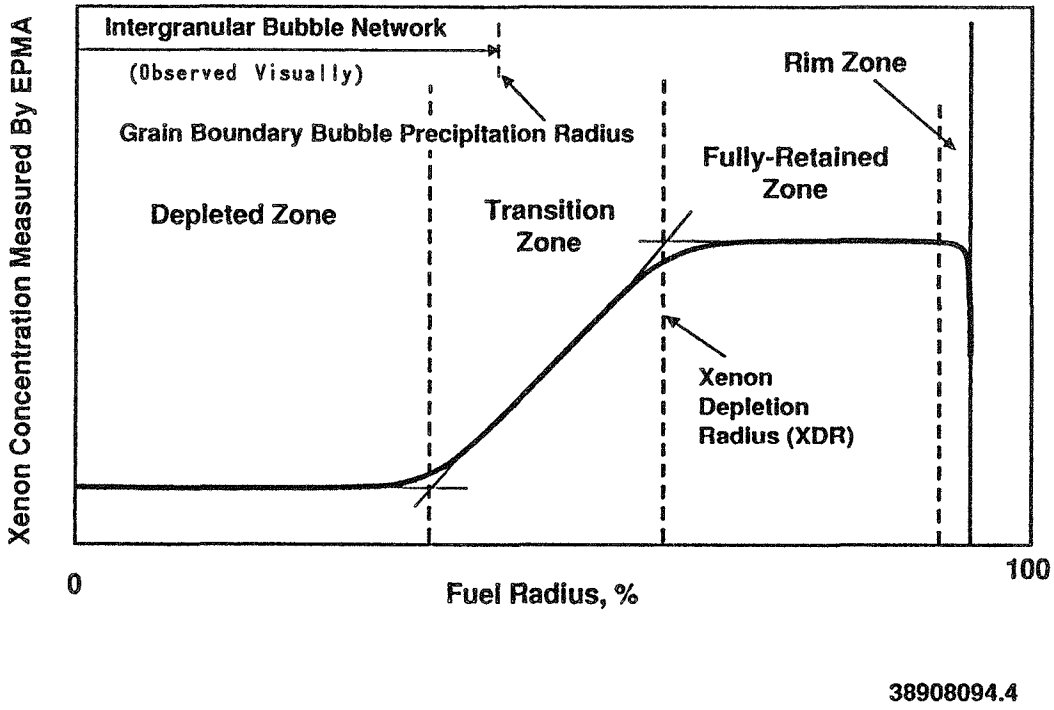

FIGURE 4.15. Definition of Grain Boundary Bubble Precipitation Radius (GBBPR) and Xenon Depletion Radius (XDR)

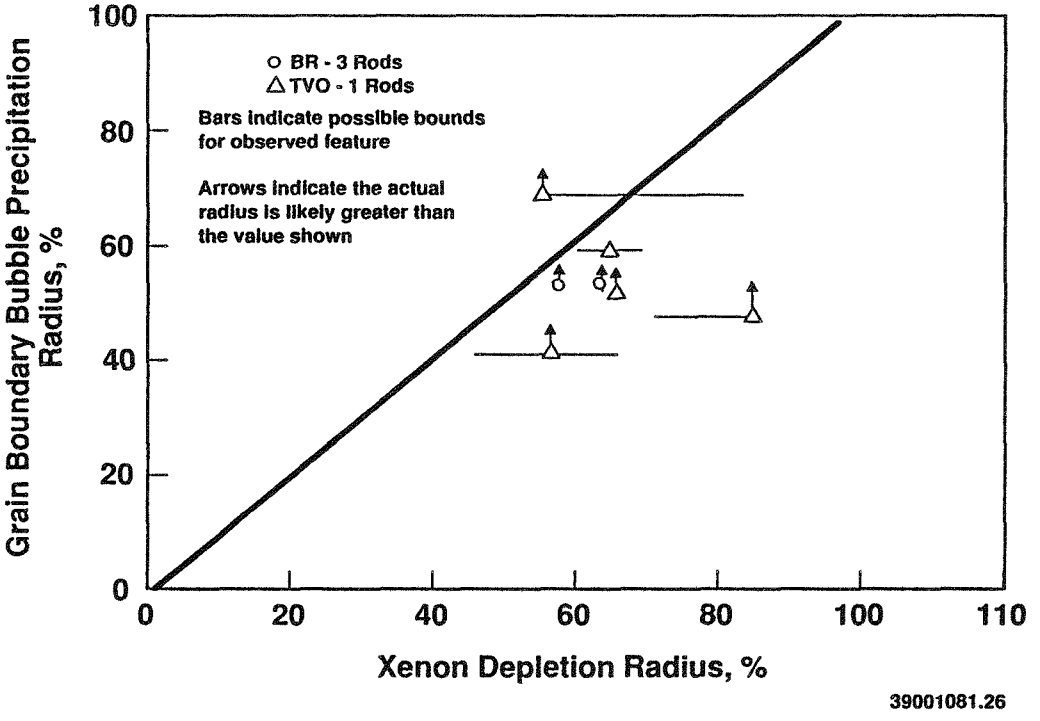

FIGURE 4.16. Relationship Between Intergranular Bubble Network and Xenon Depletion Radius for Task 3 Fuel Rods (Excluding Original Task 3 Rods)

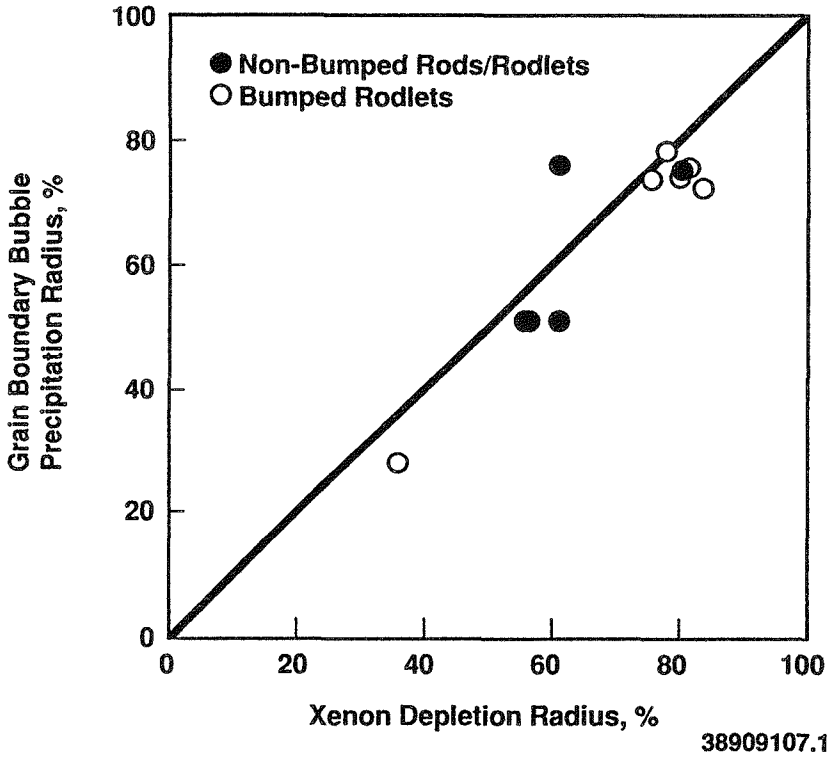

FIGURE 4.17. Relationship Between Intergranular Bubble Network and Xenon Depletion Radius for Task 2 Fuel Rods

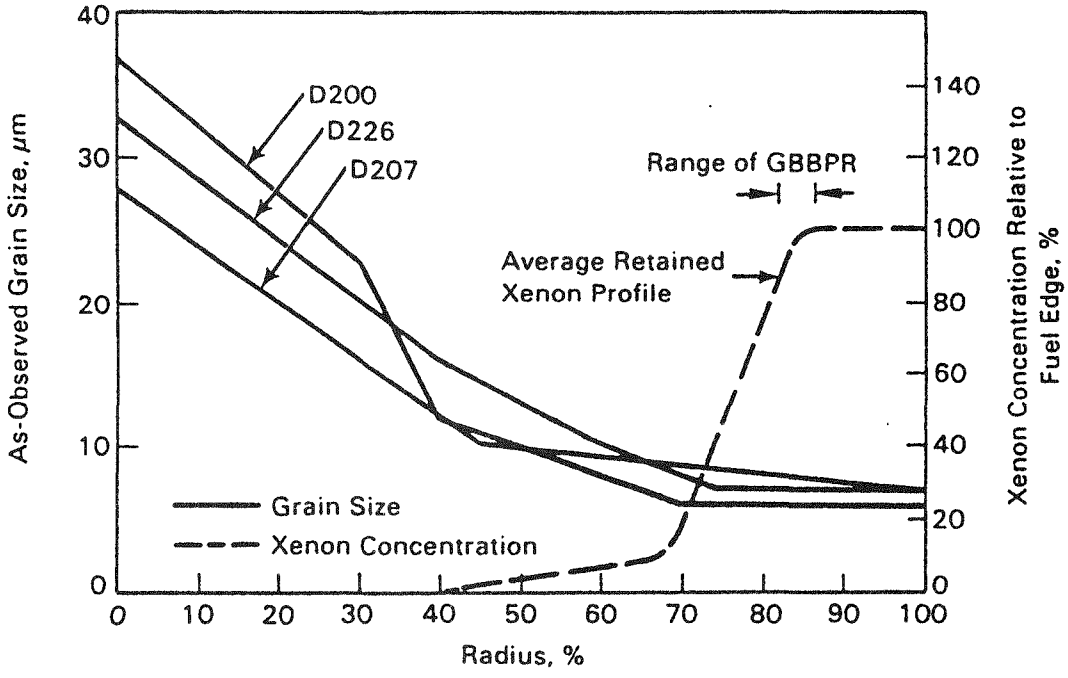

FIGURE 4.18. Grain Growth and Xenon Retention for Power-Bumped KWU/CE PWR Rodlets

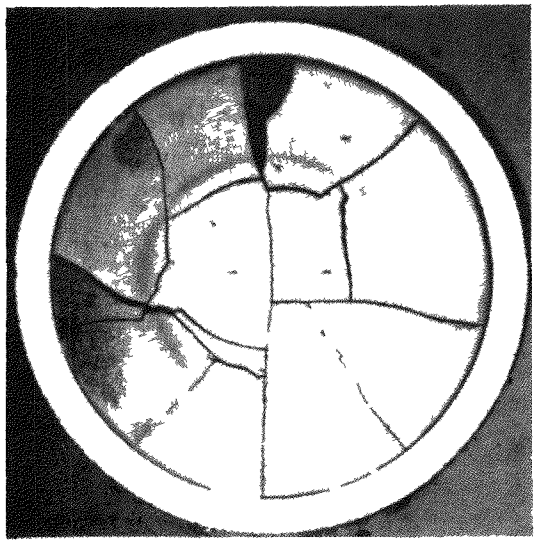

Dark-Etch Ring (6X Magnification, Etched Surface)

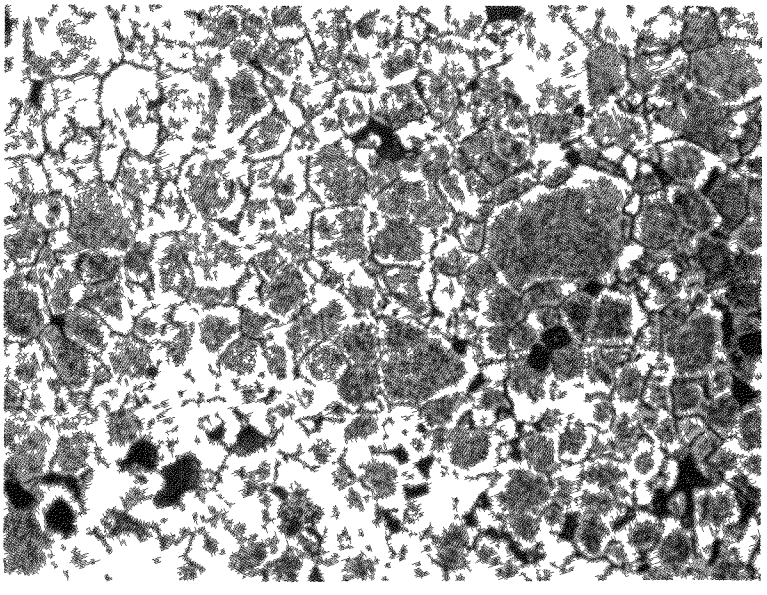

Intragranular Porosity Within Dark-Etch Ring (500X, Etched Surface)

FIGURE 4.19. Example of "Dark-Etch" Ring and Intragranular Porosity in Grains in Ring (Rod H8/36-4 at 48.2 cm)

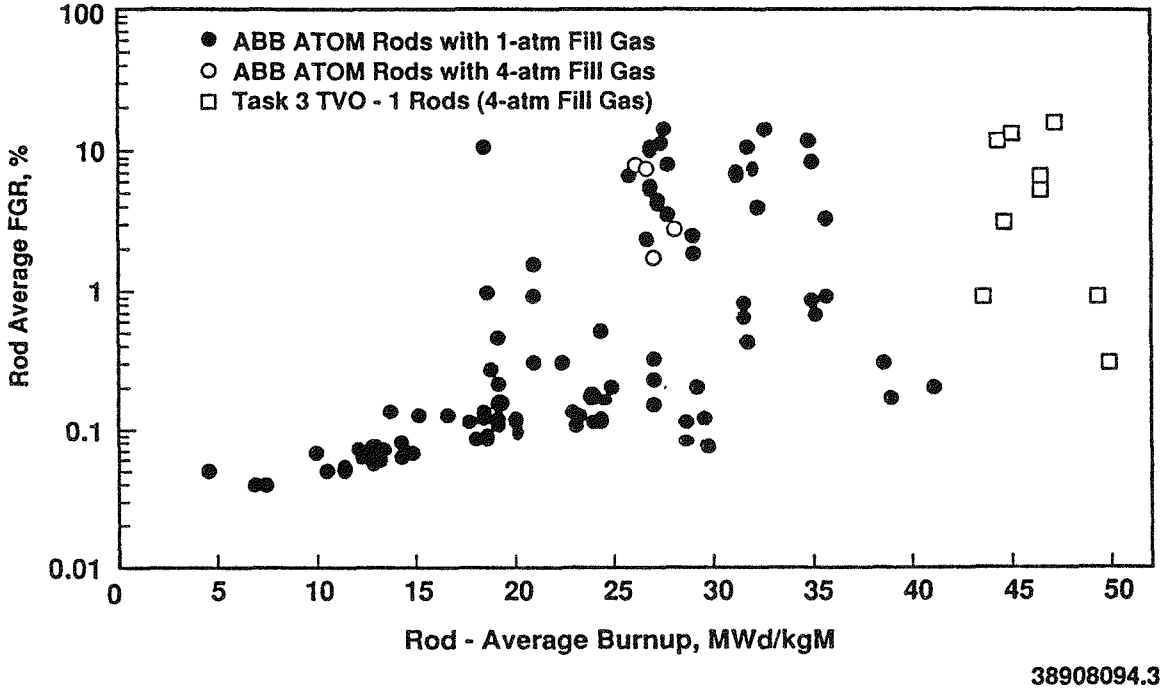

FIGURE 4.20. Comparison of FGR Data from TVO-1 Rods to Other ABB ATOM Rods

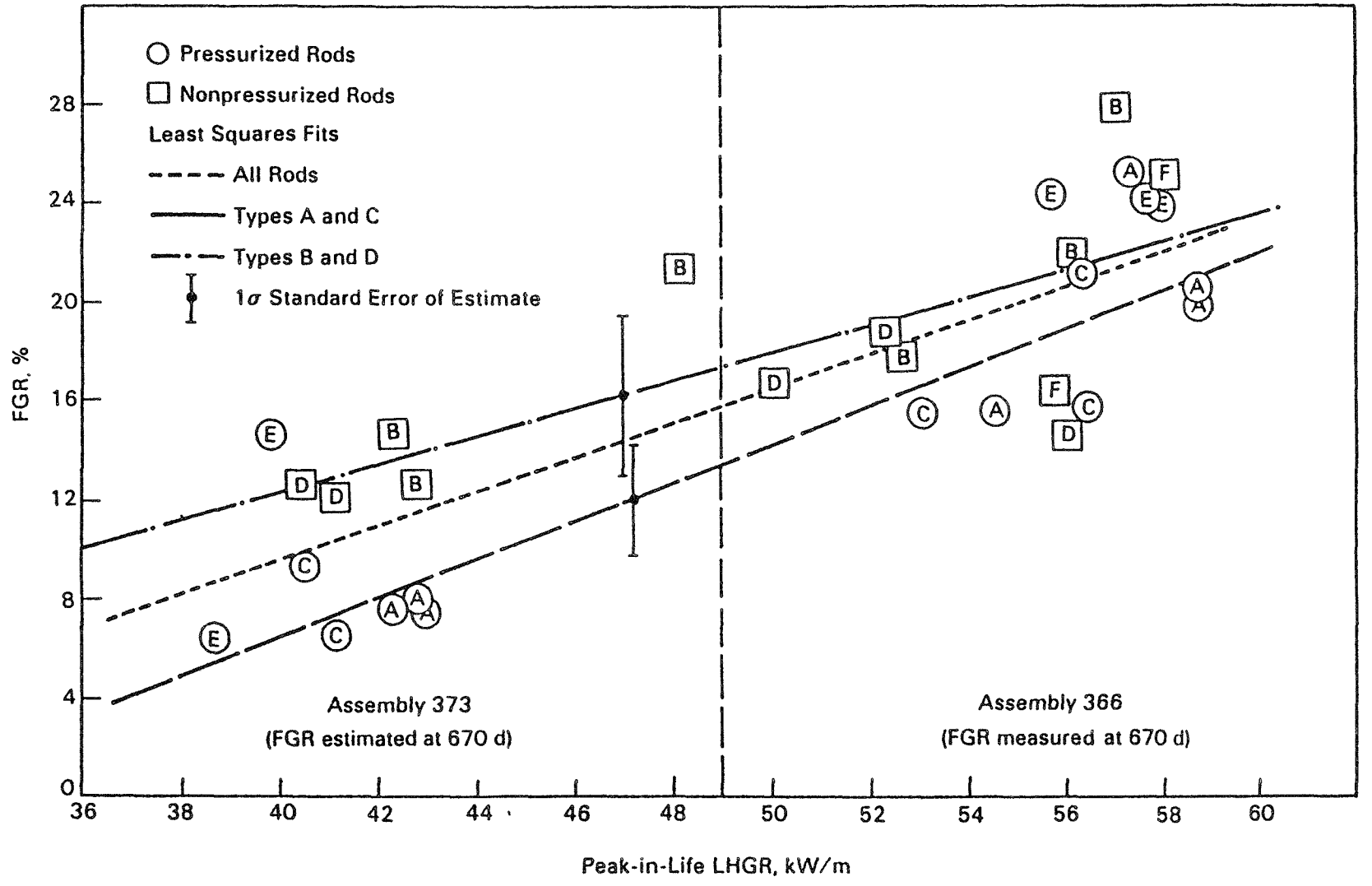

FIGURE 4.21. Comparison of FGR Data from BNFL Assemblies 373 and 366

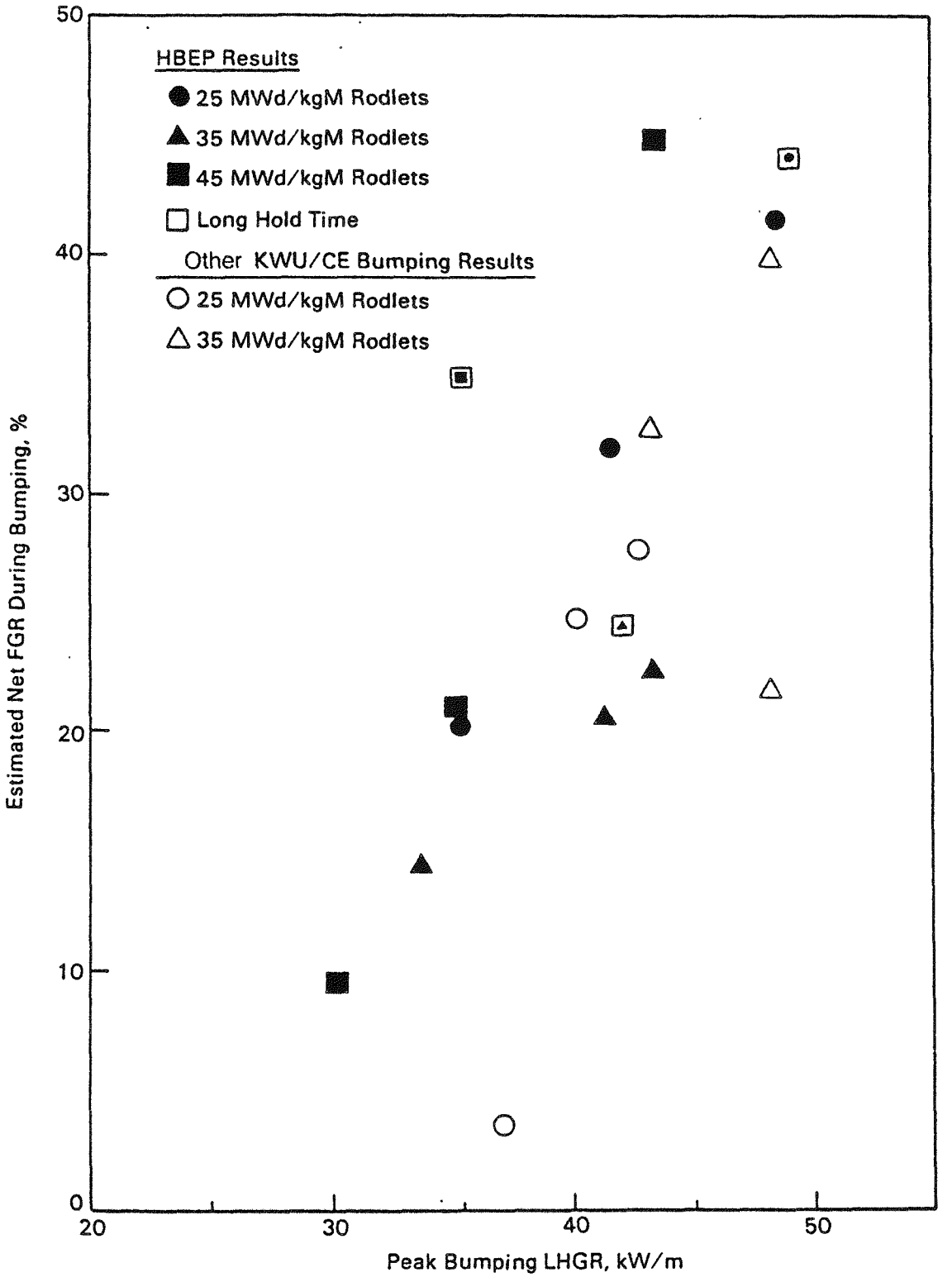

FIGURE 4.22. Net FGR During Power-Bumping for Task 2 KWU/CR PWR Rodlets and Other Power-Bumped KWU/CE PWR Rodlets

5.0 REFERENCES

HBEP Publications

HBEP-01(1P1). 1982. A State-of-the-Technology Assessment.

HBEP-05(2B2). 1981. Irradiation History of BNFL Rods - Task 2A.

HBEP-10(1P2). 1982. Fission Gas Release Data Evaluation - Published Data.

HBEP-25(2P4). 1987. Qualification of Fission Gas Release Data from Task 2 Rods.

HBEP-41(2/3P9). 1989. Sectioning Diagrams for HBEP Rods and Rodlets.

HBEP-50(2P16). 1988. Summary of Postirradiation Examinations - Task 2.

HBEP-51(3P17). 1988. Fabrication, Preirradiation Characterization, and Irradiation History for TVO-1 Rods - Task 3.

HBEP-60(3P26). 1990. Qualification of Fission Gas Release Data from Task 3 Rods.

Freshley, M.D. 1981. The Investigation of High Burnup Effects in Sintered UO_2 Pellet Fuel with Emphasis on Fission Gas Release - Program Plan (Revision 3). Prepared for the Sponsors of the High Burnup Effects Program by Battelle, Pacific Northwest Laboratory, Richland, Washington.

Other Publications

Andersson, S.O., et al. 1986. "The Finnish-Swedish High Burnup Fuel Evaluation Programme." In Proceedings of Improvements in Water Reactor Fuel Technology and Utilization, Stockholm, Sweden, September 15-19, 1986.

Baron, D, C. Forat, and E. Maffeis. 1988. "FRAGEMA Experience in Fission Gas Release Under Base and Transient Operating Conditions." In Proceedings of the International Topical Meeting on LWR Fuel Performance, Williamsburg, Virgina, April 17-20, 1988.

Beyer, C.E., and R.O. Meyer. 1976. "Semiempirical Model for Radioactive Fission Gas Release from UO_2," Trans. Am. Nuc. Soc., Vol 23, pg 172.

Beyer, C.E. 1982. "An Evaluation of Published High Burnup Fission Gas Release Data." In Proceedings of the Topical Meeting on LWR Extended Burnup - Fuel Performance and Utilization, Williamsburg, Virginia, April 4-8, 1982.

Cunningham, M. E. and C. E. Beyer. 1984. GT2R2: An Updated Version of GAPCON-THERMAL-2. NUREG/CR-3907 (PNL-5178), Pacific Northwest Laboratory, Richland, Washingon.

Franklin, D. G., S. Djurle, and D. Howl. 1985. "Performance of Niobia-Duped Fuel in Power-Ramp Tests." Nuclear Fuel Performance, BNES, London, England.

Grimoldby, R.D., and B. Crossley. 1982. Pre-irradiation characaterization data for the PWR fuel assembly No. 366. BNFL Report 439(S), British Nuclear Fuels Limited, England.

Knudsen, P., et al. 1988. "Fission Gas Release in High-Burnup Fuel During Power Transients." In Proceedings of the International Topical Meeting on LWR Fuel Performance, Williamsburg, Virginia, April 17-20, 1988.

Lanning, D.D. 1986a. Experimental Support and Development of Single-Rod Fuel Codes Program - Summary Report. NUREG/CR-4718 (PNL-5972), Pacific Northwest Laboratory, Richland, Washington.

Lanning, D.D. 1986b. Irradiation History and Final Postirradiation Data for IFA-432. NUREG/CR-4717 (PNL-5971), Pacific Northwest Laboratory, Richland, Washington.

LaVake, J.C. and M. Gaertner. 1984. High Burnup PWR Ramp Test Program: Final Report. DOE/ET/34030-10, U.S. Department on Energy, Washington, D.C.

Manzel, R., F. Sontheimer, and H. Stehle. 1985. "Fission Gas Release of PWR Fuel Under Steady and Transient Conditions up to High Burnup." In Proceedings of the American Nuclear Society Topical Meeting on Light Water Reactor Fuel Performance, Orlando, Florida, April 21-24, 1985.

NRC. 1982. Background and Derivation of ANS-5.4 Standard Fission Product Release Model. NUREG/CR-2507, Compiled by Southern Science Applications, Inc., Dunedin, Florida.

Pati, S.R., A.M. Garde, and L.J. Clink. 1988. "Contribution of Pellet Rim Porosity to Low Temperature Fission Gas Release at Extended Burnups." In Proceedings of the International Topical Meeting on LWR Fuel Performance, Williamsburg, Virgina, April 17-20, 1988.

Pati, S.R. and A.M. Garde. 1985. "Fission Gas Release from PWR Fuel Rods at Extended Burnups." In Proceedings of the American Nuclear Society Topical Meeting on Light Water Reactor Fuel Performance, Orlando, Florida, April 21-24, 1985.

Une, K., I. Tanabe, and M. Oguma. 1988. "Effects of Additives and the Oxygen Potential on the Fission Gas Diffusion in UO_2 Fuel." In Journal of Nuclear Materials, 150:93-99.

APPENDIX A

SUMMARY OF FUEL ROD DESIGNS, IRRADIATION HISTORIES, AND PIE DATA

APPENDIX A

SUMMARY OF FUEL ROD DESIGNS, IRRADIATION HISTORIES, AND PIE DATA

Presented in this appendix are summaries of fuel rod design, preirradiation characterization, and irradiation conditions data (Tables A.1 through A.11). Also presented are plots summarizing the irradiation histories for the rods evaluated as part of the HBEP (Figures A.1 through A.10). Best-estimate burnup values are presented in Tables 3.2 and 3.3; derivation of the values was presented in HBEP-25 and HBEP-60.

TABLE A.1. Summary of BNFL Fuel and Rod Designs (Task 2A)

Rod	Fuel Enrichment, % U-235	Fuel Density, % TD	Rod Gas Pressure, MPa @ 0°C	Cladding Type(a)
DF	9	93.6	1.38	C-W
BK	9	93.6	1.38	C-W
AK	9	93.6	1.38	C-W
AU	7.1	95.5	1.38	C-W
AP	7.1	95.3	1.38	C-W
BN	5.9	92.8	1.38	annealed
BW	5.9	92.8	1.38	annealed
DE	9	93.1	0.094	C-W
AL	9	93.6	0.094	C-W
BH	9	93.2	0.094	C-W
CQ	7.1	95.5	0.094	C-W
BP	7.1	95.5	0.094	C-W

Fuel Outer Diameter = 9.265 mm
Cladding Inner Diameter = 9.53 mm
Cladding Outer Diameter = 10.77 mm
Active Stack Length = 1005 mm
Rod Void Volume = 11.1 cm^3

All rods are part of Task 2A

(a) C-W = 15% cold-worked, stress-relieved
annealed = 650°C for 4 h

TABLE A.2. Summary of KWU/CE PWR Fuel and Rodlet Designs (Task 2)

Rodlet	Fuel Enrichment, % U-235	Fuel Density, % TD	Rod Fill Pressure, MPa @ 0°C	Task	Other Comments
D198	3.2	94.3	2.1	2C	25 MWd/kgM rod group
D199	3.2	94.3	2.1	2C	
D200	3.2	94.3	2.1	2C	
D201	3.2	94.3	2.1	2C	
D202	3.2	94.3	2.1	2A	
D205	3.2	94.3	2.1	2C	35 MWd/kgM rod group
D206	3.2	94.3	2.1	2C	
D207	3.2	94.3	2.1	2C	
D208	3.2	94.3	2.1	2C	
D209	3.2	94.3	2.1	2A	
D219	3.2	94.3	2.1	2C	45 MWd/kgM rod group
D226	3.2	94.3	2.1	2C	
D227	3.2	94.3	2.1	2C	
D220	3.2	94.3	2.1	2C	
D228	3.2	94.3	2.1	2A	
D244	3.2	94.0	2.1	2A	4% Gd_2O_3
D245	3.2	94.0	2.1	2A	
D267	3.0	95.1	2.1	2B	large UO_2 grains
D268	3.0	95.1	2.1	2B	
D346	3.2	94.3	0.2	2B	low pressure
D347	3.2	94.3	0.2	2B	

Fuel Outer Diameter = 9.040, 9.112 mm(a)
Cladding Inner Diameter = 9.283 mm
Cladding Outer Diameter = 10.76 mm
Active Stack Length = 317 mm
Rod Void Volume = 3.2, 2.9 cm^3(a)

(a) Rodlets D219, D226, D227, D220, D228, D244, D245, D267, and D268 had the larger pellet diameter and lower void volume.

TABLE A.3. Bumping Conditions for KWU/CE PWR Rodlets (Task 2C)

Rodlet	Terminal LHGR, kW/m		Hold Time, h
	Rodlet-Peak	Rodlet-Average	
D198	48.8	45.5	191
D199	48.2	44.8	48
D200	46.4	38.2	48
D201	35.2	32.5	48
D205	41.9	38.7	195
D206	45.2	42.0	48
D207	41.2	38.0	48
D208	33.6	31.2	48
D219	35.2	32.4	191
D226	43.2	39.7	48
D227	35.0	32.5	48
D220	30.2	27.7	48

Power-Bumping Ramp Rate = 5 W/cm/h

TABLE A.4. Summary of KWU/CE BWR Fuel and Rodlet Designs (Task 2)

Rodlet	Fuel Enrichment, % U-235	Fuel Density, % TD	Fill Gas Pressure, MPa @ 0°C	Task
S26H	3.0	96.1	0.1	2A
S34H	3.0	96.1	0.1	2A
S17W	3.0	96.1	0.1	2B
S24W	3.0	96.1	0.1	2B

Fuel Outer Diameter = 10.60 mm
Cladding Inner Diameter = 10.80 mm
Cladding Outer Diameter = 12.53 mm
Active Stack Length = 325 mm
Rod Void Volume = 4.9 cm^3

TABLE A.5. Summary of GE BWR Fuel and Rodlet Designs (Task 2)

Rodlet	Fuel Enrichment, % U-235	Fuel Density, % TD	Fill Gas Pressure, MPa @ 0°C	Task
8D10-2	2.88	95.4	0.09	2A
8D10-1	2.88	95.4	0.09	2C
0A07-3	2.88	95.4	0.09	2A
0A07-1	2.88	95.4	0.09	2C
5D17-4	2.88	95.4	0.09	2C
5D04-3	2.88	95.4	0.09	2B
8D14-3	2.88	95.4	0.09	2C
8D14-2	2.88	95.4	0.09	2B

Fuel Outer Diameter = 10.57, 10.95 mm(a)
Cladding Inner Diameter = 10.80, 11.14 mm(a)
Cladding Outer Diameter = 12.52 mm
Active Stack Length = 756 mm
Rod Void Volume = 12.5 cm^3

(a) The larger diameters are for Rodlets 8D14-3 and 8D14-2.

TABLE A.6. Bumping Conditions for GE BWR Rodlets (Task 2C)

Rodlet	Ramp Rate, W/cm/h	Rodlet-Peak Terminal LHGR, kW/m	Hold Time, h
0A07-1	4.5	45.0	0(a)
8D10-1	3.4	42.5	48
8D14-3	2.0	36.0	48
5D17-4	2.0	42.5	51

(a) Rodlet failed upon reaching terminal LHGR level.

TABLE A.7. Summary of FGA/CEA Fuel and Rodlet Designs (Task 3)

Rod	Fuel Enrichment, % U-235	Fuel Density, % TD	Fill Gas Pressure, MPa @ 0°C	Number of Irradiation Cycles
BK370	7.07	93.2	2.88	3
BK363	7.07	93.2	1.40	4
BK365	7.07	93.2	2.88	4

Fuel Outer Diameter = 8.19 mm
Fuel Hole Diameter = 2.48 mm
Cladding Inner Diameter = 8.36 mm
Cladding Outer Diameter = 9.50 mm
Active Stack Length = 1017 mm
Rod Void Volume = 12.0 cm^3

TABLE A.8. Summary of BN Fuel and Rodlet Designs (Task 3)

Rod	Fuel Enrichment, % U-235	Fuel Density, % TD	Fill Gas Pressure, MPa @ 0°C	Number of Irradiation Cycles
3-74	8.25	94.6	1.96	2
3-89	8.25	94.6	1.96	2
3.86	8.25	94.6	1.96	3
3-128	8.25	94.6	1.96	3
3-138	8.25	94.6	1.96	3
3-337	8.25	94.6	1.96	3

Fuel Outer Diameter = 8.04 mm
Cladding Inner Diameter = 8.24 mm
Cladding Outer Diameter = 9.50 mm
Active Stack Length = 1000 mm
Rod Void Volume = 7.6 cm^3

TABLE A.9. Summary of WEC Fuel and Rodlet Designs (Task 3)

Rod	Fuel Hole Diameter, mm	Fuel Stack Length, mm	Rod Void Volume, cm^3
01-7-A	--	990	7.15
03-8-C	2.17	976	11.5
08-8	2.17	976	11.5

Fuel Outer Diameter = 8.19 mm
Cladding Inner Diameter = 8.36 mm
Cladding Outer Diameter = 9.50 mm
Fuel Enrichment = 5.74 % U-235
Fuel Density = 94.5% TD
Rod Fill Gas Pressure = 1.26 MPa @ 0°C
Number of Irradiation Cycles = 3

TABLE A.10. Summary of HBEP-Built Fuel and Rodlet Designs (Task 3)

Rod	Fuel Enrichment, % U-235	Fuel Density, % TD	Fill Gas Pressure, MPa @ 0°C	Rod Void Volume, cm^3	Number of Irradiation Cycles
BSH-01	7.98	95.1	2.24	8.0	1
BSH-06	7.98	95.1	2.24	8.0	3
BSH-08	7.98	95.1	2.24	8.0	3
BSH-11	7.98	95.1	2.24	8.0	3
BSH-12	7.98	95.1	2.24	8.0	3
BSM-21	7.98	95.1	0.47	7.9	1
BSM-25	7.98	95.1	0.47	7.9	3
BSM-27	7.98	95.1	0.47	7.9	3
BSM-29	7.98	95.1	0.47	7.9	3
BSM-30	7.98	95.1	0.47	7.9	3
BAH-41	7.89	94.2	1.68	11.5	1
BAH-50	7.89	94.2	1.68	11.5	3
BAH-51	7.89	94.2	1.68	11.5	3
BLH-61	7.84	95.3	2.24	8.0	1
BLH-64	7.84	95.3	2.24	8.0	3
BLH-65	7.84	95.3	2.24	8.0	3

Fuel Outer Diameter = 8.08 mm
Fuel Hole Diameter for BAH Rods = 2.48 mm
Cladding Inner Diameter = 8.27 mm
Cladding Outer Diameter = 9.49 mm
Active Stack Length = 1000 mm

TABLE A.11. Summary of TVO-1 Fuel and Rodlet Designs (Task 3)

Rod	Normal (N) or Peripheral (P) Rod[a]	Fuel Enrichment, % U-235	Number of Irradiation Cycles
H8/36-6	P	1.38	5
F1/3-6	N	3.06	5
A1/8-6	P	2.34	5
E8/27-6	N	2.34	5
H8/36-4	P	1.38	6
A3/6-4	N	3.07	6
A1/8-4	P	2.34	6
H5/27-4	N	2.34	6
E8/27-4	N	2.34	6

Parameter	Normal Rod	Peripheral Rod
Fuel Outer Diameter, mm	10.44	9.94
Cladding Inner Diameter, mm	10.65	10.15
Cladding Outer Diamter, mm	12.25	11.75
Rod Void Volume, cm^3	35	32

Fuel Stack Length = 3680 mm
Rod Fill Gas Pressure = 0.37 MPa @ 0°C
Fuel Density = 95.7% TD

(a) Normal or Peripheral is a designation used by ABB ATOM (see HBEP-51). Peripheral rods, as designated by ABB ATOM, are the three rods of smaller diameter at each corner of the assemblies. All rods acquired for the HBEP were from the periphery, i.e., outer edges, of the assemblies, but were not necessarily Peripheral as defined by ABB ATOM.

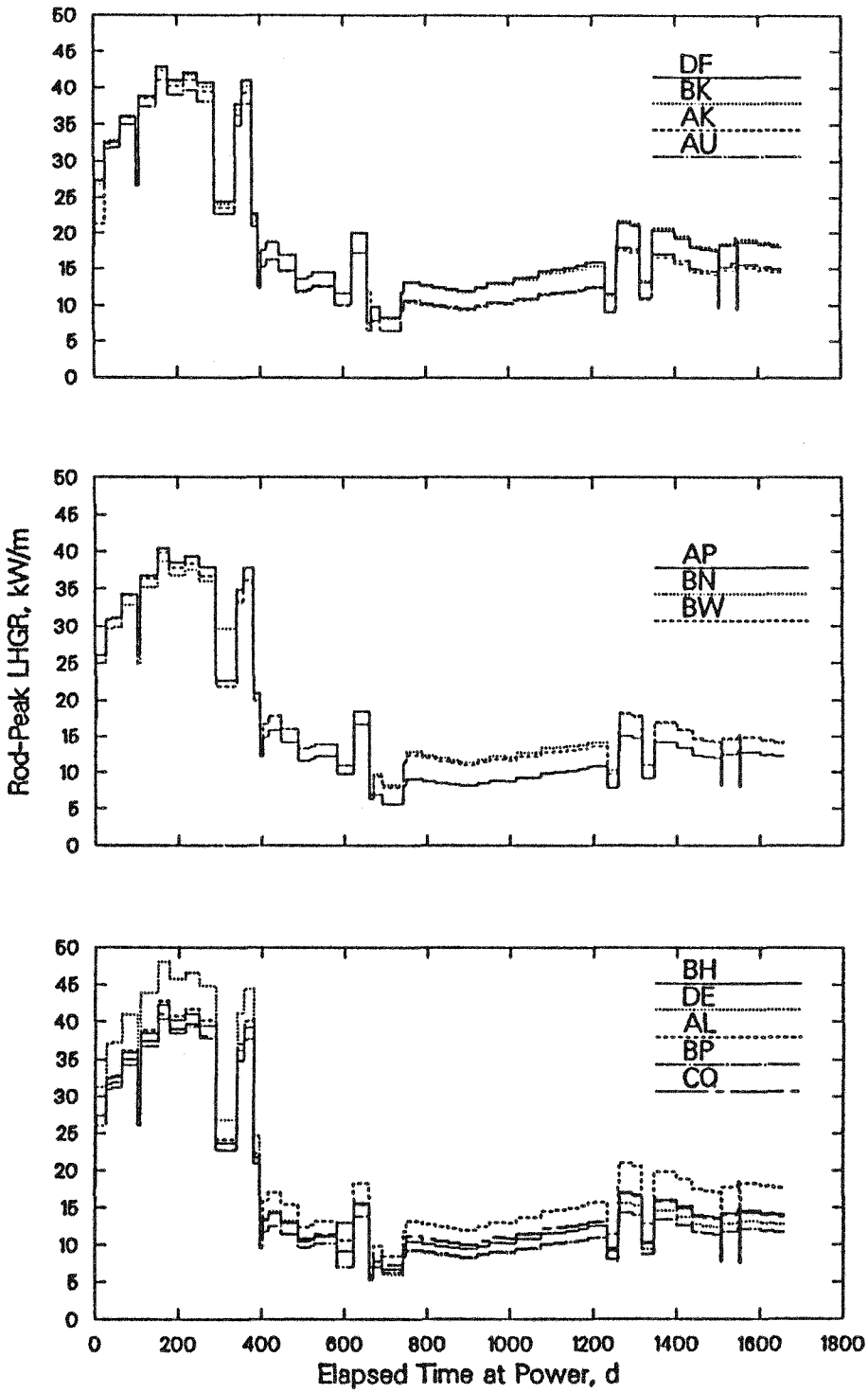

FIGURE A.1. Irradiation Histories for BNFL PWR Rods (Task 2) (From histories provided in HBEP-05; peak-node LHGR values, time corrected for percentage of nominal power.)

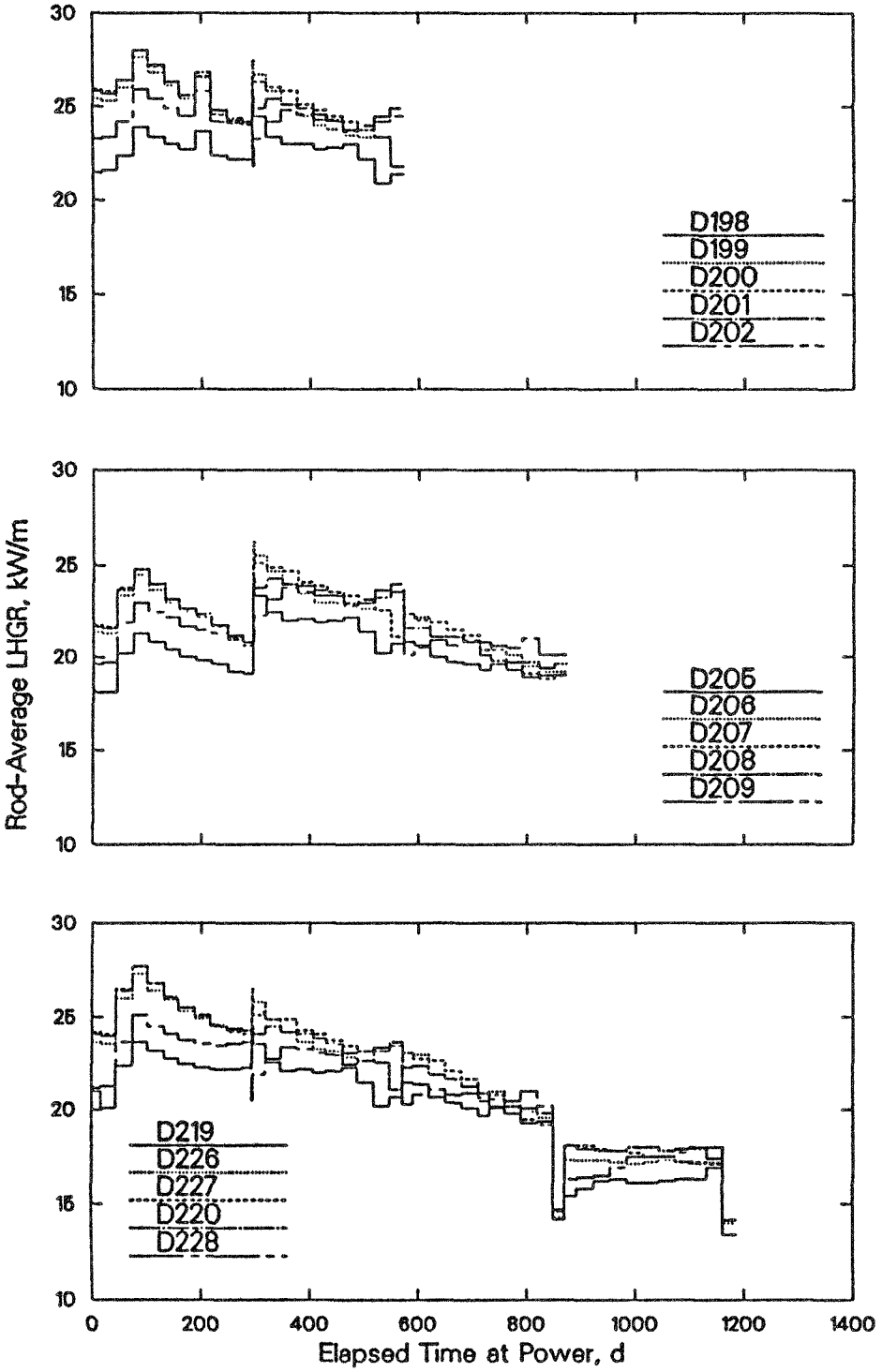

FIGURE A.2. Commercial Irradiation Histories for Standard KWU/CE PWR Rodlets (Task 2) (From histories provided in HBEP-03 and HBEP-20.)

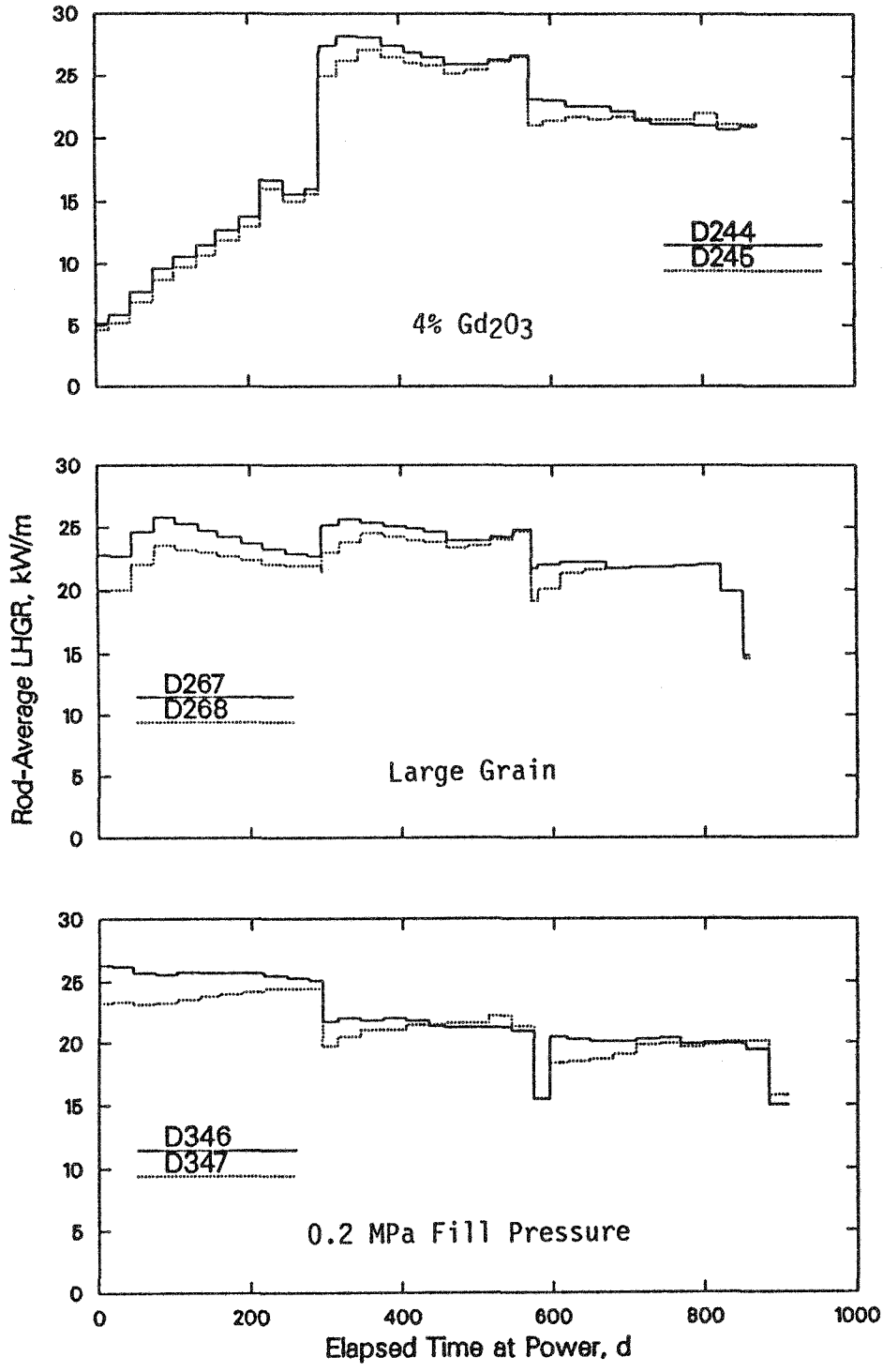

FIGURE A.3. Commercial Irradiation Histories for Variant KWU/CE PWR Rodlets (Task 2) (From histories provided in HBEP-03, HBEP-19, and HBEP-20.)

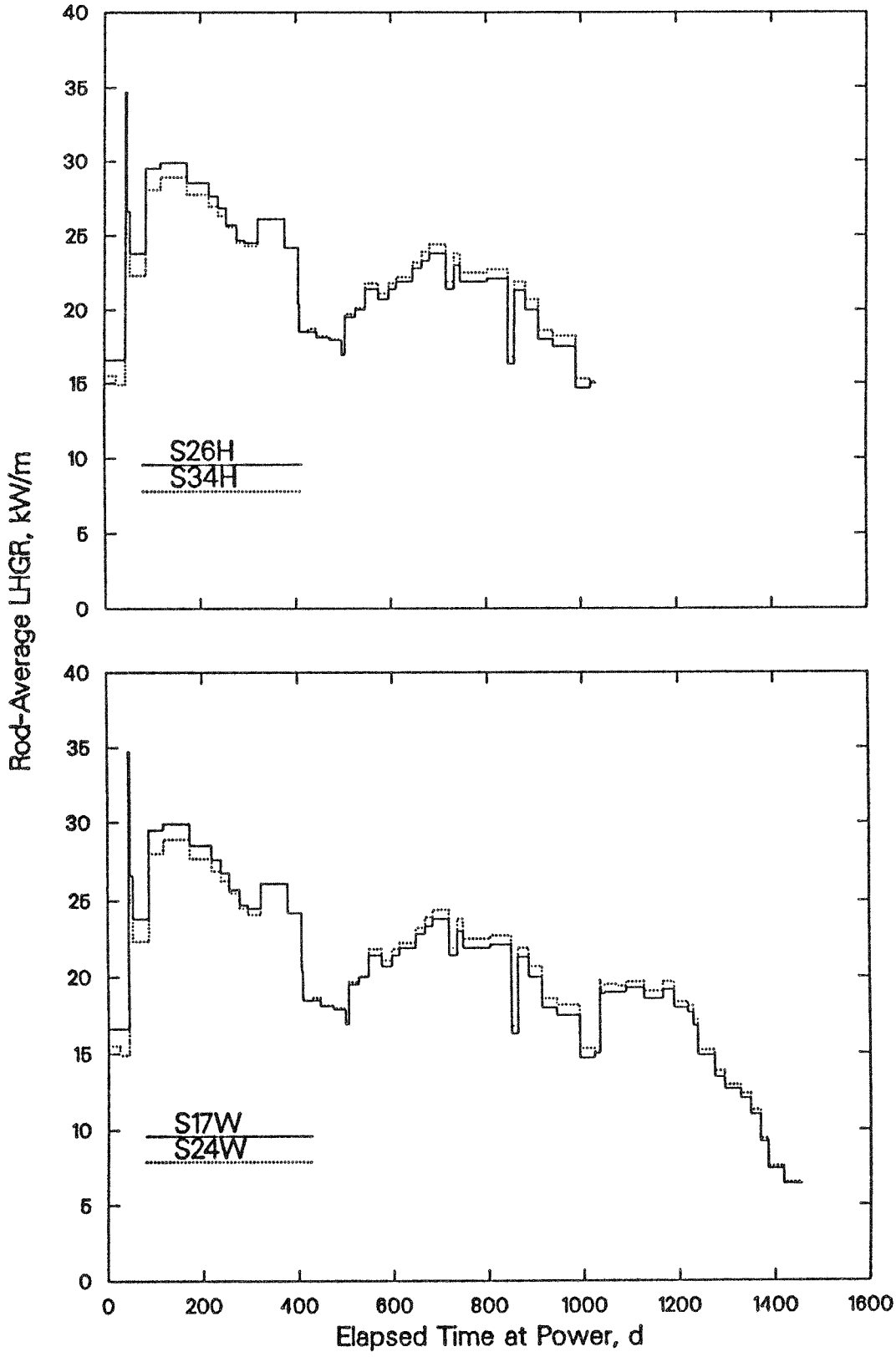

FIGURE A.4. Commercial Irradiation Histories for Standard KWU/CE BWR Rodlets (Task 2)
(From histories provided in HBEP-03 and HBEP-19.)

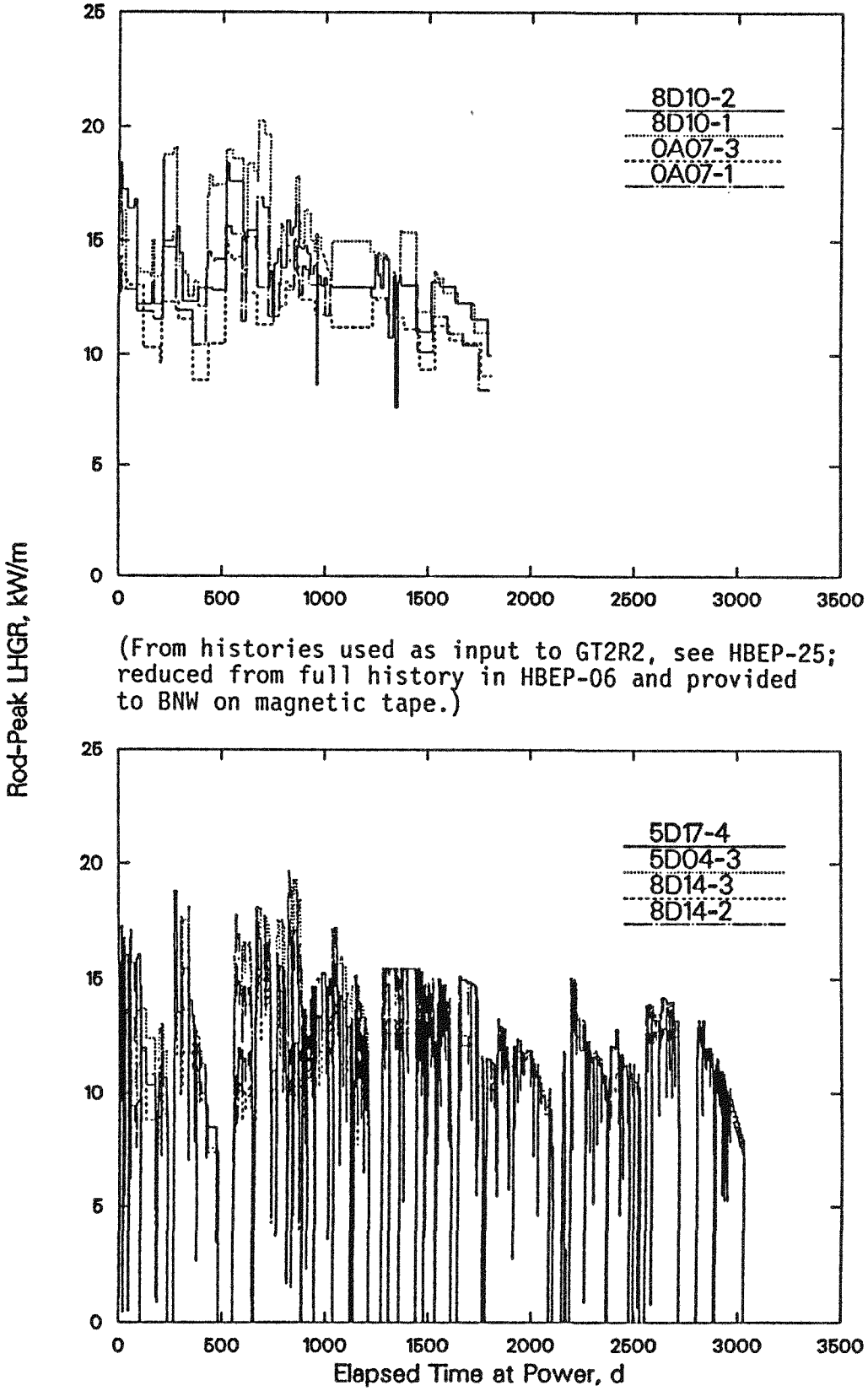

(From histories used as input to GT2R2, see HBEP-25; reduced from full history in HBEP-06 and provided to BNW on magnetic tape.)

FIGURE A.5. Commercial Irradiation Histories for GE BWR Rodlets (Task 2)
(From histories provided in HBEP-32.)

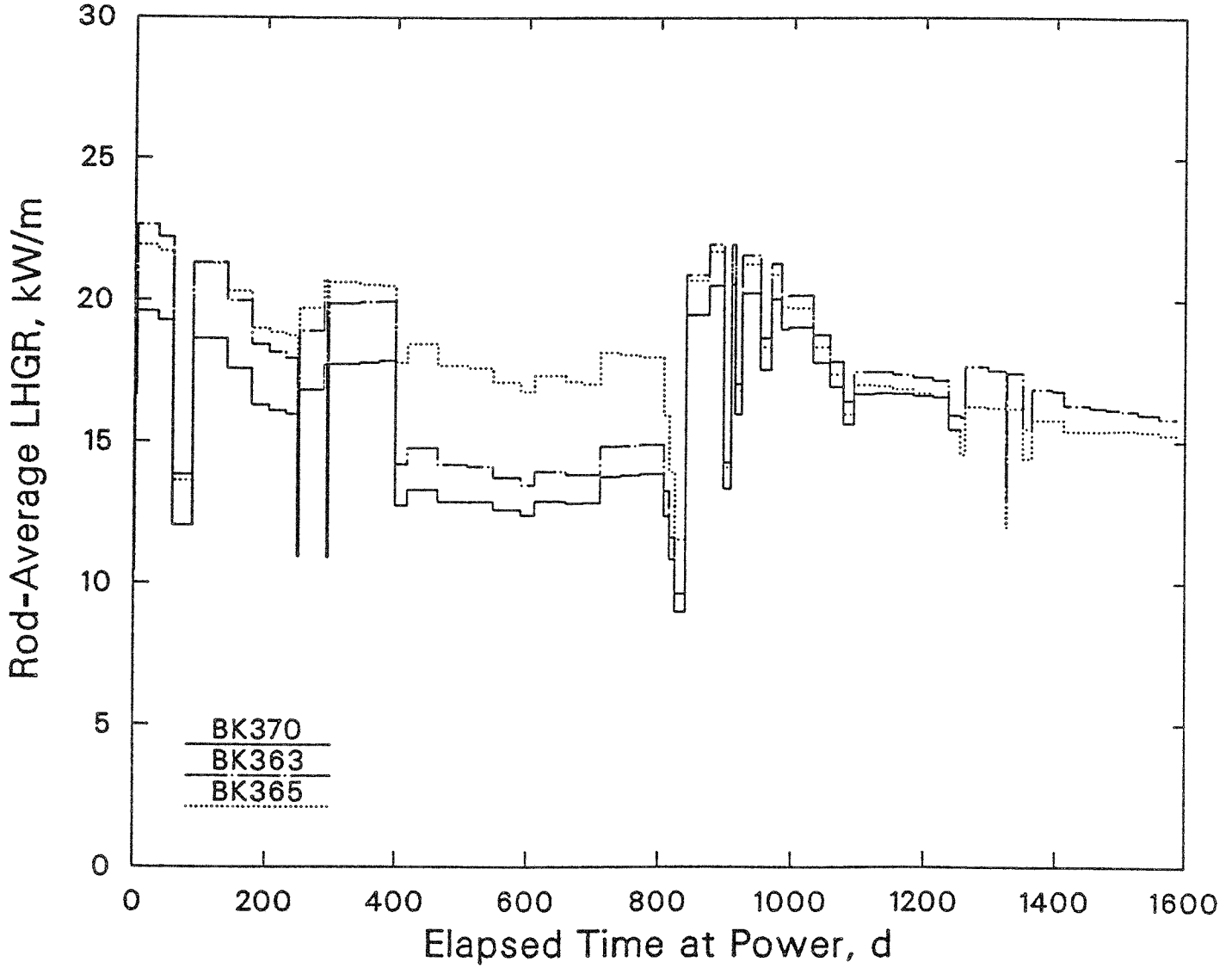

FIGURE A.6. Irradiation Histories for FGA/CEA PWR-Type Rods (Task 3) (From histories provided in HBEP-43 and HBEP-53; average LHGR value derived by BNW after normalizing axial LHGR profile to 10 equal-length segments.)

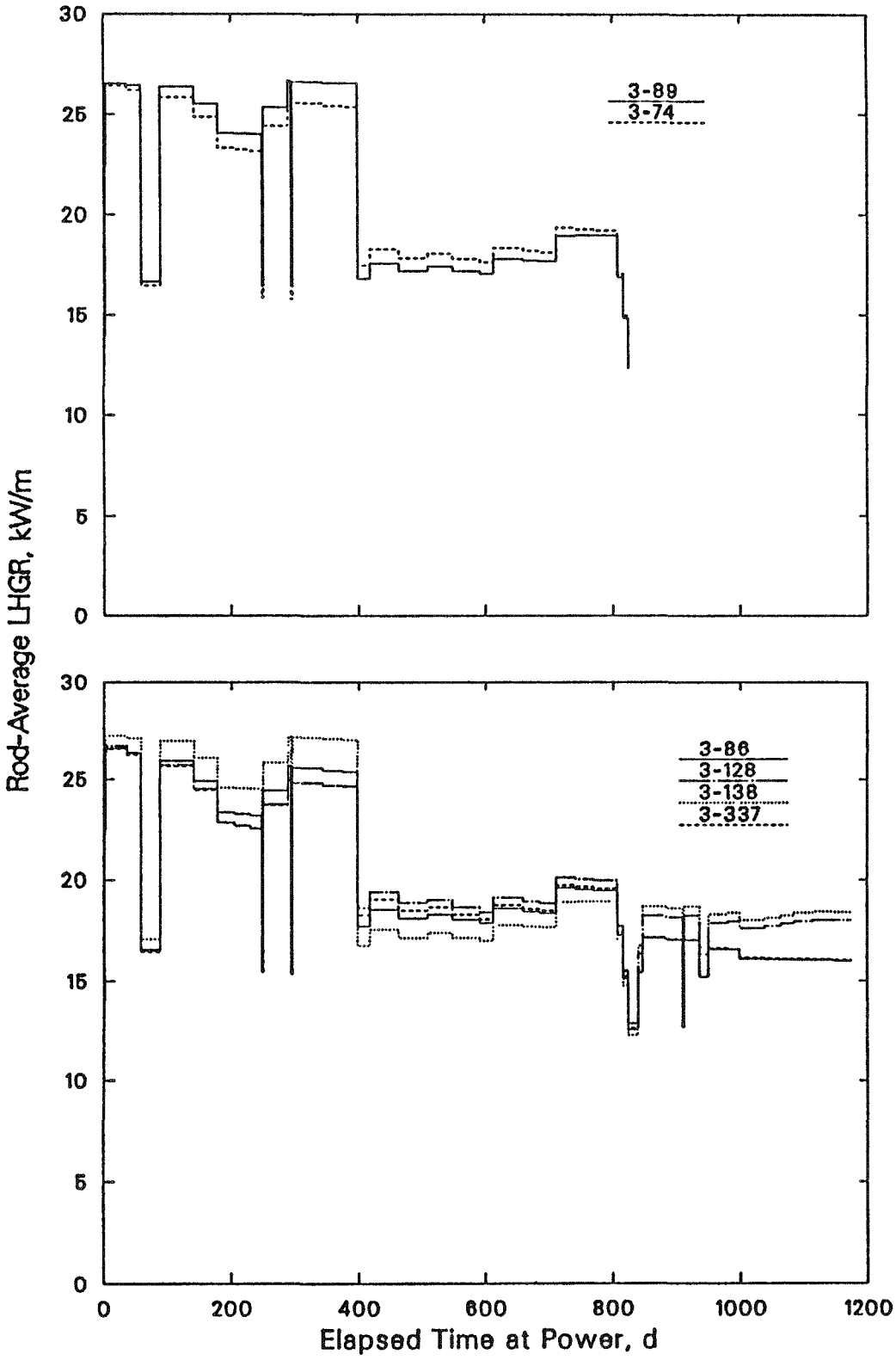

FIGURE A.7. Irradiation Histories for BN PWR-Type Rods (Task 3) (From histories provided in HBEP-43 and HBEP-53; average LHGR value derived by BNW after normalizing axial LHGR profile to 10 equal-length segments.)

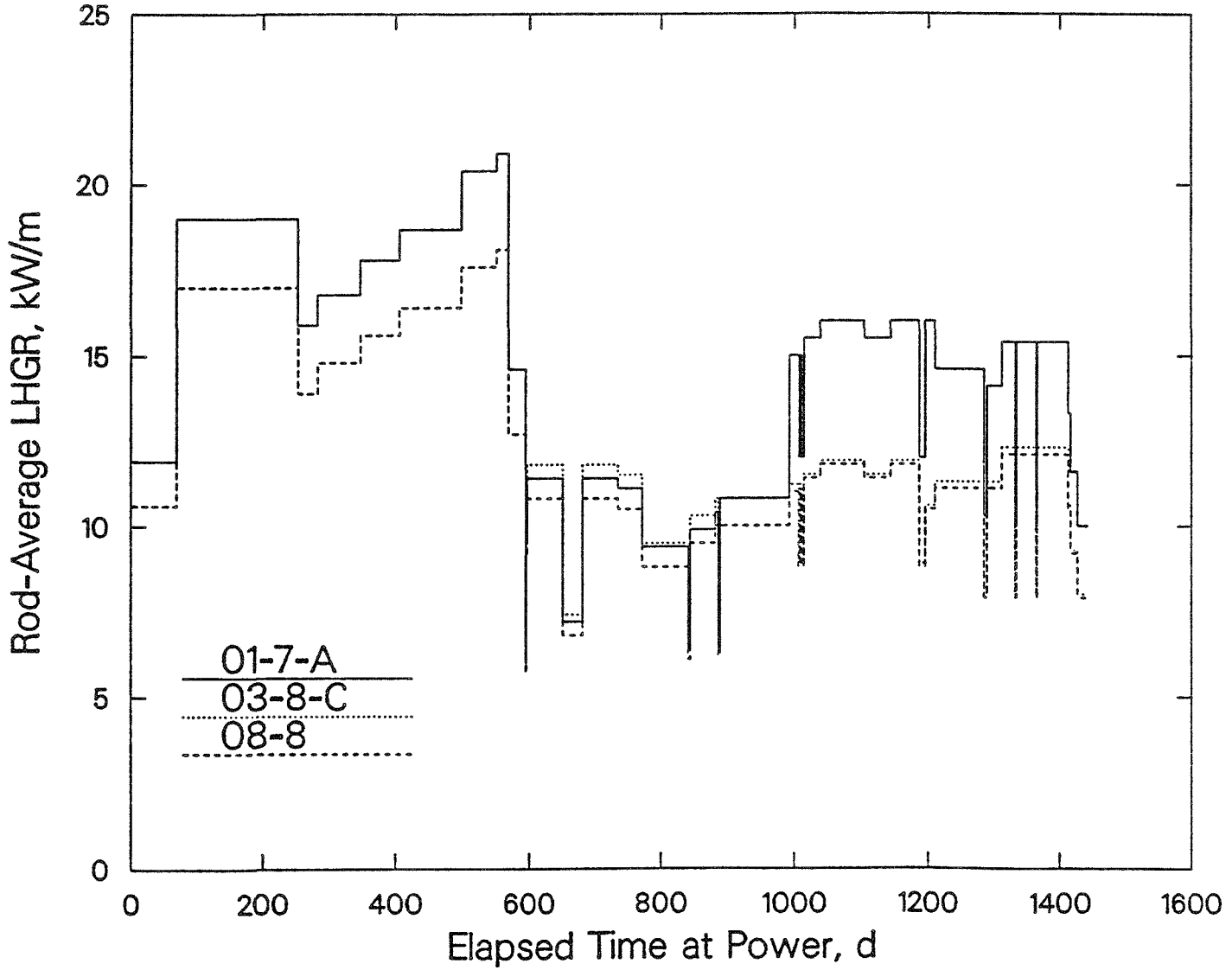

FIGURE A.8. Irradiation Histories for WEC PWR-Type Rods (Task 3) (From histories provided in HBEP-47.)

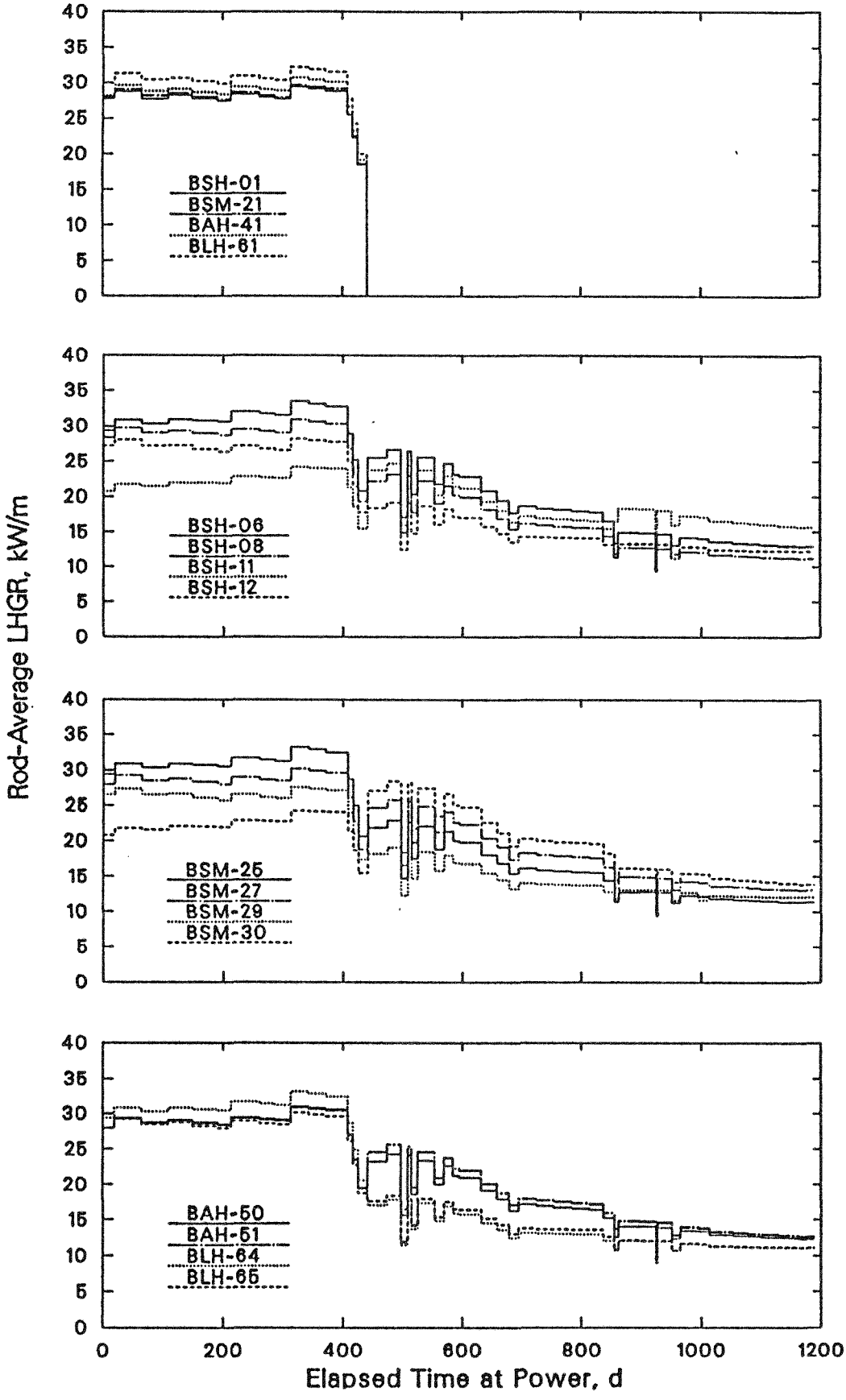

FIGURE A.9. Irradiation Histories for HBEP-Built PWR-Type Rods (Task 3) (From histories provided in HBEP-31, HBEP-44, and HBEP-53; average LHGR values derived by BNW after normalizing axial LHGR profile to 10 equal-length segments.)

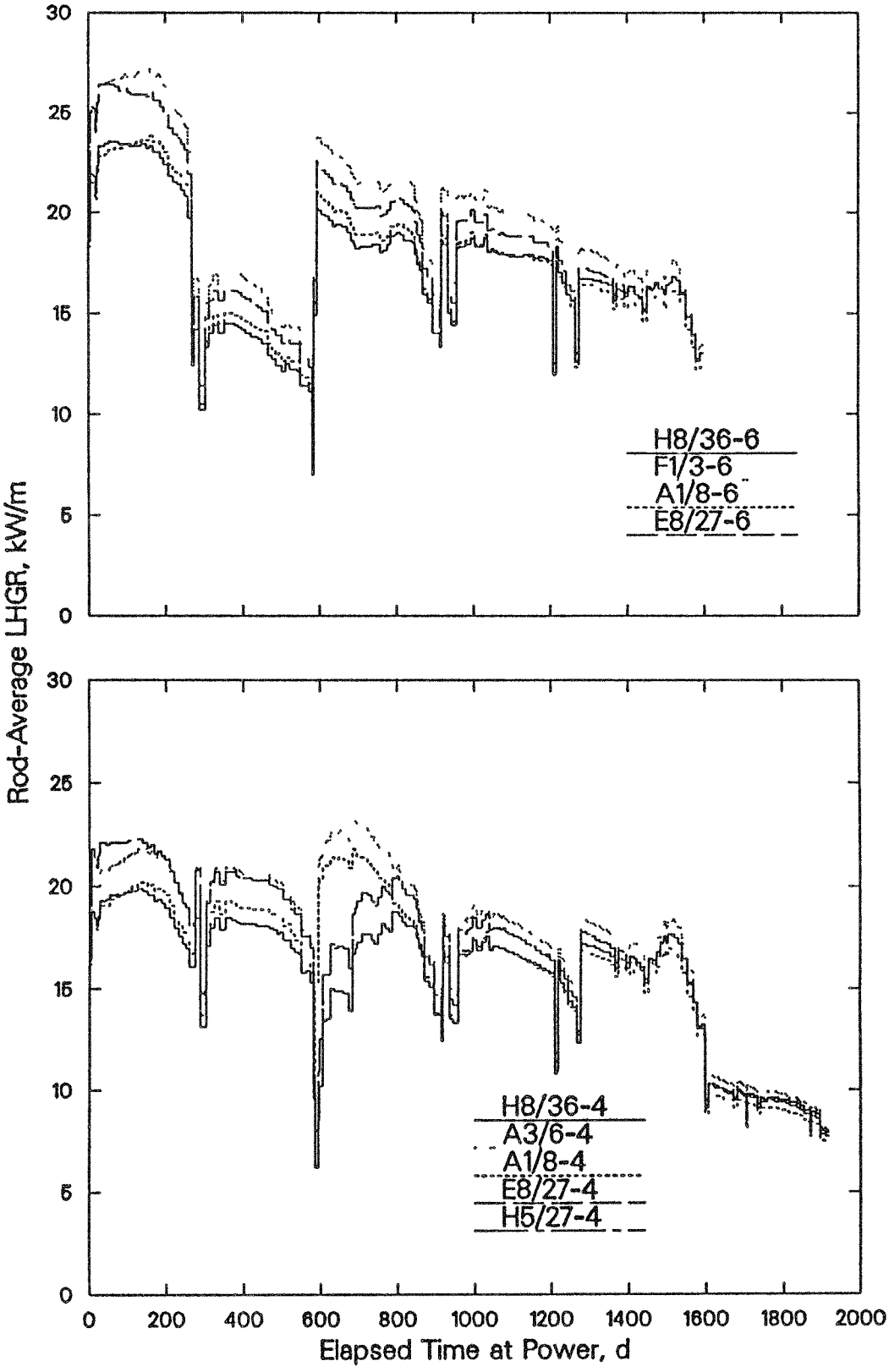

FIGURE A.10. Commercial Irradiation Histories for TVO-1 BWR Rods (Task 3) (From histories provided in HBEP-51.)

APPENDIX B

HBEP BIBLIOGRAPHY

APPENDIX B

HBEP BIBLIOGRAPHY

Presented in this appendix is a bibliography of material published by the HBEP, and tables cross-referencing specific data to the HBEP reports. The HBEP formal reports are listed in Table B.1, dates of HBEP status reports are listed in Table B.2, dates of HBEP meetings are listed in Table B.3 (handouts were prepared and distributed for these meetings), and other HBEP publications are listed in Table B.4.

A considerable amount of data ranging from preirradiation characterization to special examination has been generated and published by the HBEP. To improve the ease with which data can be found in the reports, data type and reporting document are cross-referenced for the various rod groups in Tables B.5 through B.9 and Figure B.1.

TABLE B.1. HBEP Formal Reports

Report No.[a]	Title and Date
HBEP-01(1P1)	A State-of-the-Technology Assessment. June 1982.
HBEP-02(2K1)	Fabrication and Pre-irradiation Characterization of KWU/CE Rods - Task 2A and Task 2C (Group 1). April 1981.
HBEP-03(2K2)	Irradiation Histories and NDT Examination (Karlstein) of KWU/CE Rods - Task 2A and Prebump Task 2C (Group 1). April 1981.
HBEP-04(2B1)	Pre-irradiation Characterization of BNFL Rods - Task 2A. April 1981.
HBEP-05(2B2)	Irradiation History of BNFL Rods - Task 2A. April 1981.
HBEP-06(2G1)	Fabrication, Pre-irradiation Characterization and Irradiation History of GE Rods - Task 2A, Task 2B (Partial), and Task 2C. April 1981.
HBEP-07(2G2)	NDT Examinations of GE Rods - Task 2A and Prebump Task 2C (Group 1). April 1981.
HBEP-08(2G3)	Power Bumping of GE Rods - Task 2C (Group 1). April 1981.
HBEP-09(3P1)	Design, Fabrication and Pre-irradiation Characterization of BR-3 Rods - Task 3. April 1981.
HBEP-10(1P2)	Fission Gas Release Data Evaluation - Published Data. March 1982.
HBEP-11(2K3)	Fabrication and Preirradiation Characterization of KWU/CE Rods - Task 2B and Task 2C (Group 2). June 1981.
HBEP-12(2/3P3)	Archive Fuel Characterization - Task 2 and Task 3. January 1982.

(a) Key to report numbers HBEP-a(bcd):
- a = overall report sequence number
- b = applicable Task number
- c = letter referring to rod group
  - K = KWU/CE Task 2 rods
  - B = BNFL Task 2 rods
  - G = GE Task 2 rods
  - P = Task 3 rods, and is also used for BNW reports
- d = report sequence number for rod group

For example: HBEP-22(2K12) is the 22nd HBEP report, applies to Task 2, and was the 12th report generated relative to the KWU/CE rodlets.

HBEP-13(2G4)	Postirradiation Examination of GE Rods - Task 2A and Task 2C (Group 1). November 1981.
HBEP-14(2K4)	Prebump and Postbump NDT and Power Bumping at JRC - Task 2C (Group 1, 20 MWd/kgM Rods). November 1981.
HBEP-15(2K5)	Prebump and Postbump NDT and Power Bumping at JRC - Task 2C (Group 1, 30 MWd/kgM Rods). November 1981.
HBEP-16(2K6)	Prebump and Postbump NDT Examinations and Fission Gas Measurements at ECN - Task 2C (Group 1). October 1981.
HBEP-17(2K7)	Prebump and Postbump Gamma Scan Measurements at ECN - Task 2C (Group 1, 20 MWd/kgM Rods). October 1981.
HBEP-18(2K8)	Prebump and Postbump Gamma Scan Measurements at ECN - Task 2C (Group 1, 30 MWd/kgM Rods). October 1981.
HBEP-19(2K9)	Irradiation Histories and NDT Examination (Karlstein) of KWU/CE Rods - Task 2B (Group 1). January 1982.
HBEP-20(2K10)	Irradiation Histories and NDT Examination (Karlstein) of KWU/CE Rods - Task 2B (Group 2) and Task 2C (Group 2). May 1982.
HBEP-21(2K11)	Postbump Ceramography Results from ECN - Task 2C (Group 1, 20 MWd/kgM Rods). October 1982.
HBEP-22(2K12)	Postbump Ceramography Results from ECN - Task 2C (Group 1, 30 MWd/kgM Rods). October 1982.
HBEP-23(2K13/2B3)	NDT Examinations of KWU/CE and BNFL Rods at Windscale - Task 2A. October 1982.
HBEP-24(2K14/2B4)	Destructive Examinations of KWU/CE and BNFL Rods at Windscale - Task 2A. October 1982.
HBEP-25(2P4) (Original Draft)	Qualification of Fission Gas Release Data from Tasks 2A and 2B/2C (Groups 1) Rods. October 1982.
HBEP-25(2P4) (Rev. 1, Draft)	Qualification of Fission Gas Release Data from Task 2 Rods. October 1983.
HBEP-25(2P4) (Rev. 2, Draft)	Qualification of Fission Gas Release Data from Task 2 Rods. October 1984.
HBEP-25(2P4) (Rev. 3, Draft)	Qualification of Fission Gas Release Data from Task 2 Rods. June 1987.
HBEP-25(2P4) Final Report	Qualification of Fission Gas Release Data from Task 2 Rods. November 1987.

HBEP-26(2K15)	Prebump and Postbump NDT and Power Bumping at JRC - Task 2C (Group 2). November 1982.
HBEP-27(2B5/3P5)	Fluence Calculations for Assembly 373 (Task 2A) and Radial Power Generation Calculations for BSH Type Rods (Task 3). November 1982.
HBEP-28(2K16)	Prebump and Postbump NDT Examinations and Fission Gas Release Measurements at ECN - Task 2C (Group 2). April 1983.
HBEP-29(2K17)	Prebump and Postbump Gamma Scan Measurements Performed at ECN - Task 2C (Group 2). August 1983.
HBEP-30(2K18)	Destructive Examinations of KWU/CE Rods at Windscale - Task 2B. October 1983.
HBEP-31(3P6)	BR-3 Cycle 4C Irradiation Data - Task 3. December 1983.
HBEP-32(2G5)	Irradiation History for GE Rodlets - Task 2B and 2C (Groups 2). March 1984.
HBEP-33(2K19)	Postbump Ceramography Results from ECN - Task 2C (Group 2). January 1984.
HBEP-34(2G6)	NDT Examinations of GE Rodlets - Task 2B and Prebump Task 2C (Group 2). February 1984.
HBEP-35(2K20)	Special Examination Results from ECN - Task 2C. April 1984.
HBEP-36(2G7)	Power Bumping of GE Rodlets - Task 2C (Group 2). April 1984.
HBEP-37(3P7) (Draft)	Postirradiation Examination of Four Fuel Rods Irradiated One Cycle in BR-3 - Task 3. September 1984.
HBEP-37(3P7)	Postirradiation Examination of Four Fuel Rods Irradiated One Cycle in BR-3 - Task 3. May 1986.
HBEP-38(2K21/2B5) (Draft)	Special Postirradiation Examination Results - Task 2. September 1984.
HBEP-38(2P8)	Special Postirradiation Examination Results -Task 2. April 1986.
HBEP-39(2P8) (Draft)	Summary of Task 2 Results. November 1984.
HBEP-40(2G8) (Draft)	Postirradiation and Special Examination Results for GE Rodlets - Tasks 2B and 2C (Groups 1 and 2). May 1985.

HBEP-40(2G8)	Postirradiation and Special Examination Results for GE Rodlets - Tasks 2B and 2C (Groups 1 and 2). November 1988.
HBEP-41(2/3P9) (Draft)	Sectioning Diagrams for HBEP Rods/Rodlets. March 1985.
HBEP-41(2/3P9)	Sectioning Diagrams for HBEP Rods/Rodlets. August 1989.
HBEP-42(2K22)	Pre- and Postbump Fission Gas Release Measurements (^{85}Kr) from Petten - Task 2C. March 1986.
HBEP-43(3P10)	Irradiation Data for BN and FGA/CEA Rods, BR-3 Cycles 4B, 4C, and 4D1 - Task 3. July 1986.
HBEP-44(3P11)	BR-3 Cycle 4D1 Irradiation Data - Task 3. August 1986.
HBEP-45(3P12)	Fabrication and Preirradiation Characterization of FRAGEMA/CEA BR-3 Rods - Task 3. August 1986.
HBEP-46(3P13)	Fabrication and Preirradiation Characterization of BN BR-3 Rods - Task 3. March 1987.
HBEP-47(3P14)	Fabrication, Preirradiation Characterization, and Irradiation History for Westinghouse BR-3 Rods - Task 3. June 1987.
HBEP-48(2G9)	Special Postirradiation Examination Results for GE Rodlets - Task 2. January 1988.
HBEP-49(3P15)	Archive Fuel Characterization - Task 3 BN and FGA/CEA Fuel. September 1987.
HBEP-50(2P16)	Summary of Postirradiation Special Examinations - Task 2. June 1988.
HBEP-51(3P17)	Fabrication, Preirradiation Characterization, and Irradiation History for TVO-1 Rods--Task 3. March 1988.
HBEP-52(3P18)	Archive Fuel Characterization for TVO-1 Rods - Task 3. August 1988.
HBEP-53(3P19)	BR-3 Cycle 4D2 Irradiation Data - Task 3. April 1988.
HBEP-54(3P20)	NDT Examinations of Six Fuel Rods Irradiated for Two or Three Cycles in BR-3 - Task 3. August 1988.
HBEP-55(3P21)	NDT Examinations of Nine BWR Fuel Rods Irradiated in TVO-1 - Task 3. March 1989.
HBEP-56(3P22)	NDT Examinations of Eighteen Fuel Rods Irradiated for Three

or Four Cycles in BR-3 - Task 3. June 1989.

HBEP-57(3P23) Destructive and Special Examinations of Eight Fuel Rods Irradiated in BR-3 - Task 3. August 1989.

HBEP-58(3P24) Destructive and Special Examinations of Three BWR Fuel Rods Irradiated in TVO-1 - Task 3. July 1989.

HBEP-59(3P25) XRF at Risø

HBEP-60(3P26) (Draft) Qualification of Fission Gas Release Data from Task 3 Rods. August 1989.

HBEP-60(3P26) Qualification of Fission Gas Release Data from Task 3 Rods. January 1990.

HBEP-61(3P27) (Draft) High Burnup Effects Program - Final Report. September 1989.

HBEP-61(3P27) Revision 1 High Burnup Effects Program - Final Report. January 1990.

HBEP-61(3P27) Final High Burnup Effects Program - Final Report. April 1990.

TABLE B.2. HBEP Status Reports

Report No.	Date
1	June 13, 1980 (HBEP Review Meeting Summary)
2	October 1980
3	December 1980
4	April 1981
5	September 1981
6	March 1982
7	May 1982
8	August 1982
9	January 1983
10	April 1983
11	September 1983
12	January 1984
13	May 1984
14	October 1984
15	February 1985
16	March 1985
17	May 1985
18	August 1985
19	February 1986
20	June 1986
21	May 1987
22	December 1987
23	July 1988
24	November 1988
25	July 1989
26	November 1989

TABLE B.3. HBEP Meetings

Meeting No.	Location and Date
0	Seattle, Washington. September 1978. (First Organizational Meeting)
1	Portland, Oregon. May 4, 1979.
2	San Francisco, California. November 16, 1979.
3	Las Vegas, Nevada. June 13, 1980.
4	San Francisco, California. December 4, 1981.
5	Washington, D.C. November 19, 1982.
6	San Francisco, California. November 4, 1983.
7	Washington, D.C. November 16, 1984.
8	Orlando, Florida. April 25, 1985.
9	Wengen, Switzerland. June 9, 1986.
10	Los Angeles, California. November 20, 1987.
11	Washington, D.C. November 4, 1988.
12 (Final)	Kyoto, Japan. October 25, 1989.

TABLE B.4. Other HBEP Publications

Program Planning Documents

Program Plan (Revision 1)	The Investigation of High Burnup Effects in Sintered UO_2 Pellet Fuel with Emphasis on Fission Gas Release. May 1979.
Program Plan (Revision 2)	The Investigation of High Burnup Effects in Sintered UO_2 Pellet Fuel with Emphasis on Fission Gas Release. April 1980.
Program Plan (Revision 3)	The Investigation of High Burnup Effects in Sintered UO_2 Pellet Fuel with Emphasis on Fission Gas Release. May 1981.

Related Topical Reports

BNFL Report 439(S)	Pre-Irradiation Characterization Data for the PWR Fuel Assembly No. 366. July 1982.

Open Literature Publications

"An Evaluation of Published High Burnup Fission Gas Release Data." C.E. Beyer. Proceedings of Topical Meeting on LWR Extended Burnup - Fuel Performance and Utilization, Williamsburg, Virginia, April 4-8, 1982.

Handouts

Atlanta, Georgia. April 8-9, 1980 (DOE/EPRI Fuel Performance Contractors' Overview Meeting).

Washington, D.C. September 9, 1980 (DOE Program Review).

Boulder, Colorado. January 6-7, 1982 (DOE/EPRI Fuel Performance Contractors' Overview Meeting)

Williamsburg, Virginia. April 4-8, 1982 (ANS Topical Meeting on LWR Extended Burnup-Fuel Performance and Utilization).

TABLE B.5 Cross-Reference of Data and Reports for Task 2 BNFL Rods

	Number of HBEP Report Containing Applicable Data[a]						
Rod	As-Fab	LHGR	NDT	FGR	Burnup	Ceram.	Special
DF	4,12	5,27	23	23	-	-	-
BK	4,12	5,27	23	23	24	24	38
AK	4,12	5,27	23	23	-	-	-
AU	4,12	5,27	23	23	24	24	-
AP	4,12	5,27	23	23	-	-	-
BN	4,12	5,27	23	23	-	24	-
BW	4,12	5,27	23	23	24	24	-
DE	4,12	5,27	23	23	-	24	-
AL	4,12	5,27	23	23	24	24	-
BH	4,12	5,27	23	23	-	-	-
CQ	4,12	5,27	23	23	-	-	-
BP	4,12	5,27	23	23	-	-	-

(a) As-Fab: preirradiation characterization data
LHGR: irradiation history data
NDT: nondestructive examination data
FGR: fission gas release data
Burnup: burnup measurement data
Ceram: ceramographic examination data
Special: special examination data

TABLE B.6 Cross-Reference of Data and Reports for Task 2 KWU/CE PWR Rods

	Number of HBEP Report Containing Applicable Data[a]								
Rod	As-Fab	LHGR	NDT-1	NDT-2	FGR	Burnup	Ceram.	Gamma	Special
D198	2,12	3,14	3,14,16	14,16	16	-	-	17	42
D199	2,12	3,14	3,14,16	14,16	16	-	21	17	42
D200	2,12	3,14	3,14,16	14,16	16	-	21	17	35,38,42
D201	2,12	3,14	3,14,16	14,16	16	-	21	17	42
D202	2,12	3	3,23	-	23	24	24	-	38
D205	2,12	3,15	3,15,16	15,16	16	-	22	18	42
D206	2,12	3,15	3,15,16	15,16	16	-	22	18	42
D207	2,12	3,15	3,15,16	15,16	16	-	22	18	35,38,42
D208	2,12	3,15	3,15,16	15,16	16	-	22	18	42
D209	2,12	3	3,23	-	23	24	24	-	38
D219	11,12	20,26	20,26,28	26,28	28	-	33	29	42
D226	11,12	20,26	20,26,28	26,28	28	-	33	29	38,42
D227	11,12	20,26	20,26,28	26,28	28	-	33	29	35,42
D220	11,12	20,26	20,26,28	26,28	28	-	33	29	42
D228	11,12	20	20,30	-	30	30	30	-	38
D244	2,12	3	3,23	-	23	24	24	-	38
D245	2,12	3	3,23	-	23	-	24	-	38
D267	11,12	19	19,30	-	30	-	-	-	-
D268	11,12	19	19,30	-	30	30	30	-	-
D346	11,12	20	20,30	-	30	30	30	-	-
D347	11,12	20	20,30	-	30	-	-	-	-

(a) As-Fab: preirradiation characterization data
LHGR: irradiation history data
NDT-1: nondestructive examination data after steady-state operation
NDT-2: nondestructive examination data after bumping irradiation
FGR: fission gas release data
Burnup: burnup measurement data
Ceram: ceramographic examination data
Gamma: axial gamma scanning data, pre- and post-bumping irradiation
Special: special examination data

TABLE B.7 Cross-Reference of Data and Reports for Task 2 KWU/CE BWR Rods

	Number of HBEP Report Containing Applicable Data[a]						
Rod	As-Fab	LHGR	NDT	FGR	Burnup	Ceram.	Special
S26H	2,12	3	3,23	23	24	24	-
S34H	2,12	3	3,23	23	-	-	-
S17W	11,12	19	19,30	30	30	30	-
S24W	11,12	19	19,30	30	-	-	-

(a) As-Fab: preirradiation characterization data
LHGR: irradiation history data
NDT: nondestructive examination data
FGR: fission gas release data
Burnup: burnup measurement data
Ceram: ceramographic examination data
Special: special examination data

TABLE B.8 Cross-Reference of Data and Reports for Task 2 GE BWR Rods

	Number of HBEP Report Containing Applicable Data[a]						
Rod	As-Fab	LHGR	NDT	FGR	Burnup	Ceram.	Special
8D10-2	6,12	6	7	7	-	13	-
8D10-1	6,12	6,8	7,13	13	13	13	-
0A07-3	6,12	6	7	7	-	-	-
0A07-1	6,12	6,8	7,13	-	-	-	-
5D17-4	6,12	6,32,36	34,40	40	40	40	48
5D04-3	6,12	6,32	34,40	40	40	40	-
8D14-3	6,12	6,32,38	34,40	40	40	40	-
8D14-2	6,12	6,32	34	34	-	-	-

(a) As-Fab: preirradiation characterization data
LHGR: irradiation history data
NDT: nondestructive examination data
FGR: fission gas release data
Burnup: burnup measurement data
Ceram: ceramographic examination data
Special: special examination data

TABLE B.9 Cross-Reference of Data and Reports for Task 3 Rods

	Number of HBEP Report Containing Applicable Data[a]						
Rod	As-Fab	LHGR	NDT	FGR	Burnup	Ceram.	Special
BK370	45,49	43	54	54	-	57	57
BK363	45,49	43,53	56	56	-	57	57
BK365	45,49	43,53	56	56	57	57	57,59
3-74	46,49	43	54	54	-	-	-
3-89	46,49	43	54	54	57	57	57
3-86	46,49	43,53	56	56	-	-	-
3-128	46,49	43,53	56	56	-	-	-
3-138	46,49	43,53	56	56	57	57	57,59
3-337	46,49	43,53	56	56	-	-	-
01-7-A	47	47	54	54	-	-	-
03-8-C	47	47	54	54	-	-	-
08-8	47	47	54	54	-	-	-
BSH-01	9,12	27,31	37	37	37	37	37
BSH-06	9,12	27,31,44,53	56	56	57	57	57,59
BSH-08	9,12	27,31,44,53	56	56	-	-	-
BSH-11	9,12	27,31,44,53	56	56	-	-	-
BSH-12	9,12	27,31,44,53	56	56	-	-	-
BSM-21	9,12	31	37	37	-	-	-
BSM-25	9,12	31,44,53	56	56	-	-	-
BSM-27	9,12	31,44,53	56	56	-	57	57
BSM-29	9,12	31,44,53	56	56	-	-	-
BSM-30	9,12	31,44,53	56	56	-	-	-
BAH-41	9,12	31	37	37	-	-	-
BAH-50	9,12	31,44,53	56	56	57	57	57
BAH-51	9,12	31,44,53	56	56	-	-	-
BLH-61	9,12	31	37	37	-	-	-
BLH-64	9,12	31,44,53	56	56	-	57	57,59
BLH-65	9,12	31,44,53	56	56	-	-	-
H8/36-6	51,52	51	55	55	58	58	58,59
F1/3-6	51,52	51	55	55	-	-	-
A1/8-6	51,52	51	55	55	-	-	-
E8/27-6	51,52	51	55	55	-	-	-
H8/36-4	51,52	51	55	55	58	58	58,59
A3/6-4	51,52	51	55	55	58	58	58
H5/27-4	51,52	51	55	55	-	-	-
E8/27-4	51,52	51	55	55	-	-	-

(a) As-Fab: preirradiation characterization data
LHGR: irradiation history data
NDT: nondestructive examination data
FGR: fission gas release data
Burnup: burnup measurement data
Ceram: ceramographic examination data
Special: special examination data

All HBEP Reports

Topics	Categories of Activities						
	Fabrication, Characterization	Archive Characterization	Commercial Irradiation History	Prebump Examination	Bumping Irradiation	PIE Results	Evaluation
Task 1							
State-of-the-Technology							01(1P1)
Evaluation-Published Data							10(1P2)
Task 2A							
KWU/CE Rods	02(2K1)	12(2/3P3)	03(2K2)			23(2K13/2B3), 24(2K14/2B4), 38(2K21/2B5)	
BNFL Rods	04(2B1)	12(2/3P3)	05(2B2) 27(2B5/3P5)			23(2K13/2B3), 24(2K14/2B4), 38(2K21/2B5)	
GE Rods	06(2G1)	12(2/3P3)	06(2G1)			07(2G2) 13(2G4)	
Task 2B							
KWU/CE Rods (Group 1)	11(2K3)	12(2/3P3)	19(2K9)			30(2K18), 38(2K21/2B5)	25(2P4) Original Rev. 1 Rev. 2 Rev. 3 Final Report
KWU/CE Rods (Group 2)	11(2P3)	12(2/3P3)	20(2K10)			30(2K18), 38(2K21/2B5)	
GE Rods	06(2G1)	12(2/3P3)	32(2G5)			34(2G6)	
Task 2C							
KWU/CE Rods (Group 1)	02(2K1)	12(2/3P3)	03(2K2)	03(2K2) 14(2K4) 15(2K5) 16(2K6) 17(2K7) 18(2K8) 42(2K22)	14(2K4) 15(2K5)	14(2K4),15(2K5), 16(2K6), 17(2K7), 18(2K8), 21(2K11), 22(2K12), 35(2K20), 38(2K21/2B5), 42(2K22)	39(2P8) Draft
GE Rods (Group 1)	06(2G1)	12(2/3P3)	06(2G1)	07(2G2)	08(2G3)	08(2G3) 13(2G4)	50(2P16)
KWU/CE Rods (Group 2)	11(2K3)	12(2/3P3)	20(2K10)	20(2K10) 26(2K15) 28(2K16) 29(2K17) 42(2K22)	26(2K15)	26(2K15), 28(2K16), 29(2K17), 33(2K19), 35(2K20), 38(2K21/2B5), 42(2K22)	
GE Rods (Group 2)	06(2G1)	12(2/3P3)	32(2G5)	34(2G6)	36(2G7)	34(2G6), 36(2G7), 40(2G8), 48(2G9)	
Task 3							
Program Rods, 1 Cycle	09(3P1)	12(2/3P3)	31(3P6) 27(2B5/3P5)			37(3P7)	
Program Rods, 3 Cycle	09(3P1)	12(2/3P3)	27(2B5/3P5) 44(3P11) 53(3P19)			54(3P20), 56(3P22), 57(3P23), 59(3P25)	
BN Rods	46(3P13)	49(3P15)	43(3P10) 53(3P19)			54(3P20), 56(3P22), 57(3P23), 59(3P25)	60(3P26)
FGA/CEA Rods	45(3P12)	49(3P15)	43(3P10) 53(3P19)			54(3P20), 56(3P22), 57(3P23), 59(3P25)	
Westinghouse Rods	47(3P14)		47(3P14)			54(3P20)	
TVO Rods	51(3P17)	52(3P18)	51(3P17)			55(3P21), 58(3P24), 59(3P25)	
Sectioning Diagrams All Tasks, 41(2/3P9), Draft, Final Report							
HBEP Summary 61(3P27)							

FIGURE B.1. HBEP Reports by Rod Group and Subject

APPENDIX C

POSTIRRADIATION EXAMINATION TECHNIQUES

APPENDIX C

POSTIRRADIATION EXAMINATION TECHNIQUES

A number of techniques were employed in the examination of the irradiated fuel rods. The objective of the techniques was to obtain detailed data on the postirradiation condition of the rods on both macro and micro scales. The techniques employed included: cladding metrology, axial gamma scanning, rod puncture and gas analysis, ^{148}Nd-based burnup, whole pellet fuel density, electron probe microanalysis (EPMA), X-ray fluorescence (XRF), and scanning electron microscopy (SEM); the techniques are briefly described in the following.

CLADDING METROLOGY

Cladding metrology was employed to determine cladding diameter, ovality, bowing, and overall rod length both before and after irradiation. Typically, cladding diameters were determined using contact transducers fitted with chisel-shaped anvils; the equipment was calibrated against three standards. Values were obtained at approximately 1 mm intervals and at four orientations (0°, 45°, 90°, and 135°). Repeatability of the measurements was to ±0.005 mm.

Postirradiation overall rod length was determined by comparison to a pre-measured Zircaloy-clad fuel rod; lengths were then corrected (by accounting for thermal expansion) to the equivalent value at a temperature of 293K. Accuracy of the rod length measurement was approximately ±0.25 mm (2σ).

ROD AXIAL GAMMA SCANNING

The majority of the fuel rods were axially gamma scanned for both total and selected isotopic activities. Fuel column length was also determined from the activity data; accuracy of the fuel column length analysis was approximately ±3 mm (2σ).

ROD PUNCTURE AND GAS ANALYSIS

For analysis of fission gas release, the rods were 1) punctured, 2) the gas collected with determination of total volume, 3) the interior void volume of the rod determined, and 4) the composition of the collected gas determined. Uncertainty levels (1σ) associated with these various steps include: ±3% for rod void volume and pressure; ±3% for collected gas volume; and ±1% for gas fractions.

^{148}Nd-BASED BURNUP

Fuel samples, approximately a whole pellet, were chemically analyzed for the quantity of ^{148}Nd, a fission product related to burnup level. Burnup levels derived from the ^{148}Nd analyses have an uncertainty level of approximately ±5% (2σ).

WHOLE PELLET FUEL DENSITY

Fuel samples, approximately a whole pellet, had postirradiation densities determined by immersion techniques. Multiple measurements of fuel density resulted in variations of ±0.03 g/cm^3.

ELECTRON PROBE MICROANALYSIS

Concentrations of selected elements as a function of radial location within a fuel cross-section were determined using EPMA. This technique analyzes the spectra given off when the sample is bombarded with an electron beam; element concentrations are determined by comparison to standards. Elements detected commonly consisted of uranium, plutonium, neodymium, xenon, cesium, iodine, etc; oxygen was not directly detected. The estimated level of uncertainty for the concentration of most measured elements is approximately ±10% (2σ).

Analyses of element concentrations were performed on areas ranging from approximately 10x20 μm to 90x15 μm, with some analyses performed on smaller areas. The depth of penetration of EPMA is approximately 1 μm, so only elements in the base matrix may be measured; elements in bubbles larger than 0.1 μm are usually not detected. Relative to XRF, EPMA analyzes

concentrations in smaller areas thus providing greater definition of position, but does not necessarily measure the total concentration.

X-RAY FLUORESCENCE

Concentrations of xenon as a function of position (radially and within the pellet rim region) were determined using XRF. This technique bombards the fuel sample surface with X-rays and then measures the fluorescent Kα X-rays given off. Only xenon is detected with this technique. The estimated level of uncertainty for the concentration of xenon is approximately ±10% (2σ).

Analysis of xenon concentration was obtained from areas approximately 350x4000 μm. The depth of penetration of XRF is approximately 20 μm, so xenon in the base matrix and in small bubbles or gaps may be measured. Relative to EPMA, XRF lacks the definition of location, but provides a measure of the total xenon present in the analyzed volume.

SCANNING ELECTRON MICROSCOPY

Scanning electron microscopy was used to examine surfaces of fuel cross-sections, both as-polished and freshley fractured by scratching with a diamond stylus. Fractured surfaces were used to expose bubble development on grain surfaces. Both back-scatter electron and secondary electron micrographs were obtained, with magnification levels from 40 to 4800X. EPMA measurements and SEM examinations were generally performed on the same fuel cross-section sample.

LEGAL NOTICE

This report was prepared by Battelle, Pacific Northwest Laboratories as an account of sponsored research activities as part of the High Burnup Effects Program (HBEP), contracts numbered 2311255301 through 2311255328, sponsored by the following:

Advanced Nuclear Fuels Corporation	USA
Babcock-Brown Boveri Reaktor	FRG
Babcock and Wilcox	USA
Belgonucleaire	Belgium
British Nuclear Fuels Limited	Great Britain
Central Research Institute of Electric Power Industry	Japan
Centre d'Etude de l'Energie Nucleaire	Belgium
Combustion Engineering, Incorporated	USA
dell' Energia Nucleare e delle Energie Alternative	Italy
Department of Energy, U.S. Government	USA
Electric Power Research Institute	USA
Fragema	France
General Electric Company	USA
Hitachi, Limited	Japan
Japan Atomic Energy Research Institute	Japan
Mitsubishi Heavy Industry, Limited	Japan
Netherlands Energy Research Foundation	The Netherlands
Nuclear Fuels Industry, Limited	Japan
Risø National Laboratory	Denmark
The Paul Scherrer Institute	Switzerland
Siemens AG	FRG
Studsvik Energiteknik AB	Sweden
Toshiba Corporation	Japan
Technical Research Center of Finland	Finland
Westinghouse Electric Corporation	USA

Neither Battelle, Pacific Northwest Laboratories, nor sponsors (identified above), nor any person acting on their behalf either: (a) **makes any warranty or representation, express or implied, with respect to the accuracy, completeness, or usefulness of the information contained in this report,** or that the use of any information, apparatus, process, or composition disclosed in this report may not infringe privately owned rights; or, (b) assumes any liabilities with respect to the use of, or for damages resulting from the use of, any information, apparatus, process or composition disclosed in this report.

This report and the information provided therein should not be released, published, or disclosed to others except in accordance with the terms of the above referenced contracts.